Centro Brasileiro de Pesquisas Físicas
Coordenação de Física Teórica
Tese de Doutorado

Nei Lopes da Silva Júnior

Effects of quantum and thermal fluctuations in systems with multiple competing scalar orders

Rio de Janeiro
2020

"EFFECTS OF QUANTUM AND THERMAL FLUCTUATIONS IN SYSTEMS WITH MULTIPLE COMPETING SCALAR ORDERS"

NEI LOPES DA SILVA JUNIOR

Tese de Doutorado em Física apresentada no Centro Brasileiro de Pesquisas Físicas do Ministério da Ciência Tecnologia e Inovação. Fazendo parte da banca examinadora os seguintes professores:

Mucio Amado Continentino – Presidente/Orientador/CBPF

Daniel Gustavo Barci – Coorientador/UERJ

Héron Carlos de Godoy Caldas - UFSJ

Rudnei de Oliveira Ramos – UERJ

George Balster Martins - UFU

Tobias Micklitz – CBPF

Rio de Janeiro, 25 de agosto de 2020.

DEDICATÓRIA

À minha família, em especial à minha mãe Nair Oliveira da Silva.

AGRADECIMENTOS

Agradeço a Deus por esta oportunidade.

À minha família pelo apoio e incentivo.

À Vivian e sua família.

Aos amigos, pelo apoio e suporte tanto nos momentos alegres quanto nos difíceis dessa jornada.

Ao Barci e a Zochil pela confiança.

Ao Programa de Pós-Graduação em Física do CBPF por esta oportunidade.

Ao professor Mucio, meu orientador, pela competência, paciência, preocupação e simplicidade.

Ao professor Barci, meu coorientador, pela competência, paciência, preocupação e simplicidade.

Aos professores que contribuíram nesta caminhada.

Aos colaboradores, os quais contribuíram para a minha formação acadêmica.

À agência de fomento (CNPq) pelo auxílio financeiro durante o período da pós-graduação (Doutorado).

A todos que contribuíram direta ou indiretamente para que este momento fosse possível.

...

“A mente que se abre para uma nova ideia jamais voltará ao seu tamanho original.”

Albert Einstein

“A leitura engrandece a alma.”

Voltaire

“Treine enquanto eles dormem, estude enquanto eles se divertem, persista enquanto eles descansam, e então, viva o que eles sonham.”

Provérbio Japonês

RESUMO

LOPES, NEI. *Efeitos de flutuações quânticas e térmicas em sistemas com múltiplas ordens escalares competivivas.* 2020. 127 f. Tese (Doutorado em Física). Centro Brasileiro de Pesquisas Físicas, Rio de Janeiro, 2020.

Nós calculamos as flutuações quânticas e térmicas sobre os diagramas de fases dos sistemas exibindo múltiplas ordens escalares competitivas usando a aproximação de um *loop* para o potencial efetivo da teoria quântica de campos. Nós consideramos diferentes tipos de acoplamentos entre os parâmetros de ordem, incluindo o bilinear, em duas situações distintas: regiões do diagrama de fases onde existe um ponto bicrítico, no qual ambas as fases são suprimidas continuamente, e o caso onde ambas as fases coexistem homegeneamente. Nós investigamos sistemas bidimensionais e tridimensionais com expoentes críticos dinâmicos $z = 1$ e $z = 2$. Nossos resultados indicam que os efeitos das flutuações quânticas dependem fortemente da simetria, dimensionalidade e dinâmica dos possíveis estados ordenados. Por outro lado, as flutuações térmicas apresentam características similares em todos os casos, levando a uma transição de fase de primeira ordem fraca em temperatura finita, na qual as fases de coexistência oriundas das flutuações quânticas tornam-se instáveis. Nós também mostramos que acima da temperatura crítica (T_c) o sistema apresenta um comportamento de escala consistente com aquele aproximando-se de um ponto crítico quântico. Abaixo da transição o calor específico possui uma contribuição ativada termicamente com o *gap* associado ao tamanho dos domínios da fase ordenada. Nós obtemos que T_c decresce como função da distância ao ponto bicrítico clássico em temperatura nula (PBCTN) na região de coexistência, implicando que na nossa abordagem, o sistema atinge a mais alta T_c acima do PBCTN.

Palavras-chave: Transições de fase. Flutuações quânticas e térmicas. Ordens escalares competitivas. Potencial efetivo.

ABSTRACT

LOPES, NEI. *Effects of quantum and thermal fluctuations in systems with multiple competing scalar orders*. 2020. 127 f. Dissertation (Doctorate in physics). Brazilian center for research in physics, Rio de Janeiro, 2020.

We compute quantum and thermal fluctuations on the phase diagram of systems with multiple competing scalar orders using the *one-loop* effective potential approximation from quantum field theory. We consider different types of couplings between the order parameters, including a bilinear one, in two distinct scenarios: regions of the phase diagram where there is a bicritical point, whereupon both phases vanish continuously, and the case where both phases coexist homogeneously. We investigate two and three-dimensional systems with $z = 1$ as well as $z = 2$. Our results indicate that quantum fluctuations strongly depend on the symmetry, dimensionality and dynamics of the possible ordered states. On the other hand, thermal fluctuations exhibit some common features leading to weak first-order temperature phase transitions, at which coexisting phases arising from quantum corrections become unstable. We show that above the critical temperature (T_c) the system presents scaling behavior consistent with that approaching a quantum critical point. Below the transition the specific heat has a thermally activated contribution with a gap related to the size of the domains of the ordered phases. We obtain that T_c decreases as a function of the distance to the zero-temperature classical bicritical point (ZTCBP) in the coexistence region, implying that in our approach, the system attains the highest T_c above the fine tuned value of this ZTCBP.

Keywords: Phase transitions. Quantum and thermal fluctuations. Multiple competing scalar orders. One-loop effective potential.

LIST OF ILLUSTRATIONS

LIST OF ABBREVIATIONS AND ACRONYMS

SCES	*Strongly correlated electronic systems*
CMP	*Condensed matter physics*
FM	*Ferromagnetism/Ferromagnet*
SDW	*Spin density wave*
MI	*Mott insulator*
CDW	*Charge density wave*
QPT	*Quantum phase transition*
Yb	*Ytterbium*
Ce	*Cerium*
U	*Uranium*
RKKY	*Ruderman-Kittel-Kasuya-Yosida*
QCP	*Quantum critical point*
AFM	*Antiferromagnetic/Antiferromagnet*
SC	*Superconductor/Superconductivity*
MF	*Mean-field*
QFT	*Quantum field theory*
PM	*Paramagnetism/Paramagnetic*
SSB	*Spontaneous symmetry breaking*
RPA	*Random phase approximation*
He	*Helium*
ZTCBP	*Zero-temperature classical bicritical point*
ZTCCP	*Zero-temperature classical critical point*

LIST OF SYMBOLS

T_c	*Critical temperature*
t	*Reduced temperature*
C	*Specific heat*
χ	*Susceptibility*
ϕ, φ_i	*Order parameter(s)*
H	*Magnetic field*
ξ	*Correlation length*
C_F	*Correlation function*
$\mathcal{F} = F/V$	*Landau's free energy density/Landau's functional*
M	*Magnetization*
k_B	*Boltzmann constant*
$\hbar$	*Planck constant*
τ_ξ	*Characteristic time*
z	*Dynamic critical exponent*
k	*Wave-vector*
b	*Scaling factor*
L	*Linear dimension*
$f(q, p)$	*Scaling function*
f_s	*Singular part of the ground state energy density*
$d_{eff} = d + z$	*Effective dimension*
d_L	*Lower critical dimension*
d_c	*Upper critical dimension*
S	*Action*
Z	*Functional generator*
j	*External source*
W	*Connected Green function*
Γ	*Effective action*
Λ	*Cut-off*
ω_n	*Matsubara frequency*

PUBLICATIONS DURING THE PhD

Publications related to this dissertation:

1. N.L. Silva Jr, Mucio A. Continentino, Daniel G. Barci. Quantum corrections for the phase diagram of systems with competing order. Journal of Physics: Condensed Matter **30** 225402 (2018);

2. Nei Lopes, Mucio A. Continentino, Daniel G. Barci. One-loop effective potential for two-dimensional competing scalar order parameters. Physics Letters A **384**, 126095 (2020);

3. Nei Lopes, Daniel G. Barci, Mucio A. Continentino. Finite temperature effects in quantum systems with competing scalar orders. Journal of Physics: Condensed Matter **32** 415601 (2020).

Collaborative publications:

1. Daniel Reyes, Nei Lopes, Mucio A. Continentino, Christopher Thomas. Influence of the symmetry of hybridization on the critical temperature of multiband superconductors. Physical Review B **99**, 224514 (2019);

2. S. Rufo, Nei Lopes, Mucio A. Continentino, Griffith M. A. R.. Multicritical behavior in topological phase transitions. Physical Review B **100**, 195432 (2019);

3. Nei Lopes, A.V. Andrade-Neto. Emergence of a non-Fowler-Nordheim-type behavior for a general planar tunneling barrier. Physics Letters A **384**, 126399 (2020).

CONTENTS

INTRODUCTION

The study of strongly correlated electronic systems (SCES) constitute a modern and exciting research area in condensed matter physics (CMP). It deals with interesting problems that arise due to interactions between electrons, also known as emergent phenomena. Currently, it is well-accepted that electronic interactions may give rise to different types of ground states in SCES at low temperatures. For instance, one can experimentally observe the most diverse phases, such as, ferromagnetism (FM), spin density wave (SDW), Mott insulator (MI), unconventional superconductivity, heavy Fermi-liquid and charge density wave (CDW) [1, 2] as a function of some fine tuned external control parameter, such as, pressure, doping or magnetic field [3, 4].

In general, SCES are very sensitive to small changes in external control parameters [2, 3] and it has been reported that these low temperature systems can sustain different ground states even for the same values of external parameters [5, 6, 7, 8, 9, 10, 11, 12, 13, 14, 15, 16, 17, 18, 19], which may lead to a competition between different orderings and eventually to coexistence.

Therefore, competing/coexisting orders are a common feature in most SCES [5, 6, 7, 8, 9, 10, 11, 12, 13, 14, 15, 16, 17, 18, 19]. They produce very rich experimental phase diagrams in terms of these well-controlled external parameters, which allow us to study these materials as they transit through a quantum phase transition (QPT) [3, 4], i.e., a transition at *zero-temperature*, between different ground states as the external parameter is varied.

Among the SCES one can point out a very interesting class, called heavy fermions materials, that comprises inter-metallic compounds containing unstable f-shell elements, as *Ytterbium* (Yb), *Cerium* (Ce) and *Uranium* (U). Since the f-ions are displayed on the sites of a lattice, these compounds have lattice translation invariance and ideally their resistivity should vanish as temperature approaches zero [2, 4, 20, 21]. The physical properties of these systems are a direct result of the competition between Kondo effect and Ruderman–Kittel–Kasuya–Yosida (RKKY) interactions, with the former favoring the formation of a non-magnetic ground state [22, 23]. At *zero-temperature*, there is a quantum critical point (QCP) separating a magnetic phase from a heavy Fermi-liquid state [3, 4]. On the other hand, at finite temperatures, in the magnetic side of the phase diagram, there is a line of magnetic transitions, in general antiferromagnetic (AFM), that vanishes at the QCP [4, 20, 21, 22], see Fig. 1. Moreover, U and Ce-based heavy fermions materials [20, 21, 23] can also present an exotic behavior at very low temperatures, where experiments have been reported that they can exhibit superconductivity (SC) near or in coexistence with an AFM phase close to the magnetic QCP [24], see Fig. 2 (a) and Fig. 2 (b).

Figure 1 - Doniach phase diagram

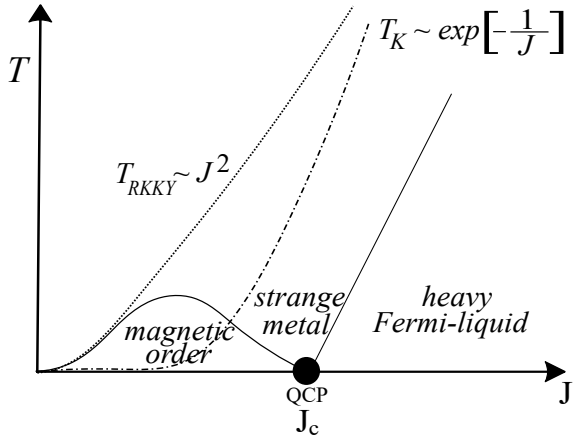

Legend: Doniach phase diagram of the Kondo lattice model Hamiltonian showing the competition between Kondo effect and RKKY interactions.

Source: Refs. [20, 22]. Adapted by the author.

There are also other important systems exhibiting unusual behavior at low temperatures. The most prominent are those presenting exotic types of competing/coexisting orderings. For example, some pnictides [12, 25, 26, 27, 28, 29], such as, $LaFeAs(O_{1-x}F_x)$, $PrFeAs(O_{1-x}F_x)$, $(Sr_{1-x}Na_x)Fe_2As_2$, $Ba(Fe_{1-x}Co_x)_2As_2$ and $(Ba_{1-x}K_x)Fe_2As_2$, exhibit competing AFM-SC order separated by a first-order phase transition and can only coexist in phase-separated macroscopic regions of the sample [5, 30, 31, 32, 33], see Fig. 2 (c). In addition, one can also find SC-AFM-Structural orders [30, 31] or even unconventional coexistence between magnetic and SC orders in some iron-based compounds [12], see Fig. 2 (d). For usual metals, it has been reported non-Fermi-liquid behavior points to the existence of underlying QCPs (see Fig. 1) and there is also the possibility of *zero-temperature* first-order transitions [24, 34, 35, 36], which are associated with the instability of the QCPs. Last but not least, magnetism and SC are also in close proximity in cuprates [8].

All of these experimental findings are in contrast with the expected behavior for conventional SC, since magnetism and SC are usually competing phenomena [8], which justifies the fact that there is a lot of ongoing efforts to understand this kind of eccentric behavior. In other words, the study of the phase diagrams of SCES with competing/coexistence orders is one of the most fundamental issues in CMP that have not yet been clarified.

Nevertheless, competing orders can be traced back to the existence of competing states with different symmetries in the ground state of the system. The usual approach to describe the mean-field (MF) phase diagram of these systems near quantum criticality, i.e., close to the QCPs, is the Landau expansion of free energy density in terms of

Figure 2 - Experimental competing/coexistence phase diagrams

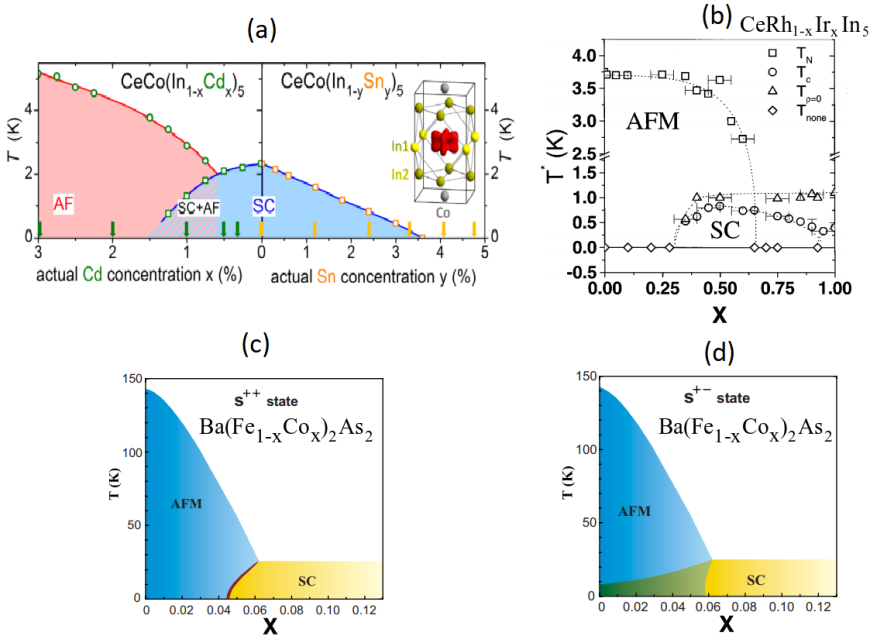

Legend: (Color online) (a,b) Experimental (c,d) Theoretical phase diagrams exhibiting competing/coexistence regions as a function of temperature and doping.

Source: (a) Ref. [9], (b) Ref. [8], (c) Ref. [5], (d) Ref. [5]. Adapted by the author.

order parameters [37]. At a microscopic level, the global phase diagram can be obtained by means of MF approximations of simplified model Hamiltonians. These procedures correctly capture those qualitative properties of the phase diagram that depend on the symmetry of the problem. For instance, in the case of two competing orders, time-reversal invariance leads to consider only quartic couplings for different fields. Examples are quadrupolar [5, 38] and spin nematic [39, 40] orderings. In general, symmetry precludes a bilinear coupling that, however, is allowed if the two order parameters transform according to the same irreducible group representation [41, 42]. In fact, this type of coupling is important to describe SDW [43, 44], orbital AFM orders [45, 46], elastic instabilities of the atomic crystal lattice [47], vortices in a multigap SC [48] and magnetic properties of the heavy fermion compound URu_2Si_2 [41].

On the other hand, quantum fluctuations may play an important role at very low temperatures. A direct consequence is that not only the symmetry, but also dynamic and dimensionality of the systems become relevant ingredients to determine the global topology of the phase diagram [3, 4]. In these cases, Landau's approach is no longer suitable.

Even in systems with a single type of order, instabilities on the phase diagram may arise due to the coupling of the order parameter to other excitations, not necessarily associated with a symmetry breaking. For example, materials as SCs with charged exci-

tations can couple to the fluctuations of the electromagnetic field [4]. Moreover, magnetic materials can couple to elastic excitations [49] and in metallic FMs the magnetization can couple to electron-hole excitations of the Fermi-liquid [34, 35, 36, 50]. In many cases the effect of these couplings is to change the order of the transition associated with the relevant order parameter and this might occur even at *zero-temperature* [34, 35, 36, 50].

In this dissertation we study the effects of quantum and thermal fluctuations on the MF phase diagrams of systems exhibiting multiple competing scalar orders for both two (2d) and three-dimensional (3d) materials. We investigate two different types of couplings, i.e., a conventional quartic and a bilinear one, whenever it is allowed by symmetry. We are interested in the case of a bicritical point where both phases vanish continuously, and that where there is a region of coexistence between the different types of ordering in the ground state. We consider the quantum dynamics of the critical modes of the competing phases by propagators associated with dynamic critical exponents $z = 1$ as well as $z = 2$ [24, 51, 52, 53]. The former can be related to the case of interacting magnetic excitons and systems characterized by linear dispersion relations, whereas the latter is normally associated with paramagnons in itinerant AFM and FM or dissipative modes in SC systems near their respective QCPs, or equivalently, systems with quadratic dispersion relations [24, 51, 52, 53].

Initially, we apply the *one-loop* effective potential approximation from quantum field theory (QFT) [24, 54, 55, 56] to obtain the quantum corrections to the classical action. We focus on a region close to the QCPs, such that, their order parameters are small and allow a Landau-type expansion of the free energy density. In general, we expect that lower dimensionalities enhance the effect of quantum fluctuations. Therefore, our initial goal is to obtain quantum corrections and verify how they modify the MF predictions. Next, in order to make the connection with experiments, we include the effects of thermal fluctuations on the effective potential through Matsubara's summation formalism [56, 57, 58, 59, 60].

We show the crucial role of considering both quantum and thermal fluctuations on the MF phase diagrams of systems with competing scalar order parameters [61, 62, 63]. The effect of quantum corrections is essential to understand the emergence of stable unconventional coexisting orders experimentally observed in SCES. Our results explicitly indicate how symmetry, dynamic and dimensionality determine the nature of the phase diagrams [61, 62]. On the other hand, thermal fluctuations lead to weak first-order temperature phase transitions, at which coexisting phases arising from quantum corrections become unstable. We also obtain thermodynamic signatures for the free energy and specific heat that might be expect in this kind of systems with multiple competing scalar orders [63].

It is worth to emphasize that the interplay between thermal and quantum fluctuations give rise to interesting effects and may provides clear predictions for the expected

behavior of these systems [63]. This brings our results to the level of a testable theory.

This dissertation is organized as follows: in chapter 1 we present classical and quantum phase transitions emphasizing the main differences between them. We discuss the requirements to the emergence of different states of matter and the description of critical phenomena through scaling theory. Then, we introduce Landau's theory for phase transitions and apply it to the well-known paramagnetic-ferromagnetic transition in order to obtain its critical exponents. Thereafter, we extend Landau's approach and the concepts of scaling theory to QPTs. In chapter 2 we present the method that will be widely used to obtain quantum and thermal fluctuations on the MF phase diagrams in this dissertation, i.e., the *one-loop* approximation from QFT. We explore some examples to make the reader more familiar with its *modus operandi*. In chapter 3 we investigate Landau's expansion for multiple competing scalar orders interacting through two different types of couplings, including an unusual bilinear one. We present the possible MF phase diagrams depending on the values of Landau's parameters. In chapter 4 we obtain the *one-loop* effective potential for multiple competing scalar orders and discuss the quantum corrections on the *zero-temperature* MF phase diagrams of systems with competing scalar orders for both 2d and 3d systems characterized by dynamic critical exponents $z = 1$ and $z = 2$. In chapter 5 we include finite temperature effects on the *one-loop* effective potential of the systems previously studied to make the link with experiments. Finally, we summarize and point out our main results.

1 CLASSICAL AND QUANTUM PHASE TRANSITIONS

In this chapter we will describe one of the most successful approaches in condensed matter and statistical physics to investigate phase transitions, that is, the conditions to the emergence of different states of matter. We will present Landau's theory for phase transitions [3, 4, 37, 64] following closely refs. [37, 64], which, from our point of view, present a very detailed and instructive way. This approach will be applied as a starting point to our problem with multiple competing scalar order parameters later.

We will point out the success and applicability of Landau's theory to find the critical behavior of the systems, i.e., to obtain its phase diagrams as well as the critical exponents [3, 4, 37, 64] that characterize distinct classes of universality for the phase transitions through the well-known paramagnetic-ferromagnetic transition [4, 37, 64].

Finally, we will extend Landau's theory to QPTs emphasizing the main differences between classical and quantum phase transitions. We will show both its peculiarities and its importance for understanding physical properties of SCES at *zero-temperature*.

1.1 Introduction

The term phase transition is commonly used to describe a system whereupon its physical properties undergo an abrupt change depending on the external parameters, such as, pressure (P) and temperature (T). We are all accustomed in our daily lives to the water phase transitions depending on the temperature and pressure at which it is found, i.e., transitions between solid (ice), liquid (water), and gaseous (gas) states of matter, see Fig. 3. However, when different materials or substances are under special conditions, that is, for very high or low temperatures, exotic states of matter may emerge, such as, plasma and SC states, respectively.

Fig. 3 shows the phase diagram of water as it goes from solid to liquid (melting point) at 0^o C and 101 kPa or changes from liquid to gas (boiling point) at 100^o C and 101 kPa. At the triple point the three phases coexist and at the critical point we find a supercritical fluid. In other words, during a phase transition of a given *medium* certain properties change, often discontinuously, as a result of the variation of external conditions, such as, temperature, pressure, or others. Therefore, in summary, as its name suggests, a phase transition is intrinsically associated with a change of phase.

Phase transitions often occur in nature and are very exciting and ongoing research topics since its principles are widely applied in many actual technologies. For example, the most prominent application related to the metal-superconductor transition are electricity generators, transmission cables, magnetic resonance and Maglevs [65].

Figure 3 - Phase diagram of water

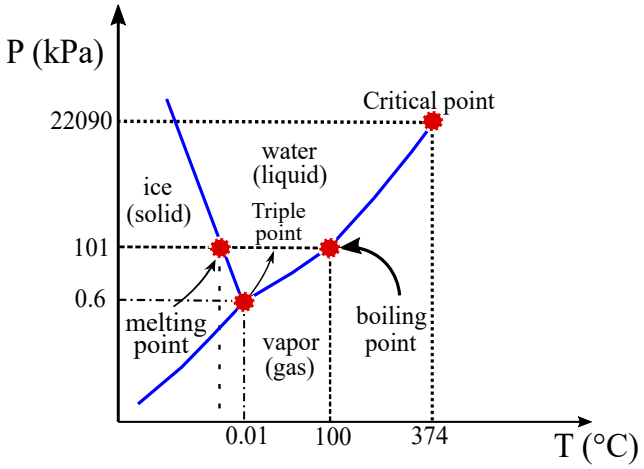

Legend: (Color online) Phase diagram showing the different states of matter for water depending on the temperature (T) and pressure (P).

Source: The author, 2020.

1.2 **Classical phase transitions**

Paul Ehrenfest (1880-1933), an Austrian physicist and mathematician, proposed that phase transitions could be classified based on the behavior of free energy as a function of thermodynamic variables. Within this scheme, phase transitions were labeled by the lowest derivative from free energy that is discontinuous at the transition, i.e., the n^{th} order if any n^{th} derivative of free energy with respect to any of its arguments yields a discontinuity at the phase transition [66]. For instance, first-order phase transitions exhibit a discontinuity in the first derivative of free energy with respect to some thermodynamic variable, and so on so forth.

The solid/liquid/gas water transitions, discussed previously, are classified as first-order transitions since they present a discontinuous change in density, which is the (inverse of the) first derivative of free energy with respect to pressure. Accordingly, second-order phase transitions are continuous in the first derivative but exhibit a discontinuity in the second derivative of free energy. These kind of transitions include paramagnetic-ferromagnetic transition in materials such as iron, where the magnetization, which is the first derivative of free energy with respect to the applied magnetic field, increases continuously from zero as temperature is lowered below the Curie temperature. However, the magnetic susceptibility, i.e., the second derivative of free energy with respect to the field, changes discontinuously [4, 37, 64].

Therefore, within Ehrenfest picture, there could be, in principle, third, fourth, and even higher-order phase transitions. However, this classification has been replaced by

a modern classification scheme whereupon phase transitions are divided into two broad categories [4, 37, 64], named similarly to Ehrenfest classes, that is, first and second-order phase transitions. The former are those that involve a latent heat and sometimes are called discontinuous one. Furthermore, in this kind of transitions one can observe coexistence of different phases since the correlation length (ξ) of the system does not diverge at the transition point. Familiar examples are the melting of ice or boiling of water, wherein the water does not instantly turn into vapor, but forms a turbulent mixture of liquid water and vapor bubbles, that is, the presence of coexistence of phases. The latter, i.e., second-order phase transitions, also called continuous one, in opposite to first-order transitions, are characterized by a divergent susceptibility, an infinite correlation length, and a power law decay of correlations near criticality [4]. Examples of continuous phase transitions are ferromagnetic, superconducting and superfluid transitions [4, 37, 59, 64, 68].

As we have discussed, Landau's approach for phase transitions is widely applied to obtain the phase diagrams as well as to describe them. The main features of classical phase transitions are related to thermal effects, i.e., with the thermodynamics. So, it is worth to emphasize that an abrupt change in the properties of the systems are intrinsically associated with a transition temperature, also known as critical temperature (T_c). Therefore, close to T_c, we describe the critical behavior of physical quantities of the system through asymptotic behaviors as a function of a thermal variable defined in the form [4, 37, 64, 67],

$$t = \frac{T - T_c}{T_c} \tag{1}$$

where t is a dimensionless variable called reduced temperature.

The thermodynamic properties of the systems that can be experimentally measured are described by a critical behavior. For instance, specific heat (C) and susceptibility (χ) may exhibit its dependence as follows [4, 37, 64, 67],

$$C \propto |t|^{-\alpha} \tag{2}$$

and

$$\chi \propto |t|^{-\gamma} \tag{3}$$

In many cases we also define a generic parameter, known as order parameter (ϕ) [3, 4, 5, 37, 40, 41, 64, 67], in order to characterize the transitions, which its detailed description will be presented later on. We know that the critical behavior of the order parameter may be expected as [3, 4, 37, 64, 67],

$$\phi \propto t^{\beta} \tag{4}$$

In the presence of external fields we are still interested in the critical behavior of ϕ in

relation to the conjugated field at the critical isotherm, which is given by [3, 4, 37, 64, 67],

$$\phi(H, t = 0) \propto H^{1/\delta} \tag{5}$$

where H is the external field.

Note from Eq. (2), Eq. (3), Eq. (4) and Eq. (5) that the critical behavior of the systems when it undergo a phase transition can be directly determined by the exponents in the relations above, i.e., α, γ, β and δ, also known as critical exponents. It is worth to point out that there are more two critical exponents that will be discussed below. Moreover, these exponents are not independent and are related to each other due to some inequalities that arises from thermodynamics [4, 37], i.e.,

- Rushbrooke Inequality,

$$\alpha + 2\beta + \gamma \geq 2 \tag{6}$$

- Griffiths first inequality,

$$\alpha + \beta(1 + \delta) \geq 2 \tag{7}$$

- Griffiths second inequality,

$$\gamma \geq \beta(\delta - 1) \tag{8}$$

- Fisher Inequality,

$$\gamma \geq (2 - \eta)\nu \tag{9}$$

- Josephson Inequality,

$$d\nu \geq 2 - \alpha \tag{10}$$

In the last two inequalities d is the dimension of the system and the critical exponents ν and η are exponents related to the critical behavior of two important quantities. They are respectively,

- Correlation length:

$$\xi \propto |t|^{-\nu} \tag{11}$$

- Correlation function: $C_F(\vec{r}) = \langle \Phi(\vec{r})\Phi(0) \rangle - \langle \Phi(0) \rangle^2$

$$C_F(\vec{r}) \propto \frac{1}{r^{d-2+\eta}} \tag{12}$$

It is important to observe that at the criticality ($t = 0$) these inequalities between critical exponents are satisfied as equalities and are known as scaling laws, which define the critical behavior of systems that undergo a phase transition [37].

Another interesting point is the universality class that emerges from the critical exponents, that is, several models that, at first view, appear to be very different may have

identical critical behaviors, which implies the same value of critical exponents [4, 37]. However, the position of the critical point and the amplitudes associated with scaling forms are, in general, non-universal and depend on the microscopic properties of each model.

1.3 **Landau's theory for phase transitions - *Mean-field* approach**

Now we discuss in details the main aspects within Landau's approach for phase transitions [3, 4, 37, 64], a phenomenological theory that arises from an idea of enormous simplicity but that involves a great physical intuition about phase transitions. From its description we will see how it is possible to extract some crucial information about phase transitions, and consequently build the phase diagrams at MF level, or equivalently, at *classical* level. The focus of this section will be to make the reader familiar with Landau's theory, which will be used later as our starting point.

Landau's theory for phase transitions was developed by the Russian physicist Lev Davidovich Landau (1908-1968) in the year 1930 to describe continuous transitions, i.e., second-order phase transitions. This theory is based on a general argument related to symmetry and well-behaved physical properties (analyticity) of the systems [68]. It is also known as phenomenological Landau theory.

Its main assumption/postulate [37] is that one can write down a function $\mathcal{F} = F/V$ known as Landau free energy density, or equivalently, the Landau functional, which depends on both coupling constants (K_i) and order parameters (ϕ_i). The latter is assumed to be small, so that $\mathcal{F}$ can be expanded to its lowest powers. For that, the system must be close to the transition point.

The order parameter ϕ is, in principle, entirely generic and its form will depend on the symmetry of the systems of interest, i.e., it can be a scalar, vector, tensor, etc. The crucial requirement about the behavior of ϕ is that its value may be defined so that in the disordered state it presents a zero value, whereas in the ordered state its value is non-zero. This kind of behavior provides a clear way to identify different phases of matter, i.e., a phase transition that may emerge in the systems. In other words, one can see that above T_c the system will be in the disordered phase ($\phi = 0$), otherwise $\phi \neq 0$. Hence,

$$\phi = \begin{cases} 0, & T > T_c \\ \neq 0, & T < T_c \end{cases} \tag{13}$$

In addition, it is assumed that $\mathcal{F}$ has the property that the state of the system is specified by its global *minimum* with respect to ϕ. In other words, the state of the system will be described by the value of ϕ that presents the minimal energy. We also assume

that thermodynamic state functions may be computed by differentiating $\mathcal{F}$ with respect to the order parameter(s).

Thus, in order to identify the explicit form of $\mathcal{F}$, it is sufficient to use the following constraints listed below on $\mathcal{F}$ [37],

1. $\mathcal{F}$ has to be consistent with the symmetries of the system;

2. Near T_c, $\mathcal{F}$ can be expanded in a Taylor-type power series in ϕ, i.e., $\mathcal{F}$ is assumed to be an analytic function of both ϕ and K_i, which means that the value of ϕ close to the transition point is small. Therefore, in a spatially dependent system of volume V, one can express $\mathcal{F}$ as follows,

$$\mathcal{F} = \frac{F}{V} = \sum_{n=0}^{\infty} a_n([K], T)\phi^n(\vec{r}) \tag{14}$$

   where a_n are Landau's phenomenological coefficients.

3. In an inhomogeneous system with a spatially varying order parameter profile ($\phi(\vec{r})$), $\mathcal{F}$ is a local function, i.e., it dependes only on $\phi(\vec{r})$ and a finite number of derivatives;

4. In the disordered phase of the system, the order parameter $\phi = 0$, whilst it is small and non-zero in the ordered phase, near to the transition point.

As stated before, for $T > T_c$, $\phi = 0$ solves the *minimum* equation for $\mathcal{F}$, whereas for $T < T_c$, $\phi \neq 0$ solves the *minimum* equation. So, for a homogeneous system, one can rewrite Eq. (14) as follows,

$$\mathcal{F} = \sum_{n=0}^{\infty} a_n([K], T)\phi^n \tag{15}$$

where we expand $\mathcal{F}$ up to $\mathcal{O}(\phi^4)$ since ϕ is assumed to be small.

We expect that all the essential physics near T_c may be encoded up to this order and, in general, this procedure is sufficient. However, whether or not the truncation of the power series for $\mathcal{F}$ is valid will turn out to depend on both dimensionality of the system and co-dimension of the singular point of interest [37].

1.3.1 Construction of $\mathcal{F}$

Once we know the assumptions/constraints associated with $\mathcal{F}$, we can build its explicit form. Let us firstly use both first and second constraints. Therefore, we perform a Taylor-type series expansion in ϕ [3, 4, 37, 64], i.e.,

$$\mathcal{F} = a_0 + a_1\phi + a_2\phi^2 + a_3\phi^3 + a_4\phi^4 + \dots \tag{16}$$

where we have truncated it up to $\mathcal{O}(\phi^4)$, as discussed previously.

Minimizing $\mathcal{F}$ in Eq. (16) with respect to ϕ, we get,

$$\frac{\partial \mathcal{F}}{\partial \phi} = a_1 + 2a_2\phi + 3a_3\phi^2 + 4a_4\phi^3 = 0 \tag{17}$$

Note that for $T > T_c$, the solution that minimizes $\mathcal{F}$ in Eq. (17) is given by $\phi = 0$ since we are in the disordered region. Hence, by construction, $a_1 = 0$.

Without loss of generality, throughout this section we only consider scalar systems characterized by a Z_2-type symmetry, i.e., Ising-like, which is associated to the symmetry of the system, or equivalently, to the first constraint. This is best seen through an example, as we will discuss below.

1.3.2 Example: Paramagnetic-Ferromagnetic transition

It is well-know that for paramagnetic-ferromagnetic (PM-FM) transition the order parameter is given by the magnetization (M) [4, 37, 64], i.e., $\phi = M$. Note that this choice satisfies all required conditions to the behavior of an order parameter, that is, when $T > T_c$, $M = 0$, otherwise $M \neq 0$. If we consider an Ising-like system at zero external magnetic field, i.e., $H = 0$, then the probability distribution P for ϕ is even in a finite system, that is, $P(\phi) = P(-\phi)$. So, from $\mathcal{F}$ in Eq. (16) we get,

$$a_3 = a_5 = a_7 = ... = 0 \tag{18}$$

where we already know that $a_1 = 0$ from Eq. (17).

Therefore, for PM-FM transition, $\mathcal{F}$ only supports, by symmetry arguments, even terms in Taylor-type series expansion and thus $\mathcal{F}$ can be written as follows [4, 37, 64],

$$\mathcal{F} = a_0([K], T) + a_2([K], T)\phi^2 + a_4([K], T)\phi^4 \tag{19}$$

The requirement that $\mathcal{F}$ be analytical in ϕ also precludes terms like $|\phi|$ in Eq. (19). In addition, one can identify that $a_0([K], T)$ in Eq. (19) is simply the value of $\mathcal{F}$ at high temperatures, i.e., for disordered phase, and we expect it to vary smoothly trough T_c. It represents the degrees of freedom of the system which are not described by the order parameter, and so may be thought of as the smooth background whereupon the singular behavior is superimposed [37]. Without loss of generality, from now on, we take $a_0 = 0$ all along this dissertation.

The coefficient $a_4([K], T)$ in Eq. (19) is assumed to be positive, otherwise $\mathcal{F}$ can be minimized by $|\phi| \to \infty$, whereas we wish to describe how the order parameter rises from zero and has a finite value as coupling constants are varied through the transition

point. In other words, $a_4([K], T)$ is taken positive to make the theory stable.

For the Ising Ferromagnet at $H = 0$, we now ask the form of $a_n([K], T)$. So, expanding a_4 in temperature near T_c we obtain,

$$a_4 = a_4^0 + (T - T_c)a_4^1 + \mathcal{O}((T - T_c)^2) \tag{20}$$

As we have discussed before, it will be sufficient just take $a_4 = a_4^0$ as a positive constant in Eq. (20). Analogously, we expand a_2 as follows,

$$a_2 = a_2^0 + \frac{(T - T_c)}{T_c}a_2^1 + \mathcal{O}((T - T_c)^2) \tag{21}$$

One can determine the form of a_2 using the fact that there is a T_c that give rise to a non-zero value to the order parameter, which will encode crucial information associated with ϕ. In other words, in opposite to a_4, one can clearly see that the leading term for a_2 in Eq. (21) is the temperature dependent one (a_2^1), which satisfies,

$$\phi = \begin{cases} 0, & T > T_c; \\ \neq 0, & T < T_c. \end{cases} \tag{22}$$

Minimizing Eq. (19) we obtain two solutions for ϕ,

$$\phi = 0 \quad \texttt{or} \quad \phi = \sqrt{\frac{-a_2(T)}{2a_4}} \tag{23}$$

Note that if ϕ is to be non-zero when $T < T_c$, then,

$$a_2^0 = 0 \quad \texttt{and} \quad a_2 = a_2^1\left(\frac{T - T_c}{T_c}\right) \tag{24}$$

where we emphasize that the higher order terms in Eq. (21) do not contribute to the leading behavior near T_c, i.e., all the essential physics will be encoded at the linear order temperature dependent term [37].

Let us now extended this treatment for $H \neq 0$, that is, in the presence of an external magnetic field. We already know that $\phi = M$, and the appropriate energy contribution term for $H \neq 0$ in this case is given by $-H\sum_i S_i = -HNM$ [37]. Therefore, we obtain $\mathcal{F}$ to describe the FM-PM transition as follows [4, 37, 64],

$$\mathcal{F} = at\phi^2 + \frac{1}{2}b\phi^4 - H\phi \tag{25}$$

where $t = (T - T_c)/T_c$, $a = a_2^1$, $\frac{1}{2}b = a_4$, and $F = V\mathcal{F} = N\mathcal{F}$ for lattice systems.

The coefficients a and b in Eq. (25) are phenomenological parameters, which, in

Figure 4 - Landau free energy density for several values of T and H

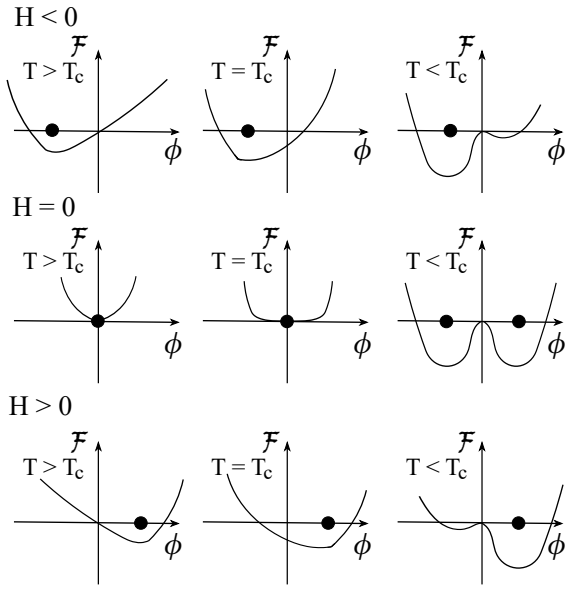

Legend: Different schematic scenarios for $\mathcal{F}$ considering several values of T and H. The • indicates the value of ϕ at which $\mathcal{F}$ achieves its global *minimum*. Since $H \neq 0$ most of the graphs depicts a first-order transition, which occurs for $T < T_c$ as H varies from a negative to a positive value. The central row depicts the continuous transition, which occurs from $H = 0$ as T is varied from above T_c to below T_c.

Source: Ref. [37]. Adapted by the author.

essence, could be obtained from an appropriate microscopic theory. In principle, a term proportional to $H\phi^3$ is also allowed by symmetry arguments in Eq.(25) but this is not a leading term near criticality [37].

Here, we have only considered the PM-FM transition, but, in general, $\mathcal{F}$ may be constructed by writing down all possible terms which are powers and products of the order parameter components that are consistent with the symmetry requirements of the particular system of interest.

1.3.3 Continuous phase transitions

From Eq. (25) one can show how Landau's theory accounts the non-analytic behavior near and below T_c as well as how to identify if the phase transition is a discontinuous or continuous one. It is very helpful to sketch possible scenarios for $\mathcal{F}(\phi, H, T)$ from Eq. (25), as shown in Fig. 4.

In this section we focus on continuous transitions, which occur for $H = 0$, as shown in the central row of the graphs in Fig. 4. For $T > T_c$, the *minimum* of $\mathcal{F}$ is located at

the origin, i.e., $\phi = 0$. For $T = T_c$, $\mathcal{F}$ has zero curvature at $\phi = 0$, but $\phi = 0$ is still the global *minimum*. For $T < T_c$, two degenerate *minima* occur at $\phi = \pm\phi_s$. The value of ϕ_s depends on the temperature, i.e., $\phi_s = \phi_s(T)$, see Eq. (23).

Thus, one can conclude that for this kind of transitions, that is, second-order transitions, the order parameter is continuous along the transition, i.e., its value does not undergo any abruptly change. In other words, in continuous transitions the order parameter varies smoothly during the order-disorder transition [4, 37, 64].

1.3.4 Critical exponents in Landau's theory

As we have seen in section 1.3.3, the PM-FM transition is continuous for $H = 0$. Therefore, with the help of Eq. (25), taking $H = 0$, one can obtain the critical exponents that characterize this transition. The critical exponent β is found from the variation of ϕ as a function of t. From Eq. (25), we get $\phi_s(t) = (-at/b)^{1/2}$, for $t < 0$, which allow us to identify $\beta = 1/2$ [3, 4, 37, 64], see Eq. (4). One can also obtain other thermodynamic critical exponents as specific heat and magnetic susceptibility, which it will be calculated below.

Note that $\mathcal{F}$ may assume two different expressions as a function of temperature, i.e.,

$$\mathcal{F} = \begin{cases} 0, & t > 0; \\ -\frac{1}{2}\frac{a^2t^2}{b}, & t < 0 \end{cases} \tag{26}$$

Then, the specific heat at constant volume (C_V) can be computed directly from,

$$C_V = -T\left.\frac{\partial^2 \mathcal{F}}{\partial T^2}\right|_V = \begin{cases} 0, & T > T_c; \\ \frac{a^2}{bT_c}, & T < T_c \end{cases} \tag{27}$$

From Eq. (27) one can clearly see that there is no power law divergence for C_V and it exhibits a discontinuity at T_c. Also note that in the ordered phase C_V exhibits a constant value, i.e., temperature independent, which implies that $\alpha = 0$ [4, 37].

To compute the remaining thermodynamic critical exponents we need to include effects of an external magnetic field ($H \neq 0$). Therefore, differentiating $\mathcal{F}$, Eq. (25), with respect to ϕ we get the magnetic equation of state for small ϕ,

$$at\phi + b\phi^3 = \frac{1}{2}H \tag{28}$$

Note that on the critical isotherm, i.e., at $t = \frac{T - T_c}{T_c} = 0$, we obtain $H \propto \phi^3$, which implies that $\delta = 3$ [4, 37], see Eq. (5). Finally, the isothermal susceptibility (recall that

$\phi = M$) is obtained by differentiating Eq. (28) with respect to H,

$$\chi_T(H) \equiv \left.\frac{\partial \phi(H)}{\partial H}\right|_T = \frac{1}{2\left(at + 3b\phi^2(H)\right)} \tag{29}$$

where $\phi(H)$ is the solution of Eq. (28). We are interested in the response function at zero external field. For $t > 0$, $\phi = 0$ and $\chi_T = (2at)^{-1}$. For $t < 0$, $\phi^2 = -at/b$ and $\chi_T = (-4at)^{-1}$. Hence, $\gamma = 1$ for both cases [4, 37].

Thus, we have obtained some of the MF critical exponents discussed in section 1.2. In order to get the last two critical exponents describing spatial correlations, i.e., ν and η, we need to extend Landau's approach to deal with inhomogeneous systems, which is beyond of the scope of this dissertation.

1.3.5 First-order transitions

Until now we have applied Landau's theory to describe second-order phase transitions with the requirement that $\phi(t)$ is arbitrarily small close to T_c, or equivalently, for $t \to 0$. As we have discussed in PM-FM transition for $H = 0$, Landau's approach provides a description of a continuous transition. However, in this section we will consider a more general expression for $\mathcal{F}$.

In constructing $\mathcal{F}$ for the PM-FM transition, we already know that there cannot be a linear term in ϕ if the symmetric phase corresponds to $\phi = 0$. However, this restriction was only due to the symmetry of the problem that have prevented us from writing down a cubic term in ϕ on $\mathcal{F}$.

Thus, let us now examine the effect of such a term, by considering,

$$\mathcal{F} = at\phi^2 + \frac{1}{2}b\phi^4 + C\phi^3 - H\phi \tag{30}$$

where a and b are positive.

So, for $H = 0$, analogously to the previous section, the equilibrium value of ϕ is obtained by minimizing $\mathcal{F}$ in Eq. (30) with respect to ϕ. In this case we get,

$$\phi = 0 \quad \texttt{or} \quad \phi = -c \pm \sqrt{c^2 - at/b} \tag{31}$$

where we have defined $c \equiv 3C/4b$.

First, note that for $c = 0$ we recover the previous results, as expected. The solution for $\phi \neq 0$ only becomes physically suitable, i.e., real, not complex, for reduced

Figure 5 - Landau free energy density for first-order transitions

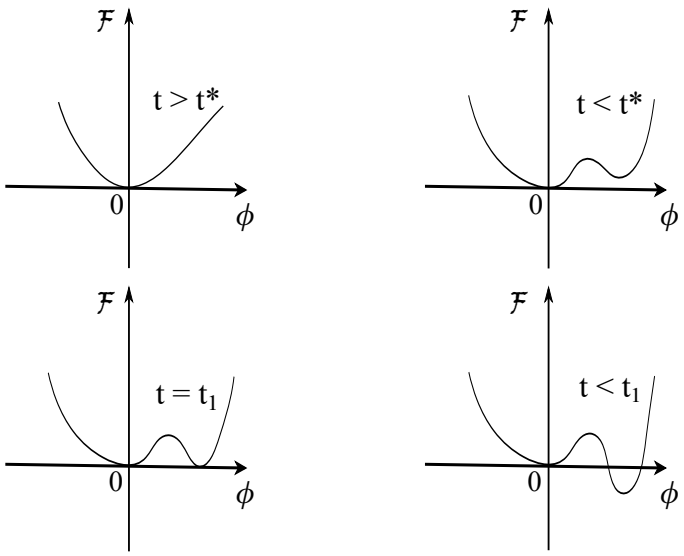

Legend: Schematic Landau free energy density from Eq. (30), taking $H = 0$, as a function of ϕ for various temperatures, exhibiting Landau's theory description of a first-order transition.

Source: Ref. [37]. Adapted by the author.

temperatures t satisfying the condition,

$$c^2 - \frac{at}{b} > 0 \tag{32}$$

i.e., for $t < t^* \equiv bc^2/a$.

Therefore, this condition occurs at a temperature higher than T_c since t^* is positive. Note that this situation is in contradiction with the description of a continuous transition, whereupon $\phi \neq 0$ only became acceptable for $t < 0$, i.e., $T < T_c$, see section 1.3.3. We can investigate it by sketching the different forms of $\mathcal{F}$ from Eq. (30), taking $H = 0$, as shown in Fig. 5.

For $t < t^*$, a secondary minimum and maximum have emerged in addition to the minimum at $\phi = 0$. So, since each minimum of $\mathcal{F}$ is associated with different phases, in this kind of transition we may expect to find one or more phases coexisting. As we reduce the temperature further to the value $t = t_1$, the value of $\mathcal{F}$ at the secondary minimum becomes the global minimum, and the value of ϕ that minimizes $\mathcal{F}$ jumps discontinuously from $\phi = 0$ to a non-zero value. This is defined as a first-order phase transition [4, 37, 64].

Note that at the first-order transition, $\phi(t_1)$ may not be arbitrarily small as $t \to t_1^-$, which means that, in principle, Landau's theory is not valid. Thus, if there is no symmetry reason that forces $C = 0$, then a cubic term will, in general, give rise to a first-order transition.

In more general situations, where ϕ has more that one component, then $\mathcal{F}$, a scalar, is constructed out by combinations of the components of ϕ that are invariants under the symmetries of the problem. Then, a sufficient, but not necessary condition for the existence of a continuous transition is that there are no cubic terms consistent with the symmetry of the problem.

One final remark is that Landau's criterion is, of course, only a statement made within the context of a MF theory. It is important to realize that effects of fluctuations, which are not taken into account within a MF approach, may change the order of a transition [4, 24, 37], as we will discuss in details later in Coleman-Weinberg potential [55], for instance.

1.4 **Quantum phase transitions**

As we have seen in section 1.2, classical phase transitions are induced by varying the temperature of the systems, where we have identified a T_c that determine the transition point. On the other hand, QPTs are defined as transitions that occur at *zero-temperature*, i.e., are associated with a change on the ground state of the system through the variation of an external control parameter of the model, such as, pressure, doping, disorder or magnetic field [3, 4].

It is worth to emphasize that, at a first view, QPTs appear to be an exclusively academic problem since, in principle, we cannot experimentally reach the *zero-temperature* limit, as defined by third law of thermodynamics. However, the presence of a QCP have been reported in several systems at very low temperatures and it is well-accepted that a QCP may affect the finite temperature region above it. This region is known as quantum critical region [3, 4], as shown in Fig. 6.

At this moment, there is no fundamental theory to describe the exotic behavior exhibited by SCES in the quantum critical region. Therefore, QPTs are a very interesting and exciting ongoing research topic in CMP. The quantum critical region, for usual metals is sometimes called non-Fermi liquid region, or equivalently, *strange* metal region. Several efforts have been dedicated by condensed matter community in order to understand its eccentric behavior since QCPs play a crucial role for SCES at very low temperatures.

Without loss of generality, from theoretical point of view, we can extrapolate it to the *zero-temperature* scenario, i.e., the presence of a QCP separates, in general, an order-disorder QPT and thus can be identified experimentally as we vary some external parameter that is not associated with the temperature and as consequence we observe a change on the ground state of the system. There are several experimental reports related to the presence of a QCP in the most varied SCES, such as, unconventional SC [5, 8, 25, 26, 27, 28, 29], U and Ce heavy-fermions materials [20, 21, 23] and recently

Figure 6 - Schematic phase diagram exhibiting the effect of a QCP

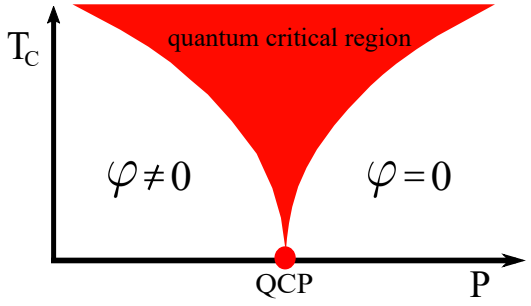

Legend: (Color online) Schematic phase diagram exhibiting the effect of a QCP at *zero-temperature* separating an order-disorder QPT, i.e., since there is a QCP will emerge a quantum critical region at finite temperature that is affected by quantum fluctuations. The parameter P is an external control parameter such as pressure, doping, disorder or magnetic field.

Source: The author, 2020.

there is a proposal of QCPs in ferroeletric systems [15, 16]. Moreover, one can also point out QPTs in topological systems [4].

Therefore, QPTs present as crucial difference when compared to classical transitions the essential need to take into account quantum effects on the systems. In fact, it is difficult to know exactly at what temperature quantum effects become important to describe a system, but it is certain that at $T = 0$ these effects are relevant [4].

Phase transitions at high temperatures in such SCES can be perfectly described by classical statistical mechanics. To understand this better, we have to define in more detail both correlation length and correlation function, which have been introduced in Eq. (11) and Eq. (12), respectively. The correlation function (density-density, spin-spin, etc.) is defined as follows [4],

$$C_F(\vec{r}) = \langle \Phi(\vec{r})\Phi(0)\rangle - \langle \Phi(0)\rangle^2 \tag{33}$$

where, depending on the system of interest, is associated with the scattering amplitudes or susceptibilities. Its general asymptotic behavior is given by [4],

$$C_F(\vec{r}) \approx e^{-r/\xi}, \ r \to \infty \tag{34}$$

Note that Eq. (34) defines the correlation length (ξ) such that if $r >> \xi$ the system is uncorrelated. On the other hand, the system exhibits its maximum correlation, i.e., $\xi \to \infty$, at the transition point, as will be discussed below.

Experimentally we know that close to the transition point there is a divergence of susceptibilities and scattering amplitudes. The former is associated, for instance, with

FMs at zero field, as discussed in section 1.3.4, whereas the latter are observed in scattering in binary liquids or neutron spreading in FMs [69]. Thus, using the expressions between fluctuations and susceptibilities, we obtain [4],

$$\chi(T,H) = \int d\vec{r}\, C_F(\vec{r},T,H) \tag{35}$$

From Eq. (35), one can conclude that near the transition point the integral must diverge. However, the correlation function is limited and if it exhibits an exponential decay behavior, given in Eq. (34), the integral in Eq. (35) is certainly convergent. Therefore, close to the transition point, the exponential decay must be dampened, which is only possible if $\xi \to \infty$ [4].

In QPTs we also consider a time length that differs in the QCP by the same argument. For this reason, continuous phase transitions are usually accompanied by a divergent length and correlation time. In this case we have to consider the correlations of long wavelength only, which are well-captured classically, even in essentially quantum models.

To sum up, one can observe experimentally that a quantum system behaves classically when the energy associated with temperature fluctuations exceeds the energy associated with the frequencies of interest [4], that is,

$$\hbar\omega^* << k_B T_c \tag{36}$$

where ω^* is the frequency associated with quantum fluctuations.

As we have seen, if the transition is accompanied by a divergent correlation time $\omega^* \to 0$ when $T \to T_c$, one can clearly see that for any transition at finite temperature we find a temperature sufficiently close to T_c such that Eq. (36) is satisfied. In other words, we always find a temperature sufficiently close to T_c in which the system behaves almost classically. However, for transitions at $T = 0$ we cannot state the same [4], which makes this kind of phase transition different and justifying its reference by QPTs.

It is worth to emphasize that the study of critical phenomena received a new attention after the introduction of the effects of quantum fluctuations.

1.4.1 Scaling theory of quantum phase transitions and its extension to finite temperatures

In the same spirit of classical phase transitions, QPTs are characterized by divergences of a characteristic length and time, as we have discussed in section 1.4, as follows [4],

$$\xi \propto |g|^{-\nu} \tag{37}$$

and

$$\tau_\xi \propto |g|^{-\nu z} \tag{38}$$

where g is the distance to the QCP and Eq. (37) and Eq. (38) define the critical exponents ν and z, respectively.

Note that the dynamic critical exponent z is defined due to the possible anisotropy between temporal and spacial dimensions. In the isotropic case we have $z = 1$ [4, 24, 51, 52] and the dimensions of time and space scale in the same way [63]. Moreover, one can also define the dynamic critical exponent so that at the critical point the characteristic frequency (ω) for fluctuations of the order parameter as a function of wave-vector (k) is proportional to k^z [70], for small k, i.e., $\omega \propto k^z$, as we will discuss later when we introduce the dynamic of the systems of interest through the propagators in section 2.2.

As we have seen before, g is associated with the distance to the QCP, i.e., $J - J_c$, where J is an arbitrary parameter of the system. Therefore, accordingly to the Kadanoff's scaling hypothesis one can write [4],

$$J' = b^{-y} J \qquad \texttt{or} \qquad h' = b^{-y} h \tag{39}$$

$$g' = b^a g \tag{40}$$

$$\tau' = b^z \tau \tag{41}$$

where the scaling factor $b = (L/L')$, L and L' are the linear dimensions of the original and scaled systems, respectively.

In that sense, a physical quantity at a given length scale is related to the same quantity in another length scale. For example, $(H'/H) = (L/L')^x = b^x$, has been justified by Kadanoff et al. [71]. Thus, we can associate the exponents y and a in Eq. (39) and Eq. (40) to the critical exponents previously discussed. The correlation length (ξ) may scales as follows [4],

$$\xi'(|g'|) = \frac{\xi(|g|)}{b} \tag{42}$$

for an arbitrary value of b.

With the help of Eq. (40) we get,

$$\xi'(b^a\,|g|) = \frac{\xi(|g|)}{b} \tag{43}$$

and taking $b^a\,|g| = 1$, or equivalently $b = |g|^{-1/a}$, we obtain the behavior of the correlation length at the criticality [4],

$$\xi = |g|^{-1/a}\,\xi' \tag{44}$$

From Eq. (37), one can recognize

$$\nu = \frac{1}{a} \tag{45}$$

In order to find the relation for z we require that the uncertainty principle [4], given by,

$$\Delta E \Delta \tau \geq \hbar \tag{46}$$

is scaling invariant.

Note that ΔE (energy) may scales in the same form of J (another energy) in Eq. (39) and consequently, the characteristic time scales with Eq. (41). Thus, one can write [4],

$$\Delta E' \Delta \tau' = \Delta E \Delta \tau \Rightarrow b^{z-y} \Delta E \Delta \tau = \Delta E \Delta \tau, \rightarrow z = y. \tag{47}$$

The singular term, labeled by the subscript s, in the free energy density at *zero-temperature* in the presence of an external magnetic field behave as [4],

$$f_s = \frac{F_s}{L^d} = J f(g, H/J) \tag{48}$$

where $f(q, p)$ is a scaling function and J is the coupling constant which has dimension of energy. At $T = 0$ this is the available energy scale to fix the energy dimension. Finally, L is the size of the system and d its Euclidean dimension.

The new free energy density and correlation length for the system where size has been rescaled by $L' = L/b$ are given by [4],

$$f'_s = b^d f_s = J' f(|g|', H'/J') \tag{49}$$

and

$$\xi'(|g|', H'/J') = b^{-1} \xi(|g|, H/J) \tag{50}$$

Using Eq. (39) and Eq. (40) into Eq. (49) and Eq. (50) and taking $b = |g|^{-1/a}$, we obtain,

$$\frac{f_s}{J} = |g|^{\frac{y+d}{a}} f\left(1, \frac{H/J}{|g|^{(x+y)/a}}\right) \tag{51}$$

and

$$\xi = |g|^{-1/a} \xi'\left(1, \frac{H/J}{|g|^{(x+y)/a}}\right) . \tag{52}$$

From the definition of the critical exponent α, associated with the singular part of the ground state energy density, we have [4],

$$f_s \propto |g|^{2-\alpha} \tag{53}$$

Using the relations to ν and z, i.e., Eq. (45) and Eq. (47) into Eq. (51) one can show that the free energy density scales as follows [4],

$$f_s \propto |g|^{\nu(d+z)} \tag{54}$$

Thus, comparing Eq. (53) and Eq. (54), we can obtain a scaling relation in the form [4],

$$2 - \alpha = \nu(d + z) \tag{55}$$

Note that the equality in Eq. (55) is identical to the Josephson's inequality satisfying as equality with a effective dimension $d + z$, see Eq. (10). As discussed before, it is intrinsic of QPTs that the dynamic of the system must be taken into account, i.e., the time appears as an additional dimension in this kind of systems [4]. If $z = 1$, time and space are isotropic, and the quantum model of d dimensions can be treated as a classical model with $d + 1$ dimensions. In this case, the relations between the critical exponents may remains valid to the effective dimension $d + 1$. In this dissertation we will consider both dynamics $z = 1$ and $z = 2$ [4, 24, 51, 52], that is, we will also investigate systems whereupon temporal length contributes in a different form for the effective dimension of the model.

In order to make direct contact with experimental results we need to extend the scaling approach for small but finite temperatures. Therefore, since temperature is a parameter, it is renormalized by the characteristic energy or coupling constant at the *zero-temperature* fixed point, see Eq. (39), as follows [4],

$$\left(\frac{T}{J}\right)' = b^z \left(\frac{T}{J}\right) \tag{56}$$

Using Eq. (56) one can obtain how temperature will appear in the scaling functions. Thus, with the help of Eq. (51) and Eq. (52) with the additional renormalization equation for temperature, Eq. (56), we get

$$f_s = |g|^{2-\alpha} f_E \left(\frac{T/J}{|g|^{\nu z}}, \frac{H/J}{|g|^{\Delta}}\right) \tag{57}$$

and

$$\xi = |g|^{-\nu} f_\xi \left(\frac{T/J}{|g|^{\nu z}}, \frac{H/J}{|g|^{\Delta}}\right) \tag{58}$$

where $\Delta = \beta + \gamma$ and we used $y = z$.

It is worth to emphasize the emergence of the dynamic critical exponent z in the free energy and correlation length, i.e., Eq. (57) and Eq. (58), respectively. This is the signature of the QPT and of the intrinsic relation between static and dynamics for these transitions [4].

When we extend quantum phase diagrams to finite temperatures we have to be aware of the *lower critical dimension* (d_L) of the system of interest, i.e., the dimension at and below which there is no finite temperature transition in the system as the zero-temperature ordered phase is immediately destroyed by thermally excited low-energy modes. For instance, $d_L = 1$ for the transverse field Ising model and $d_L = 2$ for the Heisenberg model [4]. On the other hand, we also need to identify the *upper critical dimension* (d_c), above which the critical exponents become MF-like and fluctuation effects become irrelevant [4]. In these circumstances, Landau's approach, which neglects these fluctuations, will provide the correct description of the critical behavior. For instance, $d_c = 4$ within a Gaussian approximation theory, where fluctuations, but not their interaction, are taken into account [4].

2 QUANTUM CORRECTIONS AND THE *ONE-LOOP* EFFECTIVE POTENTIAL APPROXIMATION

In this chapter we will present in details the technique that will be widely used throughout this dissertation to include quantum and thermal fluctuations on the MF phase diagrams of systems exhibiting multiple competing/coexisting scalar orders. We have applied the well-established *one-loop* effective potential approximation [24, 54, 55, 56] from QFT. We will see that this approach presents a direct and efficient procedure to take into account quantum and thermal fluctuations on the classical action. We follow closely refs. [4, 24, 69] to describe it. Finally, in order to make the reader familiar with this technique we will calculate the first-order quantum corrections term for some examples, such as, the scalar $\lambda\phi^4$ model for both 2d and 3d systems, and for the Coleman-Weinberg potential [55]. For the latter we also include finite temperature effects. We consider, in all examples within this chapter, systems that are characterized by a dynamic critical exponent $z = 1$ [4, 24, 51, 52], where time and space scales in the same form [63].

2.1 Introduction

On the ground state of SCES, or equivalently, at *zero-temperature* scenario, quantum fluctuations present a crucial role on the QPTs. Quantum effects may give rise to some important physical aspects, such as, spontaneous symmetry breaking (SSB) and change in the nature of the transitions [4, 24, 55]. All along this chapter we will describe the *one-loop* effective potential approximation [24, 54, 55, 56] and its relevance to condensed matter systems, more specifically for SCES.

The calculation of the effective potential requires knowledge of the classical action of the systems, where its free term is, in general, associated with the kinetic term of the action and thus we define it as any quadratic term of the action whereupon can be directly integrated out. It is worth to point out that identifying the free term on interacting models may not be a difficult task and we will observe that its exact form is of great importance to the results.

2.2 Dynamic of the phases and propagators

As pointed out in section 2.1, the identification of the quadratic term on the classical action, or equivalently, on the classical potential, is an important ingredient for calculating quantum fluctuations. Note that even the free part can be complicated

to be obtained and, in general, it depends on the type of fluctuations that induce the transitions. For instance, for SC heavy fermions, the SC may appear usually close to an AFM phase [8]. Therefore, in this section, we discuss different forms for the free action, which is intrinsically associated with the dynamic of the systems, and consequently to both the propagators and the dispersion relations of the systems of interest.

For simplicity, throughout this dissertation we will consider that the two different competing phases have the same dynamics described by propagators associated with dynamic critical exponents $z = 1$ as well as $z = 2$ [24, 51, 52, 53] separately. The former characterizes a non-dissipative behavior, whereas the latter exhibits a dissipative one. It results from the relation between the n^{th} order time derivatives and the gradient terms in non-stationary Ginzburg–Landau equation. In other words, one can recognize z through the relation between frequency and wave-vector dependence of the propagators at the critical point, i.e., $\omega \propto k^z$ [24, 51, 52, 53, 70].

With this two different types of dynamics considered within this dissertation, one can cover the most interesting cases of competing/coexistence orders in SCES. The case $z = 1$ is appropriate to describe magnetic phases with excitations characterized by linear dispersion relations as well as to describe SCs [4, 20, 24, 51] or superfluid liquid ^{3}He [52]. Moreover, this kind of dynamic is usually related to interacting magnetic excitons, where the effective dimension is simply increased by the unit [51]. On the other hand, the case $z = 2$ [51], that belongs to a different class of systems characterized by quadratic dispersion relations, is normally associated to paramagnons in itinerant AFM/FM [51] or overdamped modes in SCs [4] near their QCPs.

We will show explicitly that the choice of different dynamics, symmetry and dimensionality of the system may affect the final results [61, 62] for the effective potential, and consequently the effect of first-order quantum corrections on these systems. In this dissertation we will initially focus on obtaining the effective potential at *zero-temperature* (V^0_{eff}) within the *one-loop* approximation, for 2d [62] and 3d [61] systems with dynamic critical exponents $z = 1$ and $z = 2$.

The relevant propagator considering $z = 1$ is given by [4, 20, 24, 51, 69],

$$G_0^{Mink}(k) = G_0(\omega, \vec{q}) = \frac{i}{k^2 - m^2} \tag{59}$$

where k is a quadrivector $(\omega, \vec{q})$ and $k^2 = \omega^2 - q^2$ in Minkowski space.

Without loss of generality, all along this dissertation we choose to work in Euclidean space, which means that Eq. (59) can be write as follows [4, 24, 69],

$$G_0(\omega, \vec{q}) = \frac{1}{k^2 + m^2} \tag{60}$$

where $k^2 = \omega^2 + q^2$. Thus, one can clearly see the isotropic relation between time and

space associated with the dynamic critical exponent $z = 1$ since $\omega \propto k$ at the QCP.

For the case $z = 2$ we use a propagator that takes into account the electronic interaction considering a random phase approximation (RPA). Note that the electronic interaction term induces the magnetic transition and the quadratic term of the action is modified by spin fluctuations. Therefore, close to the transition the propagator of this modified action can be written as follows [4, 24, 69],

$$D_0(\omega, \vec{q}) = \frac{1}{|\omega|\,\tau + q^2 + m_p^2} \tag{61}$$

where τ is the characteristic relaxation time and m_p^2 is related to the Coulomb local repulsion U and the density of states of the fermi level $N(E_F)$,

$$m_p^2 = 1 - UN(E_F) \tag{62}$$

The propagator in Eq. (61) is also known as AFM or FM paramagnons propagator [4, 24, 69]. Moreover, in the case of an AFM instability in a SCES, the relevant propagator is also described by Eq. (61), where m_p^2 is the distance in parameter state from the magnetic transition. Note that its form exhibits a dissipative behavior and the dynamic critical exponent is given by $z = 2$. It detailed description can be found in the seminal work from Hertz [51].

2.3 The *one-loop* effective potential approximation

In this section we will present the method that will be widely applied in this dissertation to take into account quantum corrections and finite temperature effects, i.e., the *one-loop* effective potential approximation from QFT.

2.3.1 Classical limit

Initially, we define Green functions and classical solutions to show that this approximation consists in a expansion around the classical solutions. The Green function of the operators $\phi(x_1)...\phi(x_n)$ is given by [69, 72],

$$G_n(x_1, ..., x_n) = \left[\int \mathcal{D}\phi\ \phi(x_1)...\phi(x_n) e^{\frac{i}{\hbar}S[\phi]}\right]\left[\int \mathcal{D}\phi\ e^{\frac{i}{\hbar}S[\phi]}\right]^{-1} \tag{63}$$

For convenience, the notation in Eq. (63) is given in Minkowski space but one can easily transform Eq. (63) to Euclidean space through the transformation $iS[\phi] \rightarrow$

$-S_E[\phi]$ [69]. In that sense, all results within this section will remain valid to the Green functions in Euclidean space.

In the classical limit, i.e., for $\hbar \to 0$, the oscillatory behavior in the integrand of Eq. (63) indicates that the term that minimizes the action (S) is $S[\phi] = S_c[\phi_c]$, which dominates all the sum [73] and encodes all physical properties of the system. This *minimum* of the action, i.e., the classical action is given by the field ϕ_c that is solution of the equation,

$$\left.\frac{\delta S[\phi]}{\delta\phi(x)}\right|_{\phi=\phi_c} = 0 \ . \tag{64}$$

If there is only one solution, one can obtain to the Green function [69],

$$\lim_{\hbar\to 0} G_n(x_1, ..., x_n) = G_n^c(x_1, ..., x_n) = \phi_c^n \tag{65}$$

Since,

$$G_n^c(x_1, ..., x_n) = G_n^c(x_1, ..., x_{n-r}) G_n^c(x_{n-r+1}, ..., x_n) \ . \tag{66}$$

Eq. (66) indicates that there is no quantum correlation, as expected from a classical theory. On the other hand, for a quantum model, i.e., for $\hbar \neq 0$, may be somehow possible to make a series expansion in $\hbar$ around the classical solution to include terms related to quantum corrections. However, this kind of expansion is only possible on the functional W or Γ and may provide a good approach between classical and quantum theory, which will be discussed below.

2.3.2 Functional generator and the effective action

Initially, let us emphasize that the calculation of Green functions are directly associated with the theoretical solutions of several model in condensed matter and particle physics. In other words, its solutions are intrinsically related to the physical observables.

The Green functions can be generated by means of the functional given by [69, 59, 72],

$$Z[j] = \int \mathcal{D}\phi \exp\left\{\frac{i}{\hbar}\left[S[\phi] + \int j\phi\right]\right\} \tag{67}$$

where $Z[j]$ is known as functional generator and j is the external source.

Therefore, the Green functions emerge from $Z[j]$ and one can show that [69, 59, 72],

$$\frac{1}{Z[0]}\frac{1}{i^{n-1}}\left.\frac{\delta^n Z[j]}{\delta j(x_1)...j(x_n)}\right|_{j=0} = \langle 0\,|T[\phi(x_1)...\phi(x_n)]|\,0\rangle = G(x_1, x_2, ..., x_n) \ . \tag{68}$$

Note, from Eq. (68), that the functional derivatives with respect to the external source ($j(x_i)$) at $j = 0$ provides the Green functions of n-points [72]. In CMP, one can

identify that $Z[j]$ is associated with the partition function of the problem. However, this functional encodes too much information [69, 72] since the physical observables are always related to the connected Green functions whereupon are generated by the alternative functional W given by [69, 59, 72],

$$W[j] = -i\hbar \ln(Z[j]) \ . \tag{69}$$

It is worth to point out that one can easily recognize that the physical observables are associated with the connected Green functions (W) since they are related to the logarithm of the partition function. The average of the field in the presence of an external source can be calculated as follows,

$$\bar{\phi}(x, j) = \frac{\delta W}{\delta j(x)} \tag{70}$$

To obtain the other useful functional Γ we need to suppose that one can invert, in an univocal form, the functional dependence in $\bar{\phi}(x, j)$ in order to write the external source dependence in the form $j = j(x, \bar{\phi})$. If this is possible, one can define a functional which depends on $\bar{\phi}$ for a Legendre transformation [69, 59, 72], that is,

$$\Gamma[\bar{\phi}] = W[j] - \hbar \int dx \ \bar{\phi}(x) j(x, \bar{\phi}) \tag{71}$$

Although the procedure applied to obtain Eq. (71) seems simple, and analogous to what one can get in thermodynamic to define several potentials depending on the different sets of variables, the finding of the functional for $\bar{\phi}$ using the implicit dependence of j on $\bar{\phi}$ may be quite complicated.

Note that,

$$\frac{\delta \Gamma[\bar{\phi}]}{\delta \bar{\phi}(x)} = -\hbar j(x) \tag{72}$$

Therefore, in the limit $\hbar \to 0$ we obtain,

$$\frac{\delta \Gamma_0[\bar{\phi}]}{\delta \bar{\phi}(x)} = 0 \tag{73}$$

Note that the condition in Eq. (73) is the *minimum* equation satisfied by the classical action when $\phi = \phi_c$ and $j = 0$, see Eq. (64). So, in this case, $\bar{\phi} = \phi_c$ and consequently one can recognize $\Gamma_0[\bar{\phi}]$ as the classical action, that is,

$$\lim_{\hbar \to 0} \Gamma[\bar{\phi}] = \Gamma_0[\bar{\phi}] = S[\bar{\phi}] \tag{74}$$

The complete action $\Gamma[\bar{\phi}]$ is thus interpreted as a quantum generalization of the classical action $S[\bar{\phi}]$ [69, 72]. In that sense, $\Gamma[\bar{\phi}]$ is also known as effective action of the

theory, which encodes classical and quantum effects, and in the limit $\hbar \to 0$ its reduces to the classical action. Thus, the expansion in $\hbar$, performed in the effective action, may represent an useful approach to include quantum effects on the theory.

2.3.3 First-order quantum corrections

Let us deduce the first-order quantum corrections term from the classical solution starting with the normalized functional generator [69, 59, 72],

$$\tilde{Z}[j,\phi] = \int \mathcal{D}\phi \; e^{\frac{i}{\hbar}\left[S[\phi]+\int j\phi\right]} \tag{75}$$

For simplicity, the renormalization is supposed implicit, such that

$$S[\phi] = S_R[\phi] + \hbar\delta S[\phi] \tag{76}$$

where $S_R[\phi]$ is the renormalized action and $\hbar\delta S[\phi]$ are the counterterms necessary to make the theory *cut-off* independent [69].

As we have seen before, in the limit $\hbar \to 0$ the field $\phi = \phi_c[j]$ is the classical solution, which satisfies,

$$\left.\frac{\delta S_R}{\delta\phi(x)}\right|_{\phi=\phi_c[j]} + j(x) = 0 \tag{77}$$

where j is an external source.

Since the action is in the presence of an external source j, one can expand $S_R + \int j\phi$ around the classical solution $\phi_c[j] = \phi_c^j$ using an Ansatz as follows [69],

$$\phi(x) = \phi_c^j + \hbar^{1/2}\eta(x) \tag{78}$$

where the new field $\eta(x)$ describes the fluctuations of the field $\phi(x)$ around the classical solution.

With the help of Eq. (78) one can rewrite Eq. (75) as follows,

$$\tilde{Z}[j,\eta] = \int \mathcal{D}\phi \exp\left\{\frac{i}{\hbar}\left[S[\phi_c^j + \hbar^{1/2}\eta] + \int d^dx \; j(x)\left(\phi_c^j + \hbar^{1/2}\eta(x)\right)\right]\right\} \tag{79}$$

Around the classical solution, i.e., $\phi = \phi_c^j$, we use the functional expansion to the

classical action $S[\phi]$,

$$\begin{aligned} S[\phi_c^j + \delta\eta] &= S[\phi_c^j] + \int d^d x_1 \left.\frac{\delta S[\phi]}{\delta\phi}\right|_{\phi=\phi_c^j} \delta\eta(x_1) + \\ &+ \frac{1}{2}\int d^d x_1 d^d x_2 \; \delta\eta(x_1) \left.\frac{\delta^2 S[\phi]}{\delta\phi(x_1)\delta\phi(x_2)}\right|_{\phi=\phi_c^j} \delta\eta(x_2) + \mathcal{O}(\delta\eta^3) \end{aligned} \tag{80}$$

If S presents a quadratic part in the form $\frac{1}{2}\phi(x)\hat{K}\phi(x)$ and a self-interacting term $U(\phi)$, the second derivative of the action is given by [69]

$$\left.\frac{\delta^2 S[\phi]}{\delta\phi(x_1)\delta\phi(x_2)}\right|_{\phi=\phi_c^j} = \int d^d x \left[\hat{K} + U''(\phi_c^j)\right] \delta(x - x_1)\delta(x - x_2) \tag{81}$$

where $U''(\phi_c^j)$ is the second derivative of the self-interacting term with respect to the field $\phi(x)$ calculated at the classical *minimum*.

In general, we have the form of free action as follows [69],

$$S_0[\phi] = \frac{1}{2}\int \left(\partial_\mu\phi\partial^\mu\phi - \frac{1}{2}m^2\phi^2\right) = -\frac{1}{2}\int \phi[\Box + m^2]\phi \tag{82}$$

where $\Box = \vec{\nabla}^2 - \partial_t^2$.

Therefore, usually we need to deal with kinetic terms in the form,

$$\hat{K} = \Box + m^2 \tag{83}$$

Replacing Eq. (81) into the functional expansion of $S[\phi_c^j + \hbar^{1/2}\eta]$ and with the help of Eq. (79) we get,

$$\begin{aligned} \tilde{Z} &= \exp\left\{i\hbar^{-1}\left(S[\phi_c^j] + \hbar\delta S[\phi_c^j] + \int j \; \phi_c^j\right)\right\} \times \\ &\times \int \mathcal{D}\eta \exp\left\{i\hbar^{1/2}\int d^d x \left(\left.\frac{\delta S}{\delta\phi}\right|_{\phi=\phi_c^j} + j\right)\eta + \frac{i}{2}\int d^d x \; \eta\left(\hat{K} + U''(\phi_c^j)\right)\eta\right\} \end{aligned} \tag{84}$$

In the deduction of Eq. (84) we have used the translation invariance of the element of integration $\mathcal{D}\phi$ and we have removed from the functional integration the constant contribution that depends on the classic solution ϕ_c^j only. Thus, the integration is now performed in the first and second order on the functional in relation to the classic solution.

Note, however, that the first-order term in η of Eq. (84) is zero since the classical field ϕ_c^j is solution to the equation [69, 72, 73],

$$\left.\frac{\delta S}{\delta\phi}\right|_{\phi=\phi_c^j} + j = 0 \; . \tag{85}$$

Thus, the first non-zero contribution comes from the second-order term in η of Eq. (84). Note also that the second-order term is quadratic in η, and consequently can be easily integrated out using the well-known relation [69, 72, 73],

$$\frac{1}{Z_0}\int \mathcal{D}\phi\ e^{-\frac{i}{2}\int d^dx\ \phi[\hat{\mathcal{V}}]\phi} = \left[\frac{\det(\hat{K})}{\det(\hat{\mathcal{V}})}\right]^{1/2} \tag{86}$$

where Z_0 is the normalization factor.

From Eq. (83) one can see that the quadratic contribution $\hat{K}$, in general, can be written in the form $\hat{K} = \Box + m^2$, such that Eq. (86) now can be written as follows,

$$\frac{1}{Z_0}\int \mathcal{D}\phi\ e^{-\frac{i}{2}\int d^dx\ \phi[\hat{\mathcal{V}}]\phi} = \left[\frac{\det(\Box + m^2)}{\det(\hat{\mathcal{V}})}\right]^{1/2} \tag{87}$$

Using the relation in Eq. (86) into Eq. (84) with $\hat{\mathcal{V}} = \hat{K} + U''$ we get,

$$Z = \exp\left\{i\hbar^{-1}\left(S[\phi_c^j] + \hbar\delta S[\phi_c^j] + \int j\ \phi_c^j\right)\right\}\left[\frac{\det(\hat{K})}{\det(\hat{K}+U'')}\right]^{1/2} \tag{88}$$

Taking the logarithm of Eq. (88) we obtain $W[j]$,

$$W[j] = -i\hbar\ln(Z) = S[\phi_c^j] + \int\ j\phi_c^j + \hbar\delta S[\phi_c^j] + \frac{i}{2}\hbar\ln\left[\frac{\det(\hat{K}+U'')}{\det(\hat{K})}\right] \tag{89}$$

Using the identity [69],

$$\ln\det\hat{\mathcal{V}} = \mathtt{Tr}\ln\hat{\mathcal{V}} \tag{90}$$

Finally, we obtain,

$$W[j] = S[\phi_c^j] + \int\ j\phi_c^j + \hbar\left\{\delta S[\phi_c^j] + \frac{i}{2}\mathtt{Tr}\ln\left[1 + \frac{U''}{\hat{K}}\right]\right\} \tag{91}$$

Note that the logarithmic term in Eq. (91) is of first-order in $\hbar$ and improves the classical solution $S[\phi_c^j]$ (zero-order in $\hbar$) to include quantum corrections [69, 72]. Moreover, the counterterms, which are necessary to renormalize the theory [72], are properly included in the term $\delta S[\phi_c^j]$.

Thus, the effective action can be identified as follows,

$$\Gamma[\phi_c^j] = W[j] - \int\ j\phi_c^j = \Gamma^{(0)}[\phi_c^j] + \hbar\Gamma^{(1)}[\phi_c^j] + \mathcal{O}(\hbar^2) \tag{92}$$

where $\Gamma^{(0)}[\phi_c^j] = S[\phi_c^j]$ is the classical contribution and the term that encodes the first-

order quantum corrections is given by,

$$\Gamma^{(1)}[\phi_c^j] = \frac{i}{2}\texttt{Tr}\ln\left[1 + U''i\hat{G}_0\right] + \texttt{counterterms} \tag{93}$$

where we have used that $i\hat{G}_0 = [\hat{K}]^{-1}$ is the propagator of the free action [73].

The first-order quantum corrections term assumes a more familiar form in *momentum* space, which is obtained performing a Fourier transform [72] in Eq. (93),

$$\Gamma_k^{(1)}[\phi_c^j] = \frac{i}{2}\int \frac{d^dk}{(2\pi)^d}\ \texttt{Tr}\ \ln[1 + U''iG_0(k)] + \texttt{counterterms} \tag{94}$$

where $iG_o(k)$ is now the free propagator in *momentum* space.

In general, for a free action in the form of Eq. (82), $iG_o(k)$ is given by [69],

$$iG_0(k) = -\frac{1}{k^2 - m^2} \tag{95}$$

It is worth to emphasize that one can recognize the *loop* expansion [69, 72, 73] if we expand the logarithm in Eq. (94), which yields

$$\Gamma_k^{(1)}[\phi_c^j] = \frac{i}{2}\int \frac{d^dk}{(2\pi)^d}\ \texttt{Tr}\left[U''iG_0 - \frac{1}{2}\left(U''iG_0(k)\right)^2 + \frac{1}{3}\left(U''iG_0(k)\right)^3 + ...\right] \tag{96}$$

In Euclidean space one can obtain a similar result for Eq. (94) as follows,

$$\Gamma_k^{(1)}[\phi_c^j] = \frac{1}{2}\int \frac{d^dk}{(2\pi)^d}\ \texttt{Tr}\ \ln[1 + U''G_0^E(k)] + \texttt{counterterms} \tag{97}$$

where $G_0^E(k)$, for $z = 1$ [4, 24, 51, 52, 69], exhibits the form given in Eq. (60), that is,

$$G_0^E(k) = G_0^E(\omega, \vec{q}) = \frac{1}{k^2 + m^2} \tag{98}$$

where $k^2 = \omega^2 + q^2$.

On the other hand, for $z = 2$ [4, 24, 51, 52, 69], we have,

$$G_0^E(k) = G_0^E(\omega, \vec{q}) = \frac{1}{|\omega|\,\tau + q^2 + m^2} \tag{99}$$

In this dissertation we will be interested in investigating this two different types of dynamics associated with the frequency dependence of the propagators described in both Eq. (98) and Eq. (99) on the systems with multiple competing scalar orders, as we will discuss later.

2.3.4 Generalization for multiple scalar fields

The previous result for the *one-loop* effective potential in Eq. (92), i.e., classical and first-order quantum corrections, is only applicable for an action that contains one-component scalar field $\phi(x)$ and terms of self-interaction. Thus, we need to generalize this method for a generic action that exhibits several scalar fields ϕ_i and coupling terms.

In general, all components of the scalar fields have kinetic terms given by Eq. (82) and thus the same free propagators. In this case, its main difference appears in the interacting terms, which can now involve interactions between the fields. Here, however, we will need an even more general method whereupon the fields can also have different free propagators.

So, the general action takes the form [69],

$$S[\phi_i] = \int d^d x \left[\sum_i \phi_i \hat{K}_i \phi_i + U(\phi_i) \right] \tag{100}$$

where $\hat{K}_i$ encodes the quadratic term contribution that, in general, is given in the form $\hat{K}_i = \Box + m^2$ and U is the potential contribution that may contain terms of self-interaction of the fields and terms of interaction between the fields.

The notation $\{\phi_i\}$ will indicate that the functional depends on a set of several fields ϕ. Thus, we define the classical solution as $\{\phi_i\} = \phi_c^j$ since the classical solution determines the values of fields so that the action in the presence of the external source $j(x)$ is minimized.

Analogously to the previous section, we expand the normalized functional generator around the classical solution,

$$\tilde{Z}[j,\eta] = \int \mathcal{D}\phi \exp\left\{ \frac{i}{\hbar} \left[S[\phi_c^j + \hbar^{1/2}\eta] + \int d^d x \; j(x) \left(\phi_c^j + \hbar^{1/2}\eta(x) \right) \right] \right\} \tag{101}$$

where,

$$\begin{aligned} S[\phi_c^j + \delta\eta] &= S[\phi_c^j] + \int d^d x_1 \sum_l \left. \frac{\delta S[\{\phi_i\}]}{\delta \phi_l} \right|_{\{\phi_i\}=\phi_c^j} \delta\eta_l(x_1) + \\ &+ \frac{1}{2} \int d^d x_1 d^d x_2 \sum_{l,m} \delta\eta_l(x_1) \left. \frac{\delta^2 S[\{\phi_i\}]}{\delta\phi_l(x_1)\delta\phi_m(x_2)} \right|_{\{\phi_i\}=\phi_c^j} \delta\eta_m(x_2) + \mathcal{O}(\delta\eta^3) \end{aligned} \tag{102}$$

The second derivative is now given by,

$$\left. \frac{\delta^2 S[\{\phi_i\}]}{\delta\phi_l(x_1)\delta\phi_m(x_2)} \right|_{\{\phi_i\}=\phi_c} = \int d^d x \left[\hat{K}_l \delta_{l,m} + \frac{\partial^2 U(\{\phi_i\})}{\partial\phi_l(x_1)\partial\phi_m(x_2)} \right] \Bigg|_{\{\phi_i\}=\phi_c} \delta(x - x_1)\delta(x - x_2) \tag{103}$$

which allow us to define the Matrix $[\tilde{M}]_{l,m}$ as follows,

$$[\tilde{M}]_{l,m} = \left[\hat{K}_l\delta_{l,m} + \frac{\partial^2 U(\{\phi_i\})}{\partial\phi_l(x_1)\partial\phi_m(x_2)}\right]\Bigg|_{\{\phi_i\}=\phi_c} \tag{104}$$

Thus, the expansion now can be written as follows,

$$\begin{aligned}\tilde{Z} &= \exp\left\{i\hbar^{-1}\left(S[\phi_c^j] + \hbar\delta S[\phi_c^j] + \int j\ \phi_c^j\right)\right\}\times \\ &\times \int \mathcal{D}\eta \exp\left\{i\hbar^{-1/2}\int d^dx\left(\sum_l \frac{\delta S[\{\phi_i\}]}{\delta\phi_l}\Big|_{\{\phi_i\}=\phi_c^j} + j\right)\eta + \frac{i}{2}\int d^dx\ \eta_l[\tilde{M}]_{l,m}\eta_m\right\}\end{aligned} \tag{105}$$

where there is an implicit sum in the last term for repeated indexes.

The linear term in η of Eq. (105) again is zero due to the *minimum* condition for the classical field. Thus, the first non-zero contribution can be easily performed using [72, 73],

$$\frac{1}{Z_0}\int \mathcal{D}\eta\ e^{-\frac{i}{2}\int d^dx\ \eta_l[\tilde{M}]_{l,m}\eta_m} = \left[\frac{\det(\hat{K}_i)}{\det(\hat{\tilde{M}})}\right]^{1/2} \tag{106}$$

The functional generator Z is thus given by,

$$Z = \exp\left\{i\hbar^{-1}\left(S[\phi_c^j] + \hbar\delta S[\phi_c^j] + \int j\ \phi_c^j\right)\right\}\left[\frac{\det(\hat{K}_i)}{\det(\tilde{M})}\right]^{1/2} \tag{107}$$

As we have calculated before, the effective action $\Gamma = -i\hbar\ln(Z) - \int j\phi_c^j$ and thus we get,

$$\Gamma[\phi_c] = \Gamma^{(0)}[\phi_c^j] + \frac{i}{2}\hbar\ln\left[\frac{\det(\tilde{M})}{\det(\hat{K}_i)}\right] + \texttt{counterterms} \tag{108}$$

The quadratic contribution now has several fields ϕ_i, but from Eq. (100) it has a diagonal form [69],

$$S_0 = \int d^{d-1}x\sum_i \phi_i\hat{K}_i\phi_i = \int d^{d-1}x\sum_{l,m}\phi_l\hat{K}_l\delta_{l,m}\phi_m \tag{109}$$

Note that the inverse of its determinant in Eq. (108) is just the product of the correspondent propagators, i.e., $i\hat{G}_0^{(l)} = [\hat{K}_l]^{-1}$. Thus, Eq. (108) can be rewritten as follows,

$$\Gamma[\phi_c] = \Gamma^{(0)}[\phi_c^j] + \frac{i}{2}\hbar\ln\left[\det\left(i\hat{G}_0^{(l)}\tilde{M}_{l,m}\right)\right] + \texttt{counterterms} \tag{110}$$

or equivalently,

$$\Gamma[\phi_c] = \Gamma^{(0)}[\phi_c^j] + \frac{i}{2}\hbar\ \texttt{Tr}\ln\left[i\hat{G}_0^{(l)}\tilde{M}_{l,m}\right] + \texttt{counterterms} \tag{111}$$

Before we proceed to calculate the first-order quantum correction term and identifying the loop expansion, we first investigate Eq. (111) in details. More specifically, we explore the matrix $[\tilde{M}]_{l,m}$ for this general case.

According to the definition for $[\tilde{M}]_{l,m}$ in Eq. (104) one can write,

$$i\hat{G}_0^{(l)}[\tilde{M}]_{l,m} = \left[\delta_{l,m} + \frac{1}{\hat{K}_l}\frac{\partial^2 U(\{\phi_i\})}{\partial\phi_l(x_1)\partial\phi_m(x_2)}\right]\Bigg|_{\{\phi_i\}=\phi_c} \tag{112}$$

From Eq. (112) we can make the expansion of the logarithm in terms of a matrix $M = -(\tilde{M} - 1)$, given by,

$$M = -\frac{1}{\hat{K}_l}\left.\frac{\partial^2 U(\{\phi_i\})}{\partial\phi_l(x_1)\partial\phi_m(x_2)}\right|_{\{\phi_i\}=\phi_c} \tag{113}$$

Therefore, the first-order quantum correction term can be written as follows [69],

$$\Gamma[\phi_c] = \Gamma^{(0)}[\phi_c^j] + \frac{i}{2}\hbar\ \mathtt{Tr}\ln\left[\mathbb{I} - M\right] + \mathtt{counterterms} \tag{114}$$

Performing a Fourier transform [72, 73] in Eq. (114) we get

$$\Gamma_k[\phi_c] = \Gamma_k^{(0)}[\phi_c^j] + \frac{i}{2}\hbar\int\frac{d^dk}{(2\pi)^d}\ \mathtt{Tr}\ln\left[\mathbb{I} - M(k)\right] + \mathtt{counterterms} \tag{115}$$

where $M(k)$ is the Fourier transform of Eq. (113),

$$M = -i\hat{G}_0^{(l)}(k)\left.\frac{\partial^2 U(\{\phi_i\})}{\partial\phi_l(x_1)\partial\phi_m(x_2)}\right|_{\{\phi_i\}=\phi_c} \tag{116}$$

and $G_0^{(l)}(k)$ is the correspondent propagator to the field ϕ_l.

In Euclidean space we obtain,

$$\Gamma_k^E[\phi_c] = \Gamma_k^{E(0)}[\phi_c^j] + \frac{1}{2}\hbar\int\frac{d^dk}{(2\pi)^d}\ \mathtt{Tr}\ln\left[\mathbb{I} - M(k)\right] + \mathtt{counterterms} \tag{117}$$

with

$$M = -\hat{G}_{E(0)}^{(l)}(k)\left.\frac{\partial^2 U(\{\phi_i\})}{\partial\phi_l(x_1)\partial\phi_m(x_2)}\right|_{\{\phi_i\}=\phi_c} \tag{118}$$

where the notation $G_{E(0)}^{(l)}(k)$ indicates the propagator in Euclidean space related to ϕ_l. For convenience, the subscript E, indicating Euclidean space, will be omitted from now on since we will use the Euclidean space notation all along this dissertation.

All calculations that we have performed in this section allow us to correctly include the first-order quantum corrections term. The direct calculation of higher order terms is very laborious and for that it is easier to take advantage of that the expansion is identified

with the expansion in loops using Feynman diagrams technique [72, 73], which is beyond the scope of this dissertation. In this dissertation we will only take into account first-order quantum corrections, i.e., at *one-loop* level.

The next section is dedicated to the theoretical study of generic first-order phase transitions at *zero-temperature*. This study is very important since one of the effects of quantum fluctuations on the ground state of the systems is to change the nature of the transition to a first-order QPT [4, 24], as we will see later.

2.4 **First-order quantum phase transitions**

The concepts of scaling theory play a crucial role to describe problems of critical phenomena at $T = 0$ [4]. Through them we can obtain some scaling relations between the critical exponents that may dominate the critical behavior of SCES close to the criticality, see section 1.4.1.

In this section we extend scaling theory to first-order QPTs [74]. Although there is no divergent ξ in first-order transitions, scaling theory have proved to be very useful to describe first-order transitions at finite temperatures [75, 76, 77, 78, 79], and therefore we expect the same suitability at *zero-temperature*.

Let us consider the free energy density scaling form on the ground state close to a QPT [4] (see Eq. (53)),

$$f_s \propto |g|^{2-\alpha} \tag{119}$$

where g is the distance to the transition point ($g = 0$).

The critical exponent α is associated with ν through the hyperscaling relation $2 - \alpha = \nu(d + z)$, where d is the dimension of the system and z is the dynamic critical exponent, as described in section 1.4.1.

In addition, the total internal energy close to the transition can be written as follows [4],

$$U(g = 0^{\pm}) = U(g = 0) \pm A_{\pm} |g|^{2-\alpha} \tag{120}$$

for $g \to 0^{\pm}$.

The existence of both a first-order phase transition at $T = 0$ with a discontinuity in dU/dg and a non-zero latent heat, implies $\alpha = 1$ [4, 69]. If the hyperscaling relation remains valid, the critical exponent of the correlation length therefore assumes the value $\nu = 1/(d + z)$. Note that this is the quantum equivalent of the classical result $\nu = 1/d$ for first-order transitions at finite temperatures [75, 76, 77, 78, 79]. Furthermore, at finite temperature, associated with this value of ν there is, on the disordered side of the phase diagram, a new energy scale, i.e., $T^* \propto |g|^{z/(d+z)}$ [4].

The presence of a discontinuity on the order parameter at the transition point

and the hypothesis that there is no-decay of its correlation function leads to the results $\beta = 0$ (as in the classic case [79]) and $d + z - 2 + \eta = 0$ [4], respectively. Also similar to what occurs at finite temperatures, the critical exponent $\delta = \infty$ and for consistency between the scaling relations, the susceptibility order parameter may diverge with critical exponent $\gamma = 1$ [79].

Another interesting aspect is the generalization of the latent heat. For instance, in pressure-induced quantum transitions $g \propto (P - P_c)/P_c$, where P_c is the critical pressure and a non-zero latent heat means, in this case, a finite amount of work, i.e., $W = A_+ + A_- = P_c \Delta V$, to transform one phase into another. This finite latent heat is associated with the change in the volume of the system since the intensive variable, in this case the pressure, remains constant at the transition. Another example would be density-induced transitions, where the chemical potential remains fixed while the number of particles varies [4, 69].

In addition to the first-order quantum phase transition itself being of great interest, there are new experimental reports indicating that they occur in distinct SCES, such as, heavy fermions and magnetic transition metals [8]. In this dissertation, we are concerned with the mechanisms that may change their continuous nature to discontinuous one close to the QCP, i.e., the quantum fluctuations. However, there are many mechanisms that may be responsible for that effect. For instance, in AFMs [80] or SCs [81] a sufficiently large external magnetic field can cause this effect. On the other hand, in compressible magnets, pressure can also be responsible.

Therefore, we will focus throughout this dissertation on the mechanisms that might become important since we cool down the temperature of real system, that is, in the same region where effects of quantum fluctuations may be relevant. Next, we will include finite temperature effects on the effective potential.

Initially, in the next sections of this chapter we will present three distinct examples associated with first-order QPTs induced by quantum fluctuations. First, we investigate the $\lambda\phi^4$ model for both 2d and 3d systems with one-component field characterized by a dynamic critical exponent $z = 1$ in order to investigate the *one-loop* effective potential approximation and its renormalization procedure. Then, we discuss the well-known Coleman-Weinberg potential [55], i.e., the interesting problem of coupling the superconducting order parameter with the electromagnetic field, which give rises to the SSB mechanism and allow us to understand the change in the nature of the quantum transition and then we introduce finite temperature effects.

2.5 Example 1: $\lambda\phi^4$ theory in (2+1) dimensions

The classical potential (V_c) for $\lambda\phi^4$ scalar theory considering one-component field, without coupling, is given by,

$$V_c(\phi) = r\phi^2 + \lambda\phi^4 \tag{121}$$

In order to obtain the *one-loop* effective potential we need to calculate the matrix elements in Eq. (118), given by the interacting terms as follows,

$$[M]_{lm} = -G_0^{(l)}(k) \left[\frac{\partial^2 V^{int}(\phi_i)}{\partial\phi_l(x_1)\partial\phi_m(x_2)}\right]\Bigg|_{\phi_i=\phi_c} \tag{122}$$

where V^{int} indicates the interacting terms, i.e., quartic-order terms in the fields.

For simplicity, we take $z = 1$ [4, 24, 51, 52], which means that we have the propagator in the form,

$$G^{(1)}(k) = G_0(w, \vec{q}) = \frac{1}{k^2 + r} \tag{123}$$

where $k^2 = \omega^2 + q^2$ (Euclidean space).

Since we get both interacting term and propagator we need to calculate the derivatives in Eq. (122) for,

$$V^{int} = \lambda\phi^4 \tag{124}$$

2.5.1 *One-loop* effective potential calculation

Calculating the derivatives in Eq. (122) yields,

$$M_{11}(k) = -\frac{1}{k^2 + r}\left[12\lambda\phi^2\right] \tag{125}$$

Thus, we need to obtain the contribution,

$$\Gamma^{(1)}[\phi] = \frac{1}{2}\int \frac{d^d k}{(2\pi)^d}\ \ln\ \det[\mathbb{I} - M(k)] + \texttt{counterterms} \tag{126}$$

With the help of Eq. (125) we get,

$$\Gamma^{(1)}[\phi] = \frac{1}{2}\int \frac{d^d k}{(2\pi)^d}\ \ln\ \left(1 + \frac{12\lambda\phi^2}{k^2 + r}\right) + \texttt{counterterms} \tag{127}$$

So, for $\lambda\phi^4$ theory in (2+1) dimensions, we have the following integral to solve,

$$\Gamma^{(1)}[\phi] = \frac{1}{2}\int \frac{d^3 k}{(2\pi)^3} \ln\left[\left(1 + \frac{b}{k^2 + r}\right)\right] + \texttt{counterterms} \tag{128}$$

where,

$$b = 12\lambda\phi^2 \ . \tag{129}$$

Note that $d^dk = S_d k^{d-1} dk$, where $S_d = (2\pi)^{d/2}/\Gamma(d/2)$ and $S_3 = 4\sqrt{2}\pi$, since $\Gamma(3/2) = \sqrt{\pi}/2$. Therefore, we need to solve this kind of integral,

$$I_1 \equiv \frac{\sqrt{2}}{(2\pi)^2} \int_0^\Lambda dk \ k^2 \ln\left(1 + \frac{b}{k^2 + r}\right) \tag{130}$$

where we take the *cut-off* Λ since the integral in Eq. (130) diverges.

In the limit of $\Lambda \to \infty$ the integral of Eq. (130) has solution of the type,

$$I_1 = \frac{1}{3}\left[3(12\lambda\phi^2)\Lambda + \pi r^{3/2} - \pi r^{3/2}\left(1 + \frac{12\lambda\phi^2}{r}\right)^{3/2}\right] \tag{131}$$

which diverges linearly with the *cut-off*.

Using Eq. (131) one can rewrite Eq. (128) as follows,

$$\Gamma^{(1)}[\phi] = \frac{\sqrt{2}}{(2\pi)^2}\left\{\frac{1}{3}\left[3(12\lambda\phi^2)\Lambda + \pi r^{3/2} - \pi r^{3/2}\left(1 + \frac{12\lambda\phi^2}{r}\right)^{3/2}\right]\right\} + \texttt{counterterms} \tag{132}$$

We have to include the counterterm in the form $-\frac{1}{2}C_1\phi^2$ to eliminate the *cut-off* (Λ) dependence, making the theory *cut-off* independent.

2.5.2 Renormalization of the theory

In order to calculate the counterterms we apply the usual definition [4, 55, 69],

$$\left[\frac{d^2\Gamma^{(1)}}{d\phi^2}\right]\Bigg|_{\phi=0} = r \tag{133}$$

Thus, we obtain,

$$-\frac{1}{2}C_1\phi^2 = -\frac{1}{2}\frac{\sqrt{2}}{(2\pi)^2}\left[24\lambda\Lambda - 12\pi\lambda r^{1/2}\right]\phi^2 \tag{134}$$

Replacing Eq. (134) into Eq. (132) one can get the *one-loop* effective potential from Eq. (117),

$$V_{eff}(\phi) = \underbrace{r\phi^2 + \lambda\phi^4}_{classical\ term} + \frac{\sqrt{2}}{(2\pi)^2}\left[6\pi\lambda r^{1/2}\phi^2 - \frac{\pi}{3}r^{3/2}\left(1 + \frac{12\lambda}{r}\phi^2\right)^{3/2} + \frac{\pi}{3}r^{3/2}\right] \tag{135}$$

where the last term (constant) does not depend on the field ϕ.

Note that we can rewrite Eq. (135) as follows,

$$V_{eff}(\phi) = \left[r + \frac{\sqrt{2}\left(6\pi\lambda r^{1/2}\right)}{(2\pi)^2} \right] \phi^2 + \lambda\phi^4 - \frac{\sqrt{2}}{(2\pi)^2} \left[\frac{\pi}{3} r^{3/2} \left(1 + \frac{12\lambda}{r}\phi^2 \right)^{3/2} - \frac{\pi}{3} r^{3/2} \right] \quad (136)$$

From Eq. (136) one can clearly see that the *mass* term was renormalized. In addition, note the field dependence in the last term of Eq. (136), which results in a first-order transition, according to the definition within Landau's approach discussed in section 1.3.5.

2.6 **Example 2: $\lambda\phi^4$ theory in (3+1) dimensions**

Let us now just change the dimensionality of the system to investigate the *one-loop* effective potential for $\lambda\phi^4$ scalar theory in $(3+1)$ dimensions, again, without coupling terms. It is worth to point out that the classical term of effective potential does not depend on the dimensionality of the system.

Thus, the classical potential, for this case, is identical to Eq. (121), that is,

$$V_c(\phi) = r\phi^2 + \lambda\phi^4 \quad (137)$$

Again, we calculate the matrix elements in Eq. (118) given by the interacting terms,

$$[M]_{lm} = -G_0^{(l)}(k) \left[\frac{\partial^2 V^{int}(\phi_i)}{\partial\phi_l(x_1)\partial\phi_m(x_2)} \right] \Bigg|_{\phi_i=\phi_c} \quad (138)$$

Taking $z = 1$ [4, 24, 51, 52] we get the propagator,

$$G^{(1)}(k) = G_0(w, \vec{q}) = \frac{1}{k^2 + r} \quad (139)$$

Therefore, we need to calculate the derivatives in Eq. (138) for,

$$V^{int} = \lambda\phi^4 \quad (140)$$

2.6.1 Calculating the *one-loop* effective potential

The calculation of Eq. (138) results,

$$M_{11} = -\frac{1}{k^2 + r} \left[12\lambda\phi^2 \right] \quad (141)$$

So, we need to obtain,

$$\Gamma^{(1)}[\phi] = \frac{1}{2}\int \frac{d^dk}{(2\pi)^d}\ \ln\ \det[\mathbb{I} - M(k)] + \texttt{counterterms} \tag{142}$$

With the help of Eq. (141) we get,

$$\Gamma^{(1)}[\phi] = \frac{1}{2}\int \frac{d^dk}{(2\pi)^d}\ \ln\ \left(1 + \frac{12\lambda\phi^2}{k^2+r}\right) + \texttt{counterterms} \tag{143}$$

For $\lambda\phi^4$ scalar theory in $(3+1)$ dimensions, we obtain the following integral do solve,

$$\Gamma^{(1)}[\phi] = \frac{1}{2}\int \frac{d^4k}{(2\pi)^4} \ln\left[\left(1 + \frac{b}{k^2+r}\right)\right] + \texttt{counterterms} \tag{144}$$

where,

$$b = 12\lambda\phi^2\ . \tag{145}$$

Again, note that $d^dk = S_dk^{d-1}dk$, where $S_d = (2\pi)^{d/2}/\Gamma(d/2)$ e $S_4 = (2\pi)^2$, since $\Gamma(4/2) = 1$. Then, we need to deal now with integrals of type,

$$I_2 \equiv \frac{1}{(2\pi)^2}\int_0^\Lambda dk\ k^3 \ln\left(1 + \frac{b}{k^2+r}\right) \tag{146}$$

where, again, the *cut-off* Λ is introduced since the integral in Eq. (146) diverges.

In the limit $\Lambda \to \infty$ the integral of Eq. (146) has solution given by [4, 69],

$$I_2 \approx \left(\frac{1}{2}b\Lambda^2 + \frac{1}{4}b^2\ln\left[\frac{b}{\Lambda^2}\right] - \frac{1}{8}b^2\right) + \left(\frac{1}{4}b + \frac{1}{2}b\ln\left[\frac{b}{\Lambda^2}\right]\right)r \tag{147}$$

which now diverges quadratically (at leading order) with the *cut-off*.

In this case, we neglect the term depending on r in I_2, as a first approximation, since we are close to the transition point, which implies that this contribution may be very small. Hence,

$$I_2 \approx \left(\frac{1}{2}b\Lambda^2 + \frac{1}{4}b^2\ln\left[\frac{b}{\Lambda^2}\right] - \frac{1}{8}b^2\right) \tag{148}$$

Using Eq. (148) one can write Eq. (144) as follows,

$$\Gamma^{(1)}[\phi] = \frac{1}{(2\pi)^2}\left(\frac{1}{2}(12\lambda\phi^2)\Lambda^2 + \frac{1}{4}(12\lambda\phi^2)^2\ln\left[\frac{12\lambda\phi^2}{\Lambda^2}\right] - \frac{1}{8}(12\lambda\phi^2)^2\right) + \texttt{counterterms} \tag{149}$$

Note that we have to include now counterterms in the form $-\frac{1}{2}C_2\phi^2$ and $-\frac{1}{24}D_1\phi^4$, through which we can eliminate the *cut-off* (Λ) dependence on the effective potential.

2.6.2 Renormalizing the theory

In order to calculate the countertems we apply the usual definitions [4, 55, 69],

$$\left[\frac{d^2\Gamma^{(1)}}{d\phi^2}\right]\Big|_{\phi=0} = r \qquad \texttt{and} \qquad \left[\frac{d^4\Gamma^{(1)}}{d\phi^4}\right]\Big|_{\phi=\langle\phi\rangle} = \lambda \tag{150}$$

where $\langle\phi\rangle$ is arbitrary and usually taken as the *minimum* of the *one-loop* effective potential [4, 24, 55, 69, 72].

Therefore, the counterterms are given by,

$$-\frac{1}{2}C_2\phi^2 = -\frac{1}{2}\frac{1}{(2\pi)^2}\left[12\lambda\Lambda\right]\phi^2 \tag{151}$$

and

$$-\frac{1}{24}D_1\phi^4 = -\frac{1}{24}\frac{1}{(2\pi)^2}\left[288\lambda^2\left(11+3\ln\left[\frac{12\lambda\left\langle\phi\right\rangle^2}{\Lambda^2}\right]\right)\right]\phi^4 \tag{152}$$

Replacing Eq. (151) and Eq. (152) into Eq. (149) we obtain the effective potential as follows,

$$V_{eff}(\phi) = \underbrace{r\phi^2+\lambda\phi^4}_{classical\ term} + \underbrace{\frac{9}{\pi^2}\lambda^2\phi^4\left(\ln\left[\frac{\phi^2}{\left\langle\phi\right\rangle^2}\right]-\frac{25}{6}\right)}_{Coleman-Weinberg-like\ term} \tag{153}$$

Note, from Eq. (153), that the first-order quantum corrections term is given by a Coleman-Weinberg-like term. This kind of term will be discussed, in details, in the next example and we will show that this contribution also results in a first-order QPT.

2.7 **Example 3: Coleman-Weinberg potential**

As a last example of mechanisms that may change the nature of quantum transitions, in this case the coupling with Goldstone modes [4, 55, 69], we will discuss the superconducting transition at $T = 0$ when we couple the order parameter to a gauge field. The gauge field then represents the non-massive mode (Goldstone mode) whose fluctuations can affect the transition [4]. Next, we extend these results to include finite temperature effects and apply scaling theory to describe it.

Note that in this section we will discuss a particular case. However, we emphasize that several results within this example might remains valid for any first-order QPT. Our starting point, following the original treatment presented by Coleman and Weinberg [55], is the Lagrangian density of the system given by [55],

$$L = -\frac{1}{4}(F_{\mu\nu})^2+\frac{1}{2}(\partial_\mu\varphi_1+qA_\mu\varphi_2)^2+\frac{1}{2}(\partial_\mu\varphi_2-qA_\mu\varphi_1)^2-\frac{1}{2}m^2(\varphi_1^2+\varphi_2^2)-\frac{\lambda}{4!}(\varphi_1^2+\varphi_2^2)^4 \tag{154}$$

Eq. (154) describes, in particle physics, mesons minimally coupled with an electromagnetic field [4, 69]. However, in condensed matter we may provide some additional explanations. First, we consider the field φ as the SC order parameter, which can be expressed by a complex or two real scalars fields [4, 69], as in Eq. (154). We could write the same Lagrangian with complex fields but to the purpose of calculating the *one-loop* effective potential the two real fields are more suitable.

Moreover, Eq. (154) represents a Ginzburg-Landau-like expansion [68] of the generalized parameter for the quantum case [4], where time dependence is also important. For simplicity, we consider a system wherein time and space are isotropic, i.e., a Lorentz invariant system [4, 24, 61]. In other words, we consider time and space scaling in the same way, which implies that we are interested in a system characterized by dynamic critical exponent $z = 1$ [4, 24, 51, 52, 61, 62, 63].

It is worth to point out that the superconducting action at $T = 0$ does not always have this isotropy and in this dissertation we will also discuss the cases of systems with $z = 2$ in the next chapters.

In the same sense of particle physics, the coupling of the order parameter with the electromagnetic field is minimal and can be understood as the first term of the expansion of a more complicated coupling. Everything else is standard, that is,

$$F_{\mu\nu} = \partial_\mu A_\mu - \partial_\nu A_\nu \tag{155}$$

where the indices μ, ν goes from 0 to $d = 3$ [69].

The coupling is associated with the electric charge (q) and, for simplicity, we take $\hbar = c = 1$. On the other hand, for the non-charged scenario, i.e., for $q = 0$, Eq. (154) describes the insulator-superfluid transition at $m^2 = 0$ [4]. Furthermore, in this example we are interested in systems with three spatial dimensions, i.e., $d = 3$, and thus the effective dimension of the quantum problem is $d_{eff} = d + z = 4$.

The effective potential at *zero-temperature* ($V^0_{eff}(\varphi_c)$) for this case is well-known and can be found in several works [4, 55, 69]. In *one-loop* approximation we obtain,

$$V^0_{eff}(\varphi_c) = \frac{m^2\varphi_c^2}{2} - \frac{m^2\varphi_c^4}{4\langle\varphi\rangle^2} + \frac{3q^4\varphi_c^4}{64\pi^2}\left[\ln\left(\frac{\varphi_c^2}{\langle\varphi\rangle^2}\right) - \frac{1}{2}\right] \tag{156}$$

where φ_c is the classical value of the field and $\langle\varphi\rangle$ is an extreme of the effective potential, such that

$$\left.\frac{dV^0_{eff}}{d\varphi_c}\right|_{\varphi_c=\langle\varphi\rangle} = 0 \tag{157}$$

If we take $m = 0$, or equivalently $m^2 = 0$, in Eq. (156) we obtain the Coleman-Weinberg-like term [55], which is very similar to the last term in Eq. (153), as discussed in the previous example.

Figure 7 - The effective potential for the Coleman-Weinberg problem

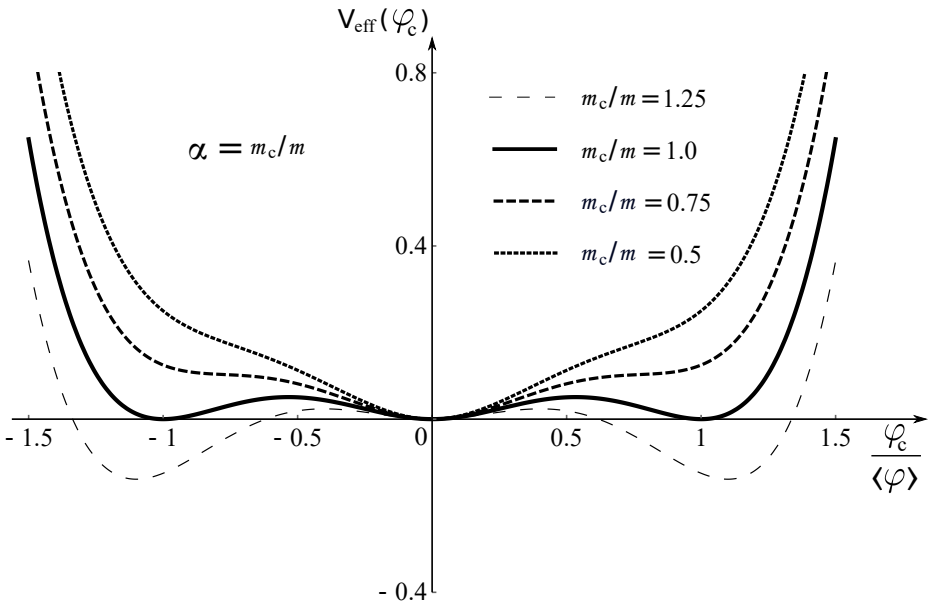

Legend: The *one-loop* effective potential for the Coleman-Weinberg problem. Note that there is a first-order quantum phase transition at the critical value $\alpha = (m_c/m)^2 = 1$.
Source: Refs. [4, 69]. Adapted by the author.

In Fig. 7 we show the plot of the effective potential for different values of mass m^2. Note that there is a critical value of m^2 given by,

$$m_c^2 = \frac{3q^4}{32\pi^2} \langle\varphi\rangle^2 \ . \tag{158}$$

At the critical value m_c^2 the system undergoes a first-order QPT for a new state of broken symmetry, i.e., $\varphi_c \neq 0$, see Fig. 7. Therefore, we will investigate the stability of this two different ground states in the vicinity of m_c. For values $m > m_c$, the stable state, given by the *minimum* of the effective potential of Eq. (156), occurs at $\varphi_c = 0$, such that, $V^0_{eff}(\varphi_c = 0) = 0$.

The value of the metastable *minimum* $\varphi_c = \langle\varphi\rangle$ is given by [4, 69],

$$V^0_{eff}(\varphi_c = \langle\varphi\rangle) = \frac{1}{4} m^2 \langle\varphi\rangle^2 \left[1 - \frac{m_c^2}{m^2}\right] \tag{159}$$

Note that at the value $m^2 = m_c^2$ the two ground states with $\varphi_c = 0$ and $\varphi_c \neq 0$ are degenerate, and for $m^2 < m_c^2$, the true ground state is associated with the phase where $\varphi_c = \langle\varphi\rangle \neq 0$, i.e., the ordered state, as shown in Fig. 7. In addition, close to m_c^2 the effective potential, that at $T = 0$ is equal to the free energy density, can be written as $V^0_{eff} \propto |m^2 - m_c^2| \propto |g|^{2-\alpha}$, which implies $\alpha = 1$, and applying the hyperscaling relation of Eq. (55) we obtain $\nu = 1/(d + z)$, verifying the scaling theory described in section 2.4.

The latent heat is given by [4],

$$L_h = (A_+ + A_-) = \frac{1}{4} m_c^2 \langle\varphi\rangle^2 \tag{160}$$

where we take $A_+ = 0$.

It is worth to point out that the results obtained are consistent with the usual theory of first-order transitions [4]. In these kind of transitions both phases coexist at a point (or line at finite temperatures) of first-order. In the vicinity of this point, one of the phases is always more stable but the another phase is still represented by the existence of a metastable *minimum*.

We define spinodals [4] as the points that mark the limit from which these metastable minima emerges, that is, in the region between spinodals the stable phase coexists with strong fluctuations in the competing phase. Note, from Fig. 7, the existence of a spinodal for $(m_c/m)^2 = 0.5$, that indicates the limit of metastability for the SC within the normal phase. On the other hand, there is always seems to be a *minimum* metastable at $\varphi_c = 0$ in the SC phase.

2.7.1 Finite-temperature effects on the Coleman-Weinberg potential

The main advantage of investigating a simple model such as the Coleman-Weinberg potential, given by Eq. (154), is that one can extend its results at $T = 0$ for finite temperatures and consequently test the validity of the scaling theory.

Note that in Euclidean QFTs at finite temperatures the effective potential is equivalent to the thermodynamic free energy [82]. Therefore, the extension of the effective potential for finite temperatures is obtained by replacing the integrals in frequency (ω) for discrete sums. This well-established technique is known as Matsubara summation formalism [57, 58, 59, 72, 73] and will be discussed in details later.

Using this technique one can show that the extension of the Coleman-Weinberg effective potential, at *one-loop* approximation, for finite temperatures, taking $k_B = 1$, is given by [4, 69],

$$V_{eff}(T) = \frac{1}{4} m^2 \langle\varphi\rangle^2 |g| \left\{ 1 + \frac{2}{\pi^2 m^2 \langle\varphi\rangle^2} \frac{T^{d+1}}{|g|} I\left(\frac{M(\varphi_c)}{T}\right) \right\} \tag{161}$$

where $g = m^2 - m_c^2$ (see Eq. (159)), $M^2(\varphi_c) = m^2 + q^2\varphi_c^2$ and,

$$I_d(y) = \int_0^\infty dx\; x^{d-1} \ln\left[1 - e^{-\sqrt{x^2+y^2}}\right] \tag{162}$$

Note that the numerical solution of the integral of Eq. (162) for three spatial

Figure 8 - Numerical solution of the integral in Eq. (162) for three spatial dimensions.

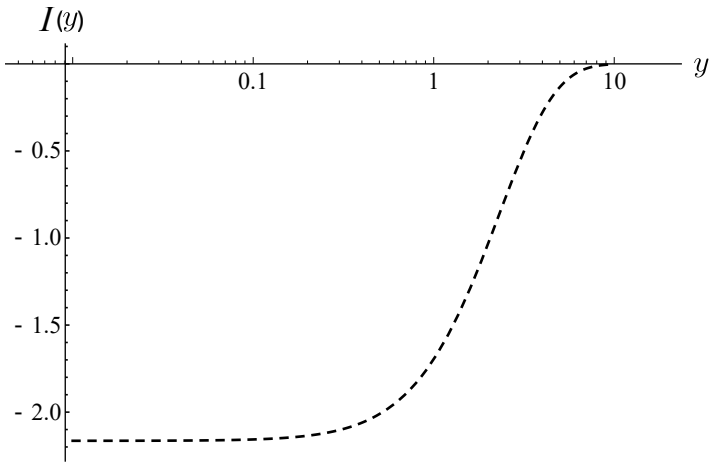

Legend: Semi-Log plot for the numerical solution of the integral in Eq. (162) for three spatial dimensions.

Source: Refs. [4, 69]. Adapted by the author.

dimensions, i.e., $I_3(y) = I(y = M(\varphi_c)/T)$ is presented in Fig. 8.

At high temperatures, i.e., for $T >> M$, and close to the transition point, one can get the effective potential ($V_{eff}(\varphi, T)$) as follows [4, 69],

$$V_{eff}(\varphi, T) = -\frac{\pi^2}{18}T^4 - \frac{1}{8}m^2T^2 + \frac{1}{2}m_T^2\varphi^2 - \frac{m_T^2}{4\left\langle\varphi\right\rangle^2}\varphi_c^4 + \frac{3q^4\varphi_c^4}{64\pi^2}\left[\ln\left(\frac{\varphi_c^2}{\left\langle\varphi\right\rangle^2}\right) - \frac{1}{2}\right] \quad (163)$$

where we have defined a renormalized *mass* (m_T), which depends on the temperature,

$$m_T^2 = \left|m^2\right|\left(1 - \frac{T^2}{T_{MF}^2}\right) \quad (164)$$

with $T_{MF}^2 \approx 12\left|m^2\right|/3q^2$.

Note that one can also rewrite m_T, replacing $T_{MF}^2 \approx 12\left|m^2\right|/3q^2$, in the form,

$$m_T^2 = m^2 + \left(\frac{q^2}{4}\right)T^2 \quad (165)$$

From Eq. (165) the line on which m_T is always zero is given by,

$$T_{MF} = \frac{2}{q}\left|m^2\right|^{1/2} \quad (166)$$

If we consider only the contribution of the first-order terms in λ, i.e., $\mathcal{O}(\lambda)$, T_{MF} will be given by $T_{MF} = \left(12\left|m^2\right|/(4\lambda + 3q^2)\right)^{1/2}$ [4], which implies that this line no longer has any special meaning in the charged case since when we cool down the system it

Figure 9 - Schematic phase diagram for a charged superfluid coupled to the electromagnetic field

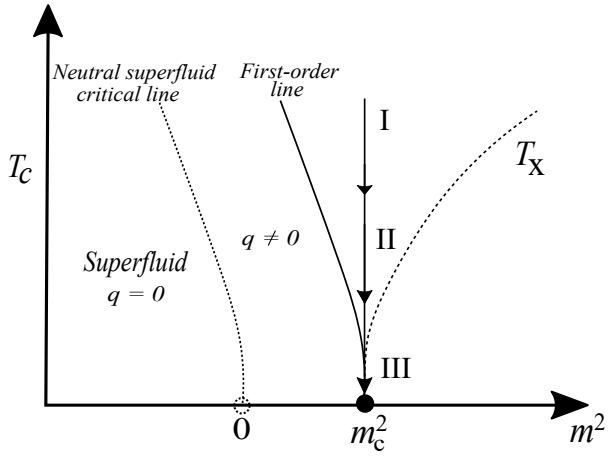

Legend: Schematic phase diagram for a charged superfluid coupled to the electromagnetic field. Along of the vertical trajectory $m^2 = m_c^2$ one can identify different scaling regimes (I, II and III) as a function of temperature.

Source: Ref. [4]. Adapted by the author.

undergoes a first-order phase transition before, as shown in Fig. 9. This first-order line is dominated by the same MF shift critical exponent, i.e., $\psi = z/(d+z-2) = 1/2$ [4], of the critical line of the neutral superfluid given by $T_{SF} = \left(12\left|m^2\right|/(4\lambda)\right)^{1/2}$.

It is worth to emphasize that in the case $d = 3$ the insulating-superfluid transition at *zero-temperature* is described exactly by the effective potential since $d_c = d + z = 4$ for this transition, which has already been extensively studied by Fisher et al. [83]. The insulating character of the disordered phase is due to the presence of an excitation gap given by $\Delta = |m^2|^{\nu z} = |m^2|^{1/2}$ since the correlation length critical exponent ν assumes its MF value for $d \geq d_c$ [4].

In the charged superfluid, i.e., the SC, the transitions are very different and occur for [4],

$$m_T^2 = m^2 - m_c^2 + \left(\frac{q^2}{4}\right) T_c^2 \tag{167}$$

where m_c^2 is given by Eq. (158).

Thus, the first-order line is given by,

$$T_c = \frac{2}{q}\sqrt{|m_c^2 - m^2|} \tag{168}$$

Note that above the QCP of the neutral superfluid, i.e., at $m^2 = 0$, there is now a

Figure 10 - Specific heat as a function of temperature

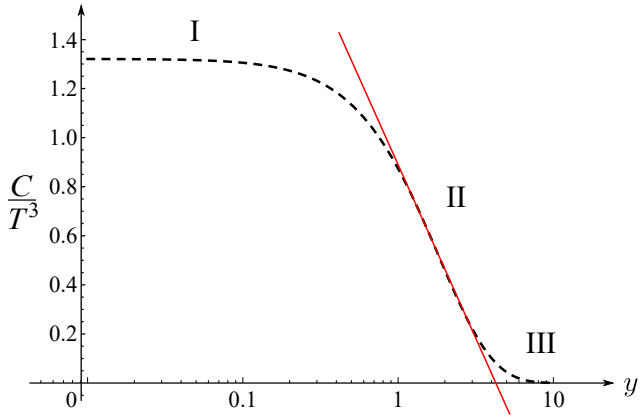

Legend: (Color online) Specific heat as a function of temperature on the vertical trajectory $m^2 = m_c^2$ related to the first-order QPT at $T = 0$. The different scaling regimes are discussed in the text. Note that the fitting (red line) in regime II indicates a non-universal logarithmic behavior, i.e., $\ln(T)$.

Source: Refs. [4, 69]. Adapted by the author.

SC instability at finite temperature, that is,

$$T_c(m^2 = 0) = \sqrt{\frac{3}{8\pi^2}} q \langle\varphi\rangle \tag{169}$$

The physical origin for this transition can be explained due to the energy acquired by the system in expelling the electromagnetic field when the system becomes an SC [4]. In the next section we carefully analyze this result applying the formalism of scaling theory to describe the critical phenomena close to a first-order QPT.

2.7.2 Scaling theory applied to the Coleman-Weinberg potential

Let us now consider the system on the fine tuned parameters, i.e., on the vertical trajectory that ends at $T = 0$ at the new transition point $m^2 = m_c^2$ in which occurs the first-order QPT, see Fig. 9. Cooling down the temperature of the system one can observe the behavior of physical observables as a function of temperature.

Fig. 10 shows the specific heat as a function of temperature, where the scaling behavior is valid up to a certain scale of temperature before breaking down in a non-universal logarithmic behavior. Note that for usual QCPs in metallic systems the vertical trajectory considered represents the trajectory whereupon we observe a non-Fermi-liquid behavior at high temperatures [4].

At high temperatures, i.e., for $T >> m_c$, which corresponds to the regime I in

Fig. 9 and Fig. 10, the numerical solution of the integral $I_3(y)$ saturates, i.e., $I_3(y < 0.12) \approx -2.16$, as can be seen in Fig. 8. In this case, the effective potential is given by,

$$V_{eff}(T) \approx \frac{1}{4} m^2 \langle\varphi\rangle^2 |g| \left\{ 1 - \frac{4.32}{\pi^2 m^2 \langle\varphi\rangle^2} \frac{T^{d+1}}{|g|} \right\} \tag{170}$$

Note that Eq. (170) can be rewritten in a scaling form as follows [4, 69],

$$V_{eff}(T) \propto |g|^{2-\alpha} F\left[\frac{T}{T_X}\right] \tag{171}$$

with $F(0) =$ constant. This scaling form can also be found in usual QCPs for continuous transitions.

For this case, i.e., for a first-order transition, the value of the critical exponent for the specific heat is given by $\alpha = 1$ [4, 69, 74] and the characteristic temperature (T_X) is [4],

$$T_X \propto |g|^{\nu z} \propto |g|^{\frac{z}{d+z}} = |g|^{\frac{1}{d+1}} = |g|^{\frac{1}{4}} \tag{172}$$

with $\nu = 1/(d+z)$ [4, 69, 74], see Fig. 9.

In the scaling regime I, along the vertical line $m^2 = m_c^2$ shown in Fig. 9, the free energy density therefore has the scale form $\mathcal{F}(m = m_c, T) \propto T^{(d+z)/z}$ and consequently the specific heat of Fig. 10 is given by [4],

$$\left.\frac{C}{T}\right|_{m=m_c,T} \propto T^{\frac{d-z}{z}} \tag{173}$$

So, the thermodynamic behavior along the vertical line $m^2 = m_c^2$ in regime I ($T >> m_c$) is the same that we observe when we approach the usual QCP observed in the neutral superfluid for $m^2 = 0$. In other words, one can imagine that at high temperatures the system is not aware of the effect of the change in the nature of the transition by quantum fluctuations and thus the charge q, i.e., the coupling, in regime I is irrelevant [4].

As we start to cool down the temperature of the system there is a non-universal intermediate regime, i.e., regime II in Fig. 9 and Fig. 10. In this transition, for $m_c < T$, the specific heat behaves according to $C/T^{d/z} \propto -\ln(T)$, as we can see from the fitting (dotted line) in the semi-log plot in Fig. 10.

Finally, at very low temperatures, i.e., for $T << m_c$ on the vertical line $m^2 = m_c^2$, or equivalently in regime III in Fig. 9 and Fig. 10, the specific heat decays exponentially as a function of temperature, that is, $C/T^{d/z} \propto \exp(-m_c/T)$. The gap for thermal excitations is related to the distance m_c of the transition point at $T = 0$. The correlation length (ξ), which increases along the line as we decrease temperature, reaches a saturation value in regime III of $\xi_S \approx m_c^{-1}$. One can understand the exponential dependence on the specific heat as a result of gapped excitations within SC regions of finite size $L \approx \xi$. Thus,

the gap between the states within these regions is given by $\Delta \approx L^{-z} \approx \xi^{-z} \approx m_c$ [4].

Although the results in this section have been obtained from a particular model, we expect that the scaling behavior for regimes I and III may be a universal characteristic of any weak first-order transition. The scaling theory applied in regime I is similar to that of continuous transitions where $T^* \propto |g|^{\nu z}$ [74] but with $\nu = 1/(d+z)$, which confirms the previous discussion related to the scaling behavior for QPTs.

For this case, the control parameter, given by the mass m (or m^2), provides the natural *cut-off* for temperatures below which the scale theory becomes invalid. The two characteristic energy scales of the system, i.e., T^* and m^2, are general concepts that may play an crucial role close to any discontinuous QPT.

One can also discuss different mechanisms that lead to the change in the nature of quantum transition. The mechanism described above was the coupling with a Goldstone mode (non-massive), represented by the electromagnetic field. The influence of these modes is discussed in a very general way in the work of Belitz et al [35]. On the other hand, not only the coupling with these non-massive modes may change the nature of the transition, but also the coupling of the order parameter with another competing phase in the same region of the phase diagram, even if the fluctuations are not critical, i.e., even for massive fluctuations. In this dissertation, we focus on the case of two competing scalar orders interacting by means of two different kind of couplings in 2d and 3d systems characterized by dynamic critical exponent $z = 1$ as well as $z = 2$ [4, 24, 51, 52, 61, 62, 63].

3 CLASSICAL ANALYSIS FOR MULTIPLE COMPETING SCALAR ORDERS

From now on, we will start discussing our results within this dissertation. In this chapter we present Landau's expansion for free energy density considering multiple competing scalar orders interacting through two different types of couplings, including an unusual bilinear one. We investigate the possible classical phase diagrams depending on the values of Landau's parameters. We focus in two distinct situations: regions of the phase diagram where there is a bicritical point, at which both phases vanish continuously, and the case where both phases coexist homogeneously.

3.1 Introduction

At very low temperatures, it has been reported that several SCES can exhibit competing/coexistence orders [5, 6, 7, 8, 9, 10, 11, 12, 13, 14, 15, 16, 17, 18, 19], which implies that exotic and very interesting phenomena may emerge in these systems. As a consequence, very rich experimental phase diagrams are obtained. For example, for usual metals one can obtain a non-Fermi liquid behavior associated with the existence of underlying QCPs [4]. In addition, there is also the possibility of first-order QPTs [24, 34, 35, 36]. Therefore, the study of the phase diagrams of SCES with multiple competing orders is one of the most fundamental issues that have not yet been clarified in condensed matter.

In this dissertation we are mainly interested in two distinct scenarios: the case of a bicritical point where both phases vanish continuously, and that where there is a region of coexistence between the different types of ordering in the ground state. Our main goal within this dissertation is to obtain explicitly how quantum corrections may modify the classical predictions depending on the symmetry, dimensionality and dynamic of the systems. Next, we include finite temperature effects to connect our results with the experiments.

We consider the cases where the coupling between the different order parameters is a usual quartic coupling, but also that of a bilinear interaction, whenever it is allowed by symmetry arguments. The latter breaks time-reversal symmetry and it is only allowed if both order parameters transform with the same group representation [41, 61]. This may occur in many real systems of ongoing research interest, such as, competing SDW [43, 44], different types of orbital AFM [45, 46], elastic instabilities of crystal lattices [47], vortices in a multigap SC [48] and also applies to describe the unusual magnetism of the heavy fermion compound URu_2Si_2 [41].

3.2 Landau's free energy density for multiple competing scalar orders

The simplest and direct way to describe classically competing orders and their phase transitions is by means of Landau's theory for phase transitions [5, 37, 40, 64]. As we have seen in section 1.3, the order parameters are a representation of a symmetry group of the system of interest and it encodes the crucial role of describing the existence or not of a respective ordering or symmetry breaking on the system.

The system is assumed, by construction, to be near its transition points, such that both order parameters are small, which implies that a series expansion of free energy density in terms of them is allowed [37]. The presence of a given term in the expansion of Landau's free energy density is dictated by symmetry arguments. The equilibrium state and its properties close to the transition can be obtained by minimizing the free energy as a function of the order parameters [37].

Let us consider the case of two one-component real order parameters ϕ_1 and ϕ_2, where each order parameter transforms with an irreducible representation of the Z_2 group symmetry [61]. We investigate both bilinear and quadratic couplings between them. Therefore, the Landau's free energy density ($\mathcal{F} = F/V$) of this system can be written as follows [41, 61],

$$\mathcal{F} = \frac{a_s}{2}\phi_1^2 + \frac{u_s}{4}\phi_1^4 + \frac{a_m}{2}\phi_2^2 + \frac{u_m}{4}\phi_2^4 + \frac{u_i}{2}\phi_1^2\phi_2^2 + \gamma\phi_1\phi_2 \tag{174}$$

where $a_{s,m}$, $u_{s,m,i}$ and γ are known as Landau's phenomenological parameters.

It is worth to emphasize that for $\gamma = 0$, $\mathcal{F}$ has two independent Ising symmetries, i.e., $Z_2 \times Z_2$, which means that $\mathcal{F}$ is invariant under the transformations $\phi_1 \to -\phi_1$ and $\phi_2 \to -\phi_2$, independently. However, the term $\gamma \neq 0$ breaks this symmetry to one single Ising symmetry, that is, $Z_2 \times Z_2 \to Z_2$, corresponding to change the sign of ϕ_1 and ϕ_2 simultaneously [61]. Moreover, note that since we are interested in transitions at *zero-temperature* the quantities $a_s = a_s(P)$ and $a_m = a_m(P)$ are functions of an external control parameter P, such as, pressure, doping or magnetic field, for example.

In the absence of the bilinear coupling, i.e., for $\gamma = 0$, these quantities vanish at the QCPs for their respective order parameters, that is, at the critical pressures P_{c_1} and P_{c_2}, such that $a_s(P_{c_1}) = 0$ and $a_m(P_{c_2}) = 0$. Furthermore, we take $u_{s,m} > 0$ in order to stabilize the theory, which implies that when the couplings u_i and γ between the order parameters vanish, we have two independent second order phase transitions at P_{c_1} and P_{c_2}. When the coupling between the order parameters, u_i and γ are positive we have competition between the different phases [5, 24, 29, 41, 61].

3.2.1 Minimums of free energy density

If we take $a_s = a_1(P - P_{c_1})$, $a_m = a_2(P_{c_2} - P)$, and both the coefficients of the quartic terms $u_{s,m,i}$ and γ as positive constants, Eq. (174) describes a variety of *zero-temperature* phase diagrams as a function of P [61]. As pointed out before, we focus in two different classical scenarios, i.e., bicritical ($P_{c_1} = P_{c_2}$) and coexistence ($P_{c_1} \neq P_{c_2}$) regions, and on the nature of the transitions at *zero-temperature* that occur in the presence of couplings between order parameters.

In order to build a sensitive MF phase diagram, we need to compare free energies at different phases. The simplest case occurs when only one-component order parameter is different from zero. In this case, Eq. (174) reduces to the standard one-component Landau free energy discussed in section 1.3.3.

So, we obtain two possibilities,

1. For $\phi_2 \neq 0$ and $\phi_1 = 0$, whereupon the *minimum* of free energy yields,

$$\phi_2^2 = -\frac{a_m}{u_m} \tag{175}$$

with corresponding free energy density in the form,

$$\mathcal{F}_{\phi_2} = -\frac{a_m^2}{4u_m} \ . \tag{176}$$

2. For $\phi_1 \neq 0$ and $\phi_2 = 0$, we obtain the *minimum* of free energy as follows,

$$\phi_1^2 = -\frac{a_s}{u_s} \tag{177}$$

with corresponding free energy given by,

$$\mathcal{F}_{\phi_1} = -\frac{a_s^2}{4u_s} \ . \tag{178}$$

However, when the possibility of coexistence ($\phi_{1,2} \neq 0$) is allowed, Eq. (174) should be minimized with respect to both order parameters ϕ_1 and ϕ_2 simultaneously. This procedure yields,

$$\frac{df}{d\phi_1} = \phi_1 \left(a_s + u_s\phi_1^2 + u_i\phi_2^2\right) + \gamma\phi_2 = 0 \tag{179}$$

$$\frac{df}{d\phi_2} = \phi_2 \left(a_m + u_m\phi_2^2 + u_i\phi_1^2\right) + \gamma\phi_1 = 0 \tag{180}$$

Therefore, we have essentially two cases,

- Case 1: Disordered phase $\rightarrow$ trivial solution, i.e., $\phi_1 = \phi_2 = 0$.

- Case 2: Coexistence, i.e., a phase with $\phi_1 \neq 0$ and $\phi_2 \neq 0$ simultaneously.

At this point, it is worth to point out that in coexistence region Eq. (179) and Eq. (180) give rise to a system of two coupled cubic equations, which can be easily solved numerically, but does not allow full analytical solution [41]. In that sense, for classical coexistence, we investigate a particular analytical solution for the coupled system.

3.2.2 Particular analytical solution for classical coexistence

For coexistence case we need to solve Eq. (179) and Eq. (180) self-consistently. Thus, a particular analytical solution can be obtained summing Eq. (179) and Eq. (180), which results,

$$\phi_1 \underbrace{\left(a_s + u_s\phi_1^2 + u_i\phi_2^2 + \gamma\right)}_{=0} + \phi_2 \underbrace{\left(a_m + u_m\phi_2^2 + u_i\phi_1^2 + \gamma\right)}_{=0} = 0 \tag{181}$$

where ϕ_i is taken, in principle, arbitrary, otherwise we obtain a trivial solution.

From Eq. (181), we obtain non-trivial solutions for both order parameters as follows,

$$\phi_1^2 = -\frac{(a_s + u_i\phi_2^2 + \gamma)}{u_s} \tag{182}$$

and

$$\phi_2^2 = -\frac{(a_m + u_i\phi_1^2 + \gamma)}{u_m}. \tag{183}$$

Replacing Eq. (182) and Eq. (183) into Eq. (179) and Eq. (180) one can find a particular analytical solution given by the condition $\phi_1 = \phi_2$, which satisfies the *minimum* equations. In other words, the values of ϕ_i cannot be as arbitrary as it seems for this particular analytical solution when we solve Eq. (181). Below, we investigate the consequences of this constraint on Landau's coefficients for $\phi_1 = \phi_2$ from solutions in Eq. (182) and Eq. (183).

Using $\phi_1 = \phi_2 = \phi$ in Eq. (182) and Eq. (183) we get,

$$\phi^2 = -\frac{a_s + u_i\phi^2 + \gamma}{u_s} = -\frac{a_m + u_i\phi^2 + \gamma}{u_m}\ . \tag{184}$$

Note that to satisfy Eq. (184) we need to take $a_s = a_m$ and $u_s = u_m$ at classical level. Therefore, in order to investigate the classical phase diagrams that $\phi_1 = \phi_2 = \phi$ admits, one can rewrite Eq. (184) as follows,

$$\phi^2 = -\frac{(a + u_i\phi_2^2 + \gamma)}{u} \tag{185}$$

Figure 11 - Schematic classical phase diagrams

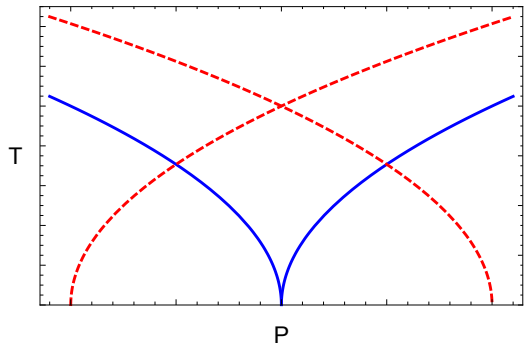

Legend: (Color online) Schematic classical phase diagrams for both types of couplings for $a_s = a_m = a = 0$ and $u_s = u_m = u > 0$. Full lines (blue) for $u_i > 0$ and $\gamma = 0$. Dashed lines (red) for $u_i = 0$ and $\gamma < 0$. In the latter case, the bilinear coupling γ induces a region of coexistence where both order parameters are finite at $a_s = a_m = 0$.
Source: Ref. [61].

where $a_s = a_m = a$ and $u_s = u_m = u$.

From Eq. (185) one can obtain three possible classical phase diagrams depending on Landau's coefficients, that is,

1. Bicritical case $\rightarrow a_s = a_m = a = 0$ and $\gamma \geq 0$, which implies that the *minimum* of free energy, Eq. (174), is given by $\phi = 0$.

2. Bicritical case, $a_s = a_m = a = 0$, that give rises to coexistence for $u_i = 0$ and $\gamma < 0$ is perfectly admitted with $\phi \neq 0$.

3. Coexistence for $a_s = a_m = a < 0$ and $\gamma < 0$, as can be seen from Eq. (185).

Therefore, at classical level, bicritical point and coexistence region are perfectly possible depending on Landau's coefficients, as shown in Fig. 11.

The crucial difference from our case when compared to different approaches [5, 41] is that in our starting point we investigate the scenario whereupon we project the bicritical point at finite-temperatures to the *zero-temperature* axis, as can be seen from the red arrow in Fig. 12 (right panel). Thus, the quantities $a_{s,m} = a_{s,m}(P)$ are functions of an external control parameter P only, i.e., it does not depend on temperature.

We can also obtain the solutions in Eq. (182) into Eq. (183) in terms of Landau's coefficient only. In that spirit, we replace Eq. (183) into Eq. (182) as follows,

$$\begin{aligned} \phi_1^2 &= -\frac{1}{u_s}\left\{a_s + \gamma + u_i\left[-\frac{(a_m + u_i\phi_1^2 + \gamma)}{u_m}\right]\right\} \\ &= -\frac{1}{u_s u_m}\left[(a_s + \gamma)u_m - u_i(a_m + u_i\phi_1^2 + \gamma)\right] \end{aligned} \tag{186}$$

Figure 12 - Projected bicritical point

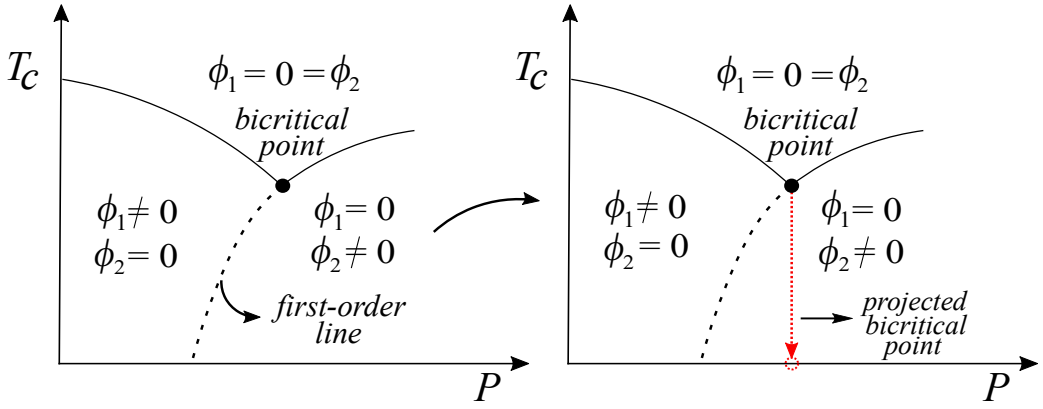

Legend: (Color online) Bicritical point at finite-temperatures projected to the *zero-temperature* axis.

Source: Ref. [5]. Adapted by the author.

Grouping ϕ_1^2 terms,

$$\left(u_s u_m - u_i^2\right)\phi_1^2 = -\left[a_s u_m - a_m u_i + \gamma(u_m - u_i)\right]. \tag{187}$$

Finally, we get,

$$\phi_1^2 = \frac{a_s u_m - a_m u_i + \gamma(u_m - u_i)}{u_i^2 - u_s u_m}, \tag{188}$$

where the stability condition for coexistence is given by $u_i < \sqrt{u_s u_m}$ for $\gamma = 0$, as stated in Refs. [5, 41, 61].

On the other hand, one can also obtain a similiar expression for ϕ_2^2. Replacing Eq. (182) into Eq. (183),

$$\begin{aligned}\phi_2^2 &= -\frac{1}{u_m}\left\{a_m + \gamma + u_i\left[-\frac{(a_s + u_i\phi_2^2 + \gamma)}{u_s}\right]\right\} \\ &= -\frac{1}{u_s u_m}\left[(a_m + \gamma)\,u_s - u_i\left(a_s + u_i\phi_2^2 + \gamma\right)\right]\end{aligned} \tag{189}$$

Grouping ϕ_2^2 terms,

$$\left(u_s u_m - u_i^2\right)\phi_2^2 = -\left[a_m u_s - a_s u_i + \gamma\,(u_s - u_i)\right], \tag{190}$$

Therefore,

$$\phi_2^2 = \frac{a_m u_s - a_s u_i + \gamma\,(u_s - u_i)}{u_i^2 - u_s u_m}, \tag{191}$$

where $a_s = a_m$ and $u_s = u_m$ in solutions of Eq. (188) and Eq. (191) for classical coexistence when $\gamma \neq 0$.

Replacing Eq. (188) and Eq. (191) into Eq. (174) one can rewrite the free energy density in the form [61],

$$\begin{aligned}\mathcal{F} &= f_s + f_m - \frac{2a_s a_m u_i}{4D_{sm}} + \frac{\gamma^2(-u_s - u_m + 2u_i)}{4D_{sm}} + \\ &+ \frac{\gamma\left[a_s u_m - a_m u_i + \gamma(u_m - u_i)\right]^{1/2}\left[a_m u_s - a_s u_i + \gamma(u_s - u_i)\right]^{1/2}}{D_{sm}}\end{aligned} \tag{192}$$

where, $f_s = \frac{a_s^2 u_m}{4D_{sm}}$, $f_m = \frac{a_m^2 u_s}{4D_{sm}}$ and $D_{sm} = u_i^2 - u_s u_m$.

Note that if we take $a_s = a_1(P - P_{c_1})$, $a_m = a_2(P_{c_2} - P)$, the coefficients of the quartic terms $u_{s,m,i}$ and γ as positive constants, Eq. (192) describe a variety of *zero-temperature* phase diagrams and phase transitions as a function of P. We consider first the classical case and the effect of each type of interaction separately. In the next chapter, we include the effect of quantum corrections and then we introduce finite temperature effects.

3.2.3 Free energy density depending on couplings

Initially, for the case of an exclusive quartic interaction, i.e., for $\gamma = 0$ in Eq. (174), or equivalently for $\gamma = 0$ in Eq. (192), we have no longer the condition for a particular analytical solution in Eq. (184), which implies that ϕ_i is now arbitrary, as can be seen from the *minimum* of free energy. Therefore, we get [61],

$$\mathcal{F} = f_m + \frac{(a_s u_m - a_m u_i)^2}{4u_m D_{sm}} = f_s + \frac{(a_m u_s - a_s u_i)^2}{4u_s D_{sm}} \tag{193}$$

where $D_{sm} = u_i^2 - u_s u_m$.

Note, from Eq. (193), that coexistence is only possible if $D_{sm} < 0$, i.e., if $u_i < \sqrt{u_s u_m}$, so that free energy density of the two coexisting phases is smaller than condensation energies of individual phases f_m and f_s [61].

It is worth to point out the particular point in the phase diagram where both phases vanish at the same critical value of external control parameter, i.e., for $P_{c_1} = P_{c_2} = P_c$. It is easy to verify, from Eq. (193), that this specific point is given by $a_s = a_m = 0$ even for finite u_i and $D_{sm} < 0$. On the other hand, this is not necessarily the case in the presence of a finite bilinear coupling γ for $u_i = 0$, as will be discussed below.

For $u_i = 0$ we obtain equilibrium values in Eq. (182) and Eq. (183) as follows [61],

$$\phi_1^2 = -\frac{a_s + \gamma}{u_s} \tag{194}$$

and

$$\phi_2^2 = -\frac{a_m + \gamma}{u_m} \ . \tag{195}$$

Using Eq. (194) and Eq. (195) in free energy density we obtain [61],

$$\mathcal{F} = f_s + f_m + \gamma\sqrt{\frac{(a_s+\gamma)(a_m+\gamma)}{u_s u_m}} + \frac{\gamma^2}{4}\left(\frac{u_s+u_m}{u_s u_m}\right) \ . \tag{196}$$

Eq. (196) shows that phase coexistence is only possible for $\gamma < 0$, such that the total free energy density of the system f is less than the sum $f_s + f_m$. This condition is also implicit in Eq. (194) and Eq. (195) [61].

Let us consider again the peculiar point in the phase diagram, i.e., $a_s = a_m = 0$. We note a quite different behavior from that of the previous case. Indeed, from Eq. (194) and Eq. (195), we realize that at classical level the system can have finite order parameters induced by bilinear coupling (γ), even for $a_s = a_m = 0$ (see Fig. 11).

For completeness, when both couplings are finite we can see from Eq. (192) that the condition for coexistence requires that $\gamma < 0$ as well as $u_i < \sqrt{u_s u_m}$, where we must consider the particular analytical solution in Eq. (184). For the special case $a_s = a_m = 0$, we notice again that both order parameters are finite due to the bilinear coupling γ as long as γ remains negative and the conditions $u_m > u_i$ and $u_s > u_i$ are satisfied. Notice that the latter automatically imply $u_i < \sqrt{u_s u_m}$ [61], or equivalently $u_i < u$ for $u_s = u_m = u$.

In the next chapter we are going to calculate the quantum corrections to the ground state energy of the system described by Eq. (174) within *one-loop* approximation. We will see that the classical phase diagrams shown in Fig. 11 are strongly affected by quantum fluctuations. However, before that, it turn out that on *one-loop* approximation, the contribution from the bilinear term to these corrections is an infinite constant independent of the fields [61]. This problem can be circumvented applying a linear transformation with det = 1 (rotation) to the classical fields, as will be presented below.

3.2.4 Linear transformation on the free energy density

The quadratic-order terms in the fields of Eq. (174) are given by,

$$\mathcal{F}_q = \frac{a_s}{2}\phi_1^2 + \frac{a_m}{2}\phi_2^2 + \gamma\phi_1\phi_2 \tag{197}$$

In that sense, we apply a linear transformation to the classical fields with det = 1, which is related to a rotation, as follows,

$$\phi_1 = \alpha\varphi_1 + \beta\varphi_2 \qquad \texttt{and} \qquad \phi_2 = -\beta\varphi_1 + \alpha\varphi_2 \tag{198}$$

where $\alpha^2 + \beta^2 = 1$.

Note that one can parametrize this transformation with just one parameter θ taking,

$$\alpha = \cos\theta \qquad \texttt{and} \qquad \beta = \sin\theta \tag{199}$$

Therefore, replacing Eq. (198) and Eq. (199) into Eq. (197) we get a diagonal form,

$$\mathcal{F}_d = r_1\varphi_1^2 + r_2\varphi_2^2 \tag{200}$$

where,

$$r_1 = \frac{a_s}{2}\cos^2\theta + \frac{a_m}{2}\sin^2\theta - \gamma\cos\theta\sin\theta \tag{201}$$

and

$$r_2 = \frac{a_s}{2}\sin^2\theta + \frac{a_m}{2}\cos^2\theta + \gamma\cos\theta\sin\theta \tag{202}$$

being that the parameter θ is defined by,

$$\tan\,(2\theta) = \frac{2\gamma}{a_m - a_s}\ . \tag{203}$$

Replacing now Eq. (198) into the remaining interaction terms of free energy, Eq. (174), we get [61],

$$\mathcal{F} = r_1\varphi_1^2 + r_2\varphi_2^2 + \lambda_1\varphi_1^4 + \lambda_2\varphi_2^4 + \lambda_{12}\varphi_1^2\varphi_2^2 + \delta_1\varphi_1^3\varphi_2 + \delta_2\varphi_1\varphi_2^3 \tag{204}$$

where,

$$\begin{aligned}
\lambda_1 &= u_s\alpha^4 + u_m\beta^4 + u_i\alpha^2\beta^2\ , \\
\lambda_2 &= u_m\alpha^4 + u_s\beta^4 + u_i\alpha^2\beta^2\ , \\
\lambda_{12} &= 6(u_s + u_m)\alpha^2\beta^2 + u_i(\alpha^4 - 4\alpha^2\beta^2 + \beta^4)\ , \\
\delta_1 &= 4u_s\alpha^3\beta - 4u_m\alpha\beta^3 + 2u_i(-\alpha^3\beta + \alpha\beta^3)\ , \\
\delta_2 &= 4u_s\alpha\beta^3 - 4u_m\alpha^3\beta + 2u_i(\alpha^3\beta - \alpha\beta^3)\ .
\end{aligned} \tag{205}$$

It is worth to emphasize that λ_i's and δ_i's in Eq. (204) are new arbitrary constants and that the bilinear coupling has been replaced by new terms of higher order in the fields (with coefficients δ_i), but with the same symmetry properties. The analysis of the classical ground state energy in this new basis is similar to that developed before. Thus, for $\gamma \neq 0$ the coexistence now is given by the condition $\lambda_{12}^2 < 4\lambda_1\lambda_2 + \delta_2\lambda_1 + \delta_1\lambda_2 + \delta_1\delta_2/4$ [61].

Finally, it is important to recall that the main effect of the coupling γ in the former basis, at classical level, is to shift the QCPs, as can be seen in Eq. (194) and Eq. (195) and is shown in Fig. 11. Therefore, the analysis in this new basis is more simple if carried out close to the new QCPs at $r_1 = 0$ and $r_2 = 0$.

4 QUANTUM CORRECTIONS ON THE *MEAN-FIELD* PHASE DIAGRAMS OF SYSTEMS WITH MULTIPLE COMPETING SCALAR ORDERS

In this chapter we will apply the *one-loop* effective potential approximation from QFT to obtain quantum corrections on the *zero-temperature* MF phase diagrams of systems exhibiting multiple competing scalar order parameters for 3d and 2d materials characterized by both dynamic critical exponents $z = 1$ and $z = 2$ [4, 24, 41, 51]. We focus in two different scenarios: a bicritical point and coexistence regions. We will discuss our results [61, 62] at *zero-temperature*, and we will see that quantum fluctuations may play a crucial role to determine the nature of the phase diagrams depending on the symmetry, dimensionality and dynamic of the propagators describing the excitations of the possible ordered states. We will show that the effect of quantum corrections is essential to understand the emergence of stable unconventional coexisting orders experimentally observed in SCES [61, 62].

4.1 Introduction

Throughout this chapter we investigate the effect of quantum corrections on the *zero-temperature* MF phase diagrams of systems with competing scalar orders taking into account two different types of coupling between the order parameters. As pointed out before, we are mainly interested in two different scenarios: the case of a bicritical point where both phases vanish continuously, and that where there is a region of coexistence between the different types of ordering in the ground state. Our goal in this chapter is to obtain explicitly how quantum corrections may modify the classical predictions within MF approach, depending on symmetry, dimensionality and dynamic of the systems.

We consider the cases whereupon the coupling between the different order parameters is a usual quartic coupling, but also that of a bilinear interaction, whenever it is allowed by symmetry arguments [61, 62]. The latter breaks time-reversal symmetry and it is only allowed if both order parameters transform with the same group representation [41, 61, 62]. Thus, bilinear coupling has been used to study many real systems of ongoing research interest, such as, competing SDW [43, 44], different types of orbital AF [45, 46], elastic instabilities of crystal lattices [47], vortices in a multigap SC [48] and also applies to describe the unusual magnetism of the heavy fermion compound URu_2Si_2 [41].

In order to obtain quantum effects we use the *one-loop* effective potential approximation from QFT [24, 54, 55], that provides the more direct and simple way to introduce

quantum corrections to the classical action. We will work in a region of parameter space close to the QCPs of the competing ground states, such that, both order parameters are small and consequently allow for a Landau-type expansion of free energy density. We will describe quantum dynamics of the critical modes for the competing phases by propagators associated with dynamic critical exponents $z = 1$ as well as $z = 2$ [4, 24, 51, 52] for 3d [61] and 2d [62] systems.

4.2 *One-loop* approximation for multiple competing scalar orders

As we have discussed in section 2.3.3 and section 2.3.4, the *one-loop* effective potential approximation provides the most simple and direct approach to investigate effects of quantum corrections on the classical phase diagrams. At *one-loop* level, the effective potential ($V_{eff}(\phi_i)$) is given by the expansion [24, 61, 62],

$$V_{eff}(\phi_i) = V_c(\phi_i) + \hbar\Gamma^{(1)}(\phi_i) + \mathcal{O}(\hbar^2) \tag{206}$$

where $V_c(\phi_i)$ is the classical potential, i.e., the Landau free energy density, and $\Gamma^{(1)}(\phi_i)$ encodes the quantum fluctuations at linear order in $\hbar$, that is, it is the first-order quantum corrections term. The fields ϕ_i are the homogeneous order parameters, which implies that the phases of the system are obtained by calculating $\partial V_{eff}/\partial\phi_i = 0$ [61, 62].

From Eq. (117) one can recognize that the first-order quantum correction term ($\Gamma^{(1)}(\phi_i)$) in Eq. (206) is given by [4, 24, 54, 55, 61, 62],

$$\Gamma^{(1)}(\phi_i) = \frac{1}{2}\int \frac{d^dk}{(2\pi)^d} \ln\left(\det\left[\mathbb{I} - M(k)\right]\right) + \texttt{counterterms}\ . \tag{207}$$

where the counterterms are necessary to renormalize the theory, and $M(k)$ is a matrix whose elements $[M]_{lm}$ can be written as follows,

$$[M]_{lm} = -G_0^{(l)}(k)\left[\frac{\partial^2 V_c^{int}(\phi_i)}{\partial\phi_l\partial\phi_m}\right]\Bigg|_{\phi_i=\phi_c}\ . \tag{208}$$

Note, from Eq. (208), that $G_0^{(l)}(k)$ are the propagators associated with the fields (ϕ_l) and V_c^{int} is the interacting part of the classical potential, that is, the Landau free energy density without mass terms ($r_{1,2}$), see Eq. (204). Finally, dynamical effects are taken into account through the frequency dependent propagators [61].

For simplicity, we will consider that the two phases have the same dynamics described by propagators associated with both dynamic critical exponent $z = 1$ and $z = 2$ [4, 24, 51, 52, 61, 62] separately. The former is characterized by a non-dissipative behavior, whereas the latter is associated with a dissipative one [51, 61, 62]. It results

from the relation between the n^{th} order time derivatives and the gradient terms in non-stationary Ginzburg–Landau equation, i.e., the frequency and wave-vector dependence of the propagators [51, 52, 61, 70], see section 2.2.

These two types of dynamics considered in this dissertation are appropriate to describe magnetic phases with excitations with linear dispersion relations ($z = 1$), SCs [4, 20, 24, 51, 61] or to superfluid liquid ^{3}He [52] as well as paramagnons in itinerant AFM/FM [51] or overdamped modes in SC [4, 62] near their QCPs ($z = 2$), as discussed in section 2.2.

The two relevant propagators are given by [4, 24, 51, 52, 61, 62],

$$G_0^{(1,2)}(k) = G_0^{(1,2)}(\omega, \vec{q}) = \frac{1}{k^2 + r_{1,2}} \tag{209}$$

and

$$D_0^{(1,2)}(k) = D_0^{(1,2)}(\omega, \vec{q}) = \frac{1}{\omega\,|\tau| + q^2 + r_{1,2}} \tag{210}$$

where $k^2 = \omega^2 + q^2$ (Euclidean space) and the propagators in Eq. (209) and Eq. (210) are associated with $z = 1$ and $z = 2$, respectively.

4.3 Quantum corrections for three-dimensional systems with linear dispersion relation

Initially, let us apply the *one-loop* effective potential approach for 3d systems characterized by linear dispersion relations, i.e., for $z = 1$, whereupon both phases have the same dynamic, which implies that $d_{eff} = 3{+}1 = 4$ [61]. The propagators, in Euclidean space, are given by [61],

$$G^{(1)}(k) = G_0(w, \vec{q}) = \frac{1}{k^2 + r_1} \qquad \texttt{and} \qquad G^{(2)}(k) = G_0(w, \vec{q}) = \frac{1}{k^2 + r_2} \tag{211}$$

where $k^2 = \omega^2 + q^2$ (Euclidean space).

In order to calculate the derivatives for Eq. (208) we need to identify V_c^{int} from Eq. (204), that is,

$$\mathcal{F} = V_c = r_1\varphi_1^2 + r_2\varphi_2^2 + \lambda_1\varphi_1^4 + \lambda_2\varphi_2^4 + \lambda_{12}\varphi_1^2\varphi_2^2 + \delta_1\varphi_1^3\varphi_2 + \delta_2\varphi_1\varphi_2^3 \tag{212}$$

As we have seen before, the two first terms in Eq. (212) are related to the free term and does not enter into the calculation of Eq. (208), which implies that V_c^{int} is thus given by,

$$V_c^{int} = \lambda_1\varphi_1^4 + \lambda_2\varphi_2^4 + \lambda_{12}\varphi_1^2\varphi_2^2 + \delta_1\varphi_1^3\varphi_2 + \delta_2\varphi_1\varphi_2^3 \tag{213}$$

From Eq. (213) we obtain $[M]_{lm}(k)$ in Eq. (208) as follows,

$$[M]_{lm}(k) = \begin{pmatrix} M_{11} = -\frac{\left[12\lambda_1\varphi_1^2+2\lambda_{12}\varphi_2^2+6\delta_1\varphi_1\varphi_2\right]}{k^2+r_1} & M_{12} = -\frac{\left[3\delta_1\varphi_1^2+3\delta_2\varphi_2^2+4\lambda_{12}\varphi_1\varphi_2\right]}{k^2+r_1} \\ M_{21} = -\frac{\left[3\delta_1\varphi_1^2+3\delta_2\varphi_2^2+4\lambda_{12}\varphi_1\varphi_2\right]}{k^2+r_2} & M_{22} = -\frac{\left[12\lambda_2\varphi_2^2+2\lambda_{12}\varphi_1^2+6\delta_2\varphi_1\varphi_2\right]}{k^2+r_2} \end{pmatrix} \quad (214)$$

Note, from Eq. (207), that to obtain the first-order quantum corrections contribution we need to calculate the following integral,

$$\Gamma^{(1)}[\varphi_{1,2}] = \frac{1}{2}\int \frac{d^dk}{(2\pi)^d}\ \ln\ \det[\mathbb{I} - M(k)] + \texttt{counterterms} \quad (215)$$

where $M(k)$ is the matrix given by Eq. (214) and the counterterms are necessary to renormalize the theory.

Calculating the determinant in Eq. (215) one can rewrite $\Gamma^{(1)}[\varphi_{1,2}]$ in the form [61],

$$\begin{aligned} \Gamma^{(1)} &= \frac{1}{2}\int \frac{d^dk}{(2\pi)^d}\ \ln\ \left[\left(1+\frac{\left[12\lambda_1\varphi_1^2+2\lambda_{12}\varphi_2^2+6\delta_1\varphi_1\varphi_2\right]}{k^2+r_1}\right)\times\right. \\ &\times \left(1+\frac{\left[12\lambda_2\varphi_2^2+2\lambda_{12}\varphi_1^2+6\delta_2\varphi_1\varphi_2\right]}{k^2+r_2}\right)+ \\ &- \left.\left(\frac{\left(3\delta_1\varphi_1^2+3\delta_2\varphi_2^2+4\lambda_{12}\varphi_1\varphi_2\right)^2}{(k^2+r_1)(k^2+r_2)}\right)\right] + \texttt{counterterms} \end{aligned} \quad (216)$$

It is worth to point out that the integral in Eq. (216) is not trivial to solve. In that sense, in order to calculate the integral in Eq. (216) we will series expand the logarithm and truncate it at $\mathcal{O}\left(3\delta_1\varphi_1^2+3\delta_2\varphi_2^2+4\lambda_{12}\varphi_1\varphi_2\right)^2$ [61].

However, before that, let us make the following identifications in Eq. (216),

$$\begin{aligned} a &= \frac{12\lambda_1\varphi_1^2+2\lambda_{12}\varphi_2^2+6\delta_1\varphi_1\varphi_2}{k^2+r_1}\ , \\ b &= \frac{12\lambda_2\varphi_2^2+2\lambda_{12}\varphi_1^2+6\delta_2\varphi_1\varphi_2}{k^2+r_2}\ , \\ c &= -\frac{1}{(k^2+r_1)(k^2+r_2)}\ . \end{aligned} \quad (217)$$

With the help of Eq. (217), one can rewrite Eq. (216) as follows,

$$\Gamma^{(1)} = \frac{1}{2}\int \frac{d^dk}{(2\pi)^d}\ln\left[(1+a)(1+b)+c\left(3\delta_1\varphi_1^2+3\delta_2\varphi_2^2+4\lambda_{12}\varphi_1\varphi_2\right)^2\right] + \texttt{counterterms} \quad (218)$$

Therefore, making a series expansion of the logarithm in Eq. (218) and truncating

at $\mathcal{O}\left(3\delta_1\varphi_1^2 + 3\delta_2\varphi_2^2 + 4\lambda_{12}\varphi_1\varphi_2\right)^2$ we obtain,

$$\begin{aligned}\Gamma^{(1)} &= \frac{1}{2}\int \frac{d^dk}{(2\pi)^d}\ln\left[(1+a)(1+b)\right] + \\ &+ \frac{1}{2}\int \frac{d^dk}{(2\pi)^d}\frac{c\left(3\delta_1\varphi_1^2 + 3\delta_2\varphi_2^2 + 4\lambda_{12}\varphi_1\varphi_2\right)^2}{(1+a)(1+b)} + \texttt{counterterms}\end{aligned} \tag{219}$$

Before solving the integrals in Eq. (219) let us first focus on the second integral of Eq. (219),

$$I_2 = \frac{1}{2}\int \frac{d^dk}{(2\pi)^d}\frac{c\left(3\delta_1\varphi_1^2 + 3\delta_2\varphi_2^2 + 4\lambda_{12}\varphi_1\varphi_2\right)^2}{(1+a)(1+b)} \tag{220}$$

Replacing back the definitions of Eq. (217) into Eq. (220) we get,

$$\begin{aligned}I_2 &= \frac{\left(3\delta_1\varphi_1^2 + 3\delta_2\varphi_2^2 + 4\lambda_{12}\varphi_1\varphi_2\right)^2}{2}\times \\ &\times \int \frac{d^dk}{(2\pi)^d}\frac{-\frac{1}{(k^2+r_1)(k^2+r_2)}}{\left(1+\frac{12\lambda_1\varphi_1^2+2\lambda_{12}\varphi_2^2+6\delta_1\varphi_1\varphi_2}{k^2+r_1}\right)\left(1+\frac{12\lambda_2\varphi_2^2+2\lambda_{12}\varphi_1^2+6\delta_2\varphi_1\varphi_2}{k^2+r_2}\right)}\end{aligned} \tag{221}$$

So,

$$I_2 = -\frac{\left(3\delta_1\varphi_1^2 + 3\delta_2\varphi_2^2 + 4\lambda_{12}\varphi_1\varphi_2\right)^2}{2}\int \frac{d^dk}{(2\pi)^d}\frac{1}{(k^2+A^2)(k^2+B^2)} \tag{222}$$

where,

$$A^2 = r_1 + 12\lambda_1\varphi_1^2 + 2\lambda_{12}\varphi_2^2 + 6\delta_1\varphi_1\varphi_2 \quad \texttt{and} \quad B^2 = r_2 + 12\lambda_2\varphi_2^2 + 2\lambda_{12}\varphi_1^2 + 6\delta_2\varphi_1\varphi_2 \tag{223}$$

Using the following identity in Eq. (222),

$$\frac{1}{(k^2+A^2)(k^2+B^2)} = \frac{1}{B^2-A^2}\left(\frac{1}{k^2+A^2} - \frac{1}{k^2+B^2}\right) \tag{224}$$

One can rewrite I_2 as follows,

$$I_2 = -\frac{\left(3\delta_1\varphi_1^2 + 3\delta_2\varphi_2^2 + 4\lambda_{12}\varphi_1\varphi_2\right)^2}{2(B^2-A^2)}\int \frac{d^dk}{(2\pi)^d}\left(\frac{1}{k^2+A^2} - \frac{1}{k^2+B^2}\right) \tag{225}$$

Therefore, from Eq. (217), Eq. (219) and Eq. (225), we obtain $\Gamma^{(1)}$ in the form [61],

$$\begin{aligned}\Gamma^{(1)} &= \frac{1}{2}\int \frac{d^dk}{(2\pi)^d}\ln\left[\left(1+\frac{b_1}{k^2+r_1}\right)\right] + \frac{1}{2}\int \frac{d^dk}{(2\pi)^d}\ln\left[\left(1+\frac{b_2}{k^2+r_2}\right)\right] + \\ &- \frac{\left(3\delta_1\varphi_1^2 + 3\delta_2\varphi_2^2 + 4\lambda_{12}\varphi_1\varphi_2\right)^2}{2(B^2-A^2)}\int \frac{d^dk}{(2\pi)^d}\left(\frac{1}{k^2+A^2} - \frac{1}{k^2+B^2}\right) + \\ &+ \texttt{counterterms}\end{aligned} \tag{226}$$

where,

$$\begin{aligned} b_1 &= 12\lambda_1\varphi_1^2 + 2\lambda_{12}\varphi_2^2 + 6\delta_1\varphi_1\varphi_2 \ ; \\ b_2 &= 12\lambda_2\varphi_2^2 + 2\lambda_{12}\varphi_1^2 + 6\delta_2\varphi_1\varphi_2 \ ; \\ A^2 &= r_1 + b_1 \ ; \\ B^2 &= r_2 + b_2 \ . \end{aligned} \tag{227}$$

It is worth to emphasize that Eq. (226) is completely general within a d-dimensional system with free energy density in the form of Eq. (212) and with order parameters characterized by dynamic critical exponents $z = 1$. Moreover, note that $d^dk = S_d k^{d-1} dk$, where $S_d = (2\pi)^{d/2}/\Gamma(d/2)$. So, for example, using this definitions in Eq. (225) for (3+1) dimensions, we have the following integrals to solve for I_2,

$$\frac{\pi^2}{(2\pi)^4} \int_0^\Lambda dk \ k^3 \frac{1}{k^2 + (A,B)^2} \tag{228}$$

where A and B, given in Eq. (227), are constants in relation to k, and Λ is the *cut-off* introduced since the integrals in Eq. (228) are divergent.

Thus, for (3+1) dimensions, we obtain $\Gamma^{(1)}$ in Eq. (226) as follows [61],

$$\begin{aligned} \Gamma^{(1)} &= \frac{1}{2}\int \frac{d^4k}{(2\pi)^4} \ln\left[\left(1 + \frac{b_1}{k^2 + r_1}\right)\right] + \frac{1}{2}\int \frac{d^4k}{(2\pi)^4} \ln\left[\left(1 + \frac{b_2}{k^2 + r_2}\right)\right] + \\ &- \frac{\left(3\delta_1\varphi_1^2 + 3\delta_2\varphi_2^2 + 4\lambda_{12}\varphi_1\varphi_2\right)^2}{2(B^2 - A^2)} \int \frac{d^4k}{(2\pi)^4} \left(\frac{1}{k^2 + A^2} - \frac{1}{k^2 + B^2}\right) + \\ &+ \texttt{counterterms} \end{aligned} \tag{229}$$

where b_1, b_2, A and B are given in Eq. (227).

In the limit of $\Lambda \to \infty$ the two first integrals in Eq. (229) have solutions in the form [4, 61],

$$I_{1,2} = \frac{\pi^2}{(2\pi)^4}\left[\frac{\Lambda^2}{2} b_{1,2} + \frac{(b_{1,2} + r_{1,2})^2}{4} \ln\left(\frac{b_{1,2} + r_{1,2}}{\Lambda^2}\right) - \frac{b_{1,2}^2}{8} - \frac{r_{1,2}^2}{4} \ln\left(\frac{r_{1,2}}{\Lambda^2}\right)\right] \tag{230}$$

On the other hand, in the limit of $\Lambda \to \infty$ the last two integrals in Eq. (229) have solutions given by [61],

$$I_{3,4} = \frac{\pi^2}{(2\pi)^4}\left[\frac{1}{2}\Lambda^2 + \frac{(A,B)^2}{2} \ln\left((A,B)^2\right) - \frac{(A,B)^2}{2} \ln\left((A,B)^2 + \Lambda^2\right)\right] \tag{231}$$

Summing Eq. (230) and Eq. (231) we get,

$$\begin{aligned}\Gamma^{(1)}_{\varphi_{1,2}} &= \frac{\pi^2}{(2\pi)^4}\left[\frac{\Lambda^2}{2}(b_1+b_2)+\frac{(b_1+r_1)^2}{4}\ln\left(\frac{b_1+r_1}{\Lambda^2}\right)+\frac{(b_2+r_2)^2}{4}\ln\left(\frac{b_2+r_2}{\Lambda^2}\right)+\right.\\ &- \frac{(b_1^2+b_2^2)}{8}-\frac{r_1^2}{4}\ln\left(\frac{r_1}{\Lambda^2}\right)-\frac{r_2^2}{4}\ln\left(\frac{r_2}{\Lambda^2}\right)+\\ &- \left.\frac{\left(3\delta_1\varphi_1^2+3\delta_2\varphi_2^2+4\lambda_{12}\varphi_1\varphi_2\right)^2}{4}\left(\ln\left(\frac{1}{\Lambda^2}\right)+\frac{B^2\ln(B^2)-A^2\ln(A^2)}{B^2-A^2}\right)\right]+\\ &+ \texttt{counterterms} \end{aligned} \tag{232}$$

where b_1, b_2, A and B are given in Eq. (227).

It is worth to point out that we have to include the counterterms to make the theory *cut-off* (Λ) independent [61, 72]. For this case, we have counterterms in the form [61],

$$\frac{1}{2}C_1\varphi_1^2\ ,\ \frac{1}{2}C_2\varphi_2^2\ ,\ C_3\varphi_1\varphi_2\ ,\ \frac{1}{4!}D_1\varphi_1^4\ ,\ \frac{1}{4!}D_2\varphi_2^4\ ,\ \frac{1}{4}D_3\varphi_1^2\varphi_2^2\ ,\ \frac{1}{6}D_4\varphi_1^3\varphi_2\ ,\ \frac{1}{6}D_5\varphi_1\varphi_2^3\ ; \tag{233}$$

where we need to identify C_i and D_i in Eq. (233).

Once we obtain Eq. (232) one can investigate the cases of interest of this dissertation, i.e., bicritical point and coexistence regions.

4.3.1 Bicritical point

Since we are close to the bicritical point one can make a series expansion of the *one-loop* effective potential in Eq. (232) for both mass terms r_1 and r_2 concomitantly [61]. Therefore, the simplest way for renormalize the *one-loop* effective potential in bicritical case, as a first approximation, is to expand Eq. (232) for small $r_{1,2}$ and then consider the values of $r_{1,2} \approx 0$ [61], which yields,

$$\begin{aligned}\Gamma^{(1)}_{\varphi_{1,2}} &= \frac{\pi^2}{(2\pi)^4}\left[\frac{\Lambda^2}{2}(b_1+b_2)+\frac{b_1^2}{4}\ln\left(\frac{b_1}{\Lambda^2}\right)+\frac{b_2^2}{4}\ln\left(\frac{b_2}{\Lambda^2}\right)-\frac{(b_1^2+b_2^2)}{8}+\right.\\ &- \left.\frac{\left(3\delta_1\varphi_1^2+3\delta_2\varphi_2^2+4\lambda_{12}\varphi_1\varphi_2\right)^2}{4}\left(\ln\left(\frac{1}{\Lambda^2}\right)+\frac{b_2\ln(b_2)-b_1\ln(b_1)}{b_2-b_1}\right)\right]+\\ &+ \texttt{counterterms} \end{aligned} \tag{234}$$

To calculate the required counterterms to make the theory *cut-off* independent we use the following definitions [61],

$$\left[\frac{d^2\Gamma^{(1)}}{d\varphi_1^2}\right]\Big|_{\varphi_{1,2}=0} = r_1 = 0\ \ ,\ \ \left[\frac{d^2\Gamma^{(1)}}{d\varphi_2^2}\right]\Big|_{\varphi_{1,2}=0} = r_2 = 0\ \ ,\ \left[\frac{d^2\Gamma^{(1)}}{d\varphi_1\varphi_2}\right]\Big|_{\varphi_1=\langle\varphi_1\rangle,\varphi_2=\langle\varphi_2\rangle} = \gamma$$

$$\left[\frac{d^4\Gamma^{(1)}}{d\varphi_1^4}\right]\Big|_{\varphi_1=\langle\varphi_1\rangle,\phi_{2=0}} = \lambda_1 \quad , \quad \left[\frac{d^4\Gamma^{(1)}}{d\varphi_2^4}\right]\Big|_{\varphi_1=0,\varphi_2=\langle\varphi_2\rangle} = \lambda_2 \quad , \quad \left[\frac{d^4\Gamma^{(1)}}{d\varphi_1^2\varphi_2^2}\right]\Big|_{\varphi_1=\langle\varphi_1\rangle,\varphi_2=\langle\varphi_2\rangle} = \lambda_{12}$$

$$\left[\frac{d^4\Gamma^{(1)}}{d\varphi_1^3\varphi_2}\right]\Big|_{\varphi_1=\langle\varphi_1\rangle,\varphi_2=\langle\varphi_2\rangle} = \delta_1 \quad , \quad \left[\frac{d^2\Gamma^{(1)}}{d\varphi_1\varphi_2^3}\right]\Big|_{\varphi_1=\langle\varphi_1\rangle,\varphi_2=\langle\varphi_2\rangle} = \delta_2 \ . \tag{235}$$

where $\langle\varphi_{1,2}\rangle$ corresponds to the minimum of the effective potential.

Calculating the derivatives of Eq. (235) we obtain the counterterms as follows [61],

$$\frac{1}{2}C_1\varphi_1^2 = -\frac{1}{2}\frac{\pi^2}{(2\pi)^4}\left[\Lambda^2(12\lambda_1+2\lambda_{12})\right]\varphi_1^2 \tag{236}$$

$$\frac{1}{2}C_2\varphi_2^2 = -\frac{1}{2}\frac{\pi^2}{(2\pi)^4}\left[\Lambda^2(12\lambda_2+2\lambda_{12})\right]\varphi_2^2 \tag{237}$$

$$C_3\varphi_1\varphi_2 = -\frac{1}{2}\frac{\pi^2}{(2\pi)^4}\left[\Lambda^2(3\delta_1+3\delta_2)\right]\varphi_1\varphi_2 \tag{238}$$

$$\begin{aligned}\frac{1}{4!}D_1\varphi_1^4 &= -\frac{1}{4!}\frac{\pi^2}{(2\pi)^4}\left[288\left(11+3\ln\left(\frac{12\lambda_1\langle\varphi_1\rangle^2}{\Lambda^2}\right)\right)\lambda_1^2 + \right.\\ &+ \left. 8\lambda_{12}^2\left(11+3\ln\left(\frac{2\lambda_{12}\langle\varphi_1\rangle^2}{\Lambda^2}\right)\right)\right]\varphi_1^4\end{aligned} \tag{239}$$

$$\begin{aligned}\frac{1}{4!}D_2\varphi_2^4 &= -\frac{1}{4!}\frac{\pi^2}{(2\pi)^4}\left[288\left(11+3\ln\left(\frac{12\lambda_2\langle\varphi_2\rangle^2}{\Lambda^2}\right)\right)\lambda_2^2 + \right.\\ &+ \left. 8\lambda_{12}^2\left(11+3\ln\left(\frac{2\lambda_{12}\langle\varphi_2\rangle^2}{\Lambda^2}\right)\right)\right]\varphi_2^4\end{aligned} \tag{240}$$

$$\begin{aligned}\frac{1}{4}D_3\varphi_1^2\varphi_2^2 &= -\frac{1}{4}\frac{\pi^2}{(2\pi)^4}\left[\left(90+36\ln\left(\frac{6\delta_1\langle\varphi_1\rangle\langle\varphi_2\rangle}{\Lambda^2}\right)\right)\delta_1^2 + \right.\\ &+ 16\lambda_1\lambda_{12}\left(9+3\ln\left(\frac{12\lambda_1\langle\varphi_1\rangle^2}{\Lambda^2}\right)\right) +\\ &+ \left(90+36\ln\left(\frac{6\delta_2\langle\varphi_1\rangle\langle\varphi_2\rangle}{\Lambda^2}\right)\right)\delta_2^2 +\\ &+ 16\lambda_2\lambda_{12}\left(9+3\ln\left(\frac{12\lambda_2\langle\varphi_2\rangle^2}{\Lambda^2}\right)\right) +\\ &+ \left. 18\delta_1\delta_2\ln\left(\frac{1}{\Lambda^2}\right)+16\lambda_{12}^2\ln\left(\frac{1}{\Lambda^2}\right)\right]\varphi_1^2\varphi_2^2\end{aligned} \tag{241}$$

$$\frac{1}{6}D_4\varphi_1^3\varphi_2 = -\frac{1}{6}\frac{\pi^2}{(2\pi)^4}\Bigg[8\left(99+27\ln\left(\frac{12\lambda_1\left\langle\varphi_1\right\rangle^2}{\Lambda^2}\right)\right)\lambda_1\delta_1 + + 4\delta_2\lambda_{12}\left(27+9\ln\left(\frac{2\lambda_{12}\left\langle\varphi_2\right\rangle^2}{\Lambda^2}\right)\right)+36\delta_1\lambda_{12}\ln\left(\frac{1}{\Lambda^2}\right)\Bigg]\varphi_1^3\varphi_2 \quad (242)$$

$$\frac{1}{6}D_5\varphi_1\varphi_2^3 = -\frac{1}{6}\frac{\pi^2}{(2\pi)^4}\Bigg[8\left(99+27\ln\left(\frac{12\lambda_2\left\langle\varphi_2\right\rangle^2}{\Lambda^2}\right)\right)\lambda_2\delta_2 + + 4\delta_1\lambda_{12}\left(27+9\ln\left(\frac{2\lambda_{12}\left\langle\varphi_1\right\rangle^2}{\Lambda^2}\right)\right)+36\delta_2\lambda_{12}\ln\left(\frac{1}{\Lambda^2}\right)\Bigg]\varphi_1\varphi_2^3 \quad (243)$$

Thus, replacing the counterterms into Eq. (234) we obtain the renormalized *one-loop* effective potential at *zero-temperature* (V^0_{eff}) for bicritical point in the form,

$$\begin{aligned}
V^0_{eff}(\varphi_1,\varphi_2) &= \underbrace{\lambda_1\varphi_1^4+\lambda_2\varphi_2^4+\lambda_{12}\varphi_1^2\varphi_2^2+\delta_1\varphi_1^3\varphi_2+\delta_2\varphi_1\varphi_2^3}_{classical\ term}+\\
&+ \frac{\pi^2}{(2\pi)^4}\Bigg[\left(36\lambda_1^2\ln\left(\frac{b_1}{12\lambda_1\left\langle\varphi_1\right\rangle^2}\right)+\lambda_{12}^2\ln\left(\frac{b_2}{2\lambda_{12}\left\langle\varphi_1\right\rangle^2}\right)\right)\varphi_1^4+\\
&+ \left(36\lambda_2^2\ln\left(\frac{b_2}{12\lambda_2\left\langle\varphi_2\right\rangle^2}\right)+\lambda_{12}^2\ln\left(\frac{b_1}{2\lambda_{12}\left\langle\varphi_2\right\rangle^2}\right)\right)\varphi_2^4+\\
&+ \left(9\delta_1^2\ln\left(\frac{b_1}{6\delta_1\left\langle\varphi_1\right\rangle\left\langle\varphi_2\right\rangle}\right)+12\lambda_1\lambda_{12}\ln\left(\frac{b_1}{12\lambda_1\left\langle\varphi_1\right\rangle^2}\right)+\right.\\
&+ \left.9\delta_2^2\ln\left(\frac{b_2}{6\delta_2\left\langle\varphi_1\right\rangle\left\langle\varphi_2\right\rangle}\right)+12\lambda_2\lambda_{12}\ln\left(\frac{b_2}{12\lambda_2\left\langle\varphi_2\right\rangle^2}\right)\right)\varphi_1^2\varphi_2^2+\\
&+ \left(36\delta_1\lambda_1\ln\left(\frac{b_1}{12\lambda_1\left\langle\varphi_1\right\rangle^2}\right)+6\delta_2\lambda_{12}\ln\left(\frac{b_2}{2\lambda_{12}\left\langle\varphi_2\right\rangle^2}\right)\right)\varphi_1^3\varphi_2+\\
&+ \left(36\delta_2\lambda_2\ln\left(\frac{b_2}{12\lambda_2\left\langle\varphi_2\right\rangle^2}\right)+6\delta_1\lambda_{12}\ln\left(\frac{b_1}{2\lambda_{12}\left\langle\varphi_1\right\rangle^2}\right)\right)\varphi_1\varphi_2^3+\\
&- \left(150\lambda_1^2\varphi_1^4+\frac{25}{6}\lambda_{12}^2\varphi_1^4+150\lambda_2^2\varphi_2^4+\frac{25}{6}\lambda_{12}^2\varphi_2^4+\frac{63}{2}\delta_1^2\varphi_1^2\varphi_2^2+\right.\\
&+ \left.\frac{63}{2}\delta_2^2\varphi_1^2\varphi_2^2+48\lambda_1\lambda_{12}\varphi_1^2\varphi_2^2+48\lambda_2\lambda_{12}\varphi_1^2\varphi_2^2+150\delta_1\lambda_1\varphi_1^3\varphi_2+\right.\\
&+ \left.150\delta_2\lambda_2\varphi_1\varphi_2^3+21\delta_2\lambda_{12}\varphi_1^3\varphi_2+21\delta_1\lambda_{12}\varphi_1\varphi_2^3\right)+\\
&+ \frac{(3\delta_1\varphi_1^2+3\delta_2\varphi_2^2+4\lambda_{12}\varphi_1\varphi_2)^2}{4}\left(\frac{b_1\ln(b_1)-b_2\ln(b_2)}{b_1-b_2}\right)\Bigg] \qquad (244)
\end{aligned}$$

where,

$$b_1 = 12\lambda_1\varphi_1^2+2\lambda_{12}\varphi_2^2+6\delta_1\varphi_1\varphi_2 \qquad \texttt{and} \qquad b_2 = 12\lambda_2\varphi_2^2+2\lambda_{12}\varphi_1^2+6\delta_2\varphi_1\varphi_2\ . \quad (245)$$

Note also that we can rewrite Eq. (244) as follows [61],

$$V^0_{eff}(\varphi_1,\varphi_2)=\tilde{\lambda}_1\varphi_1^4+\tilde{\lambda}_2\varphi_2^4+\tilde{\lambda}_{1,2}\varphi_1^2\varphi_2^2+\tilde{\delta}_1\varphi_1^3\varphi_2+\tilde{\delta}_2\varphi_1\varphi_2^3+\mathcal{O}(\varphi^6_{1,2}) \tag{246}$$

where,

$$\begin{aligned}
\tilde{\lambda}_1 &= \lambda_1+\frac{\pi^2}{(2\pi)^4}\left[36\lambda_1^2\left(\ln\left(\frac{b_1}{12\lambda_1\langle\varphi_1\rangle^2}\right)-\frac{25}{6}\right)+\lambda_{12}^2\left(\ln\left(\frac{b_2}{2\lambda_{12}\langle\varphi_1\rangle^2}\right)-\frac{25}{6}\right)+\right.\\
&+ \left.\frac{9}{4}\delta_1^2\left(\ln\left(\frac{1}{6\delta_1\langle\varphi_1\rangle\langle\varphi_2\rangle}\right)-\frac{25}{6}\right)\right]\\
\tilde{\lambda}_2 &= \lambda_2+\frac{\pi^2}{(2\pi)^4}\left[36\lambda_2^2\left(\ln\left(\frac{b_2}{12\lambda_2\langle\varphi_2\rangle^2}\right)-\frac{25}{6}\right)+\lambda_{12}^2\left(\ln\left(\frac{b_1}{2\lambda_{12}\langle\varphi_2\rangle^2}\right)-\frac{25}{6}\right)+\right.\\
&+ \left.\frac{9}{4}\delta_2^2\left(\ln\left(\frac{1}{6\delta_2\langle\varphi_1\rangle\langle\varphi_2\rangle}\right)-\frac{25}{6}\right)\right]\\
\tilde{\lambda}_{12} &= \lambda_{12}+\frac{\pi^2}{(2\pi)^4}\left[9\delta_1^2\left(\ln\left(\frac{b_1}{6\delta_1\langle\phi_1\rangle\langle\phi_1\rangle}\right)-3\right)+9\delta_2^2\left(\ln\left(\frac{b_2}{6\delta_2\langle\phi_1\rangle\langle\phi_2\rangle}\right)-3\right)+\right.\\
&+ \left.12\lambda_1\lambda_{12}\left(\ln\left(\frac{b_1}{12\lambda_1\langle\phi_1\rangle^2}\right)-\frac{7}{2}\right)+12\lambda_2\lambda_{12}\left(\ln\left(\frac{b_2}{12\lambda_2\langle\phi_2\rangle^2}\right)-\frac{7}{2}\right)\right]\\
\tilde{\delta}_1 &= \delta_1+\frac{\pi^2}{(2\pi)^4}\left[36\delta_1\lambda_1\left(\ln\left(\frac{b_1}{12\lambda_1\langle\varphi_1\rangle^2}\right)-\frac{25}{6}\right)+6\delta_2\lambda_{12}\left(\ln\left(\frac{b_2}{2\lambda_{12}\langle\varphi_2\rangle^2}\right)-\frac{7}{2}\right)\right]\\
\tilde{\delta}_2 &= \delta_2+\frac{\pi^2}{(2\pi)^4}\left[36\delta_2\lambda_2\left(\ln\left(\frac{b_2}{12\lambda_2\langle\varphi_2\rangle^2}\right)-\frac{25}{6}\right)+6\delta_1\lambda_{12}\left(\ln\left(\frac{b_1}{2\lambda_{12}\langle\varphi_1\rangle^2}\right)-\frac{7}{2}\right)\right]\\
\mathcal{O}(\varphi^6_{1,2}) &= \frac{\pi^2}{(2\pi)^4}\left[\frac{(3\delta_1\varphi_1^2+3\delta_2\varphi_2^2+4\lambda_{12}\varphi_1\varphi_2)^2}{4}\left(\frac{b_1\ln(b_1)-b_2\ln(b_2)}{b_1-b_2}\right)\right]
\end{aligned} \tag{247}$$

where b_1 and b_2 are given in Eq. (245).

The tilde quantities in Eq. (246) represent effective couplings renormalized by quantum corrections and are given together with the terms of higher orders in the fields $\mathcal{O}(\varphi^6_{1,2})$ [61]. Analogously to the classical analysis, let us analyze some particular cases for the *one-loop* effective potential in Eq. (246).

Initially, for an exclusive quartic coupling, i.e., taking $\delta_i=0$ and finite (positive) λ_{12} in Eq. (246), one can verify that the first-order quantum corrections do not introduce any qualitative change on the MF phase diagram [61]. In other words, even taking into account first-order quantum corrections, the minimum of the effective potential remains at the origin, as can be seen in Fig. 13. This implies that the bicritical point is stable in the presence of quantum corrections due to a quartic coupling.

To sum up, quantum corrections associated with an exclusive quartic coupling do not affect the classical phase diagram in Fig. 11 (full lines (blue line)) and the bicritical point survives these interactions at the classical and quantum level.

Figure 13 - Effective potential for a bicritical point in the case of an exclusive quartic coupling

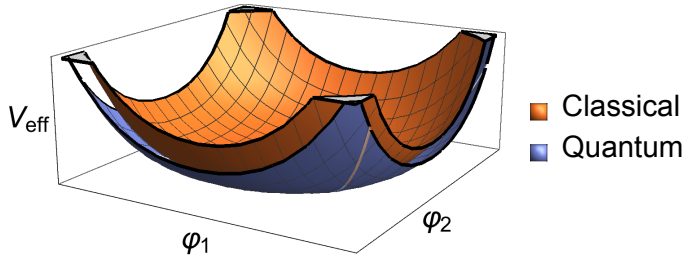

Legend: (Color online) *One-loop* Effective potential for a bicritical point in the case of an exclusive quartic coupling, with and without quantum corrections (schematic). There is no qualitative change in the classical phase diagram, i.e., the *minimum* of the effective potential is at the origin in both cases.

Source: Ref. [61].

Next, we are interested in the case that $\lambda_{12} = 0$ and a finite (positive) bilinear coupling is allowed. For simplicity, we can, without loss of generality, take the limit when $\delta_1 \to \delta_2$ and $\lambda_2 \to \lambda_1$. In addition, the terms of $\mathcal{O}(\varphi_{1,2}^6)$ in Eq. (246) can be neglected [61]. Notice also that in the presence of the bilinear coupling, the physical region of the phase diagram is that where both fields have the same sign, such that, time-reversal symmetry is preserved [61]. Thus, in order to verify the behavior of the system in this region of parameters, we make a cut in the 3d phase diagram taking $\varphi_1 = \varphi_2$ in Eq. (246).

After all these simplifications, Eq. (246) can be rewritten in the form [61],

$$\begin{aligned} V_{eff}^{0} &= \frac{1}{64\pi^2}\varphi_1^4\Bigg[\underbrace{128\pi^2(\lambda_1+\delta_2)}_{classical\ term} + 18\delta_2^2\Bigg[\ln\left(\frac{6(\varphi_1^2(2\lambda_1+\delta_2))^2}{\delta_2\left\langle\varphi\right\rangle^2}\right) + \\ &+ 4\ln\left(\frac{\varphi_1^2(2\lambda_1+\delta_2)}{\delta_2\left\langle\varphi\right\rangle^2}\right) - \frac{85}{6}\Bigg] + 288\lambda_1(\lambda_1+\delta_2)\left[\ln\left(\frac{\varphi_1^2(2\lambda_1+\delta_2)}{2\lambda_1\left\langle\varphi\right\rangle^2}\right) - \frac{25}{6}\right]\Bigg] \end{aligned} \tag{248}$$

where $\langle\varphi\rangle$ corresponds to the minimum of the effective potential.

From Eq. (248) one can identify two Coleman–Weinberg-like terms that give rise to a minimum outside the origin in the effective potential [55, 61]. Moreover, the 3d plot of the *one-loop* effective potential in Fig. 14 shows that quantum corrections due to an exclusive bilinear coupling has a dramatically different effect from that of purely quartic interactions. The quantum corrections due to the former break the symmetry of the fields and induce coexistence between these orders even for δ_i positive [61].

For completeness, we consider now the stability of the bicritical point when both couplings are present. Due to the presence of the bilinear coupling we can use the same arguments of the exclusive bilinear case to simplify the effective potential given in Eq. (246). Therefore, following the same previous procedures for the exclusive bilinear coupling, but

Figure 14 - Effective potential for a bicritical point in the case of a finite bilinear coupling

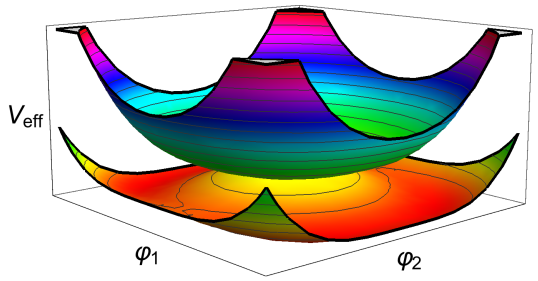

Legend: (Color online) The effective potential for a bicritical point in the case of a finite bilinear coupling, with and without quantum corrections (schematic). When we take into account quantum corrections the minima of V^0_{eff} in Eq. (246) move outside the origin, which means that the quantum corrections will induce coexistence in this case, even for δ_i positive.

Source: Ref. [61].

now for λ_{12} finite (positive) we get [61],

$$
\begin{aligned}
V^0_{eff} &= \frac{1}{192\pi^2}\varphi^4\Bigg\{\underbrace{384\pi^2\left(\lambda_1+\delta_2+\frac{\lambda_{12}}{2}\right)}_{classical\ term}+ \\
&+ 54\delta_2^2\left[\ln\left(\frac{(2\varphi^2(6\lambda_1+\lambda_{12}+3\delta_2))^2}{6\delta_2\left\langle\varphi\right\rangle^2}\right)+\right. \\
&+ \left. 4\ln\left(\frac{(\varphi_1^2(6\lambda_1+\lambda_{12}+3\delta_2))^2}{3\delta_2\left\langle\varphi\right\rangle^2}\right)-\frac{85}{6}\right]+ \\
&+ 864\lambda_1(\lambda_1+\delta_2)\left[\ln\left(\frac{\varphi_1^2(6\lambda_1+\lambda_{12}+3\delta_2)}{6\lambda_1\left\langle\varphi\right\rangle^2}\right)-\frac{25}{6}\right]+ \\
&+ 24\lambda_{12}^2\left[\ln\left(\frac{4(\varphi_1^2(6\lambda_1+\lambda_{12}+3\delta_2))^3}{\lambda_{12}\left\langle\varphi\right\rangle^2}\right)-\frac{13}{6}\right]+ \\
&+ 144\lambda_{12}\delta_2\left[\ln\left(\frac{4(\varphi_1^2(6\lambda_1+\lambda_{12}+3\delta_2))^3}{\lambda_{12}\left\langle\varphi\right\rangle^2}\right)-\frac{5}{2}\right]+ \\
&+ 288\lambda_{12}\lambda_1\left[\ln\left(\frac{\varphi_1^2(6\lambda_1+\lambda_{12}+3\delta_2)}{6\lambda_{12}\left\langle\varphi\right\rangle^2}\right)-\frac{7}{2}\right]\Bigg\}
\end{aligned}
\tag{249}
$$

Notice that for $\lambda_{12}=0$, Eq. (249) reduces to Eq. (248), as expected. In the general case, when both couplings are present, the plot of the effective potential has a behavior similar to that of the purely bilinear coupling, with minima of the effective potential outside the origin [61], as shown in Fig. 14.

Then, even in the presence of the quartic interactions, any bilinear coupling, $\delta_i > 0$, breaks the symmetry of the bicritical point and leads to a coexistence of phases for the

Figure 15 - Coexisting phases in the presence of both couplings and their particular cases

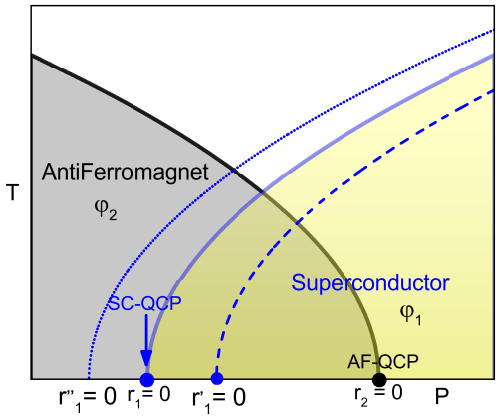

Legend: (Color online) Schematic phase diagram of coexisting phases in the presence of both couplings and their particular cases. The full (blue) line represents the classical result and the dashed line the effect of the quantum corrections (see text). In this figure the phase with $\varphi_1 \neq 0$ is identified with a superconducting phase and that with $\varphi_2 \neq 0$ with an antiferromagnet. The QCP of these phases are labeled as SC-QCP and AF-QCP, respectively.

Source: Ref. [61].

value of parameters for which both systems were critical in the absence of δ_i. This is confirmed by minimizing the effective potential, Eq. (249), to obtain $\langle\varphi\rangle$ and expanding for small δ_i and λ_{12}. We obtain that $\langle\varphi\rangle \propto \delta^{1/2}(1 + \mathcal{O}(\lambda_{12}^2) + \cdots)$ implying that any finite δ gives rise to a symmetry breaking even in the presence of the quartic interaction λ_{12} [61].

However, the two couplings are in competition, as we can easily see plotting the effective potential. For $\lambda_{12} \neq 0$, the plot for Eq. (249) is very similar to that of Fig. 14 with the only difference that the minima of the effective potential occurs for smaller values of the symmetry breaking field. The effect of the coupling λ_{12} then is to decrease the coexistence region that the δ_i coupling produces [61].

4.3.2 Coexistence region

Let us consider now the more general case where both r_1 and r_2 are different from zero. Fig. 15 shows a possible schematic phase diagram for the particular case of a SC and an AFM where both phases coexist in a region of the phase diagram.

Classically, this occurs whenever r_1 and r_2 are negative, even in the absence of a coupling between these phases [61]. In the presence of the quartic coupling λ_{12} and for $\delta_1 = \delta_2 = 0$, the required condition for coexistence, in the case of positive λ_{12}, $r_1 < 0$ and

$r_2 < 0$, is that $\lambda_{12}^2 < 4\lambda_1\lambda_2$ [61]. This guarantees that the coexistence of phases lowers the energy of the system. For $\lambda_{12} = 0$ and $\delta_{1,2} < 0$ the coexistence is always possible for $\varphi_1 = \varphi_2$, as discussed in section 3.2.2. In the general case that λ_{12} and $\delta_{1,2}$ are finite, we also obtain classical coexistence for $\varphi_1 = \varphi_2$. Moreover, the condition in this case is that $\lambda_{12}^2 < 4\lambda_1\lambda_2 + \delta_2\lambda_1 + \delta_1\lambda_2 + \delta_1\delta_2/4$ [61], with $\delta_{1,2} < 0$.

We now obtain the quantum corrections for this case of coexistence of phases. Note that the problem where $r_1 \neq 0$ and $r_2 \neq 0$ is mathematically more intricate than that of the previous section. However, we can still make analytical progress whenever the system is deep in one of the phases, but at the QCP of the other, as shown in Fig. 15.

Then, we treat here the problem where the material is in an ordered phase, such that, say $r_2 < 0$ and $\varphi_2 \neq 0$, but at the QCP of the other, i.e., with $r_1 \approx 0$, φ_1 small, although allowed to be finite. The symmetric case corresponding to r_1 small and negative, such that, the system is in the ordered φ_1 phase, but is tuned to the QCP of φ_2, i.e., to $r_2 \approx 0$ can be treated in the same way and yields equivalent results since the dynamics of the propagators are considered identical in this dissertation. For the former conditions, the effective potential is obtained expanding $\Gamma^{(1)}_{\varphi_{1,2}}$ in Eq. (232) for r_2 small but $r_1 \approx 0$. Thus, we get [61],

$$\begin{aligned}\Gamma^{(1)}_{\varphi_{1,2}} &= \frac{\pi^2}{(2\pi)^4}\left[\frac{\Lambda^2}{2}(b_1+b_2) + \frac{b_1^2}{4}\ln\left(\frac{b_1}{\Lambda^2}\right) + \frac{(b_2+r_2)^2}{4}\ln\left(\frac{b_2+r_2}{\Lambda^2}\right) - \frac{(b_1^2+b_2^2)}{8} + \right. \\ &+ \frac{\left(3\delta_1\varphi_1^2 + 3\delta_2\varphi_2^2 + 4\lambda_{12}\varphi_1\varphi_2\right)^2}{4}\left(\ln\left(\frac{1}{\Lambda^2}\right) + \frac{B^2\ln(B^2) - b_1\ln(b_1)}{B^2 - b_1}\right) + \\ &- \left.\frac{r_2^2}{4}\ln\left(\frac{r_2}{\Lambda^2}\right)\right] + \texttt{counterterms} \end{aligned} \tag{250}$$

where $B^2 = r_2 + b_2$, and $b_{1,2}$ are given in Eq. (245).

Note that both fields φ_1 and φ_2 are kept finite in this expansion even taking $r_1 \approx 0$ because of the possibility of $\varphi_1 \neq 0$ being induced by the couplings.

Again, in order to calculate the necessary counterterms we now use the definitions [61],

$$\left[\frac{d^2\Gamma^{(1)}}{d\varphi_1^2}\right]\Big|_{\varphi_{1,2}=0} = r_1 = 0 \quad , \quad \left[\frac{d^2\Gamma^{(1)}}{d\varphi_2^2}\right]\Big|_{\varphi_{1,2}=0} = r_2 \quad , \left[\frac{d^2\Gamma^{(1)}}{d\varphi_1\varphi_2}\right]\Big|_{\varphi_1=\langle\varphi_1\rangle,\varphi_2=\langle\varphi_2\rangle} = \gamma$$

$$\left[\frac{d^4\Gamma^{(1)}}{d\varphi_1^4}\right]\Big|_{\varphi_1=\langle\varphi_1\rangle,\phi_{2=0}} = \lambda_1 \quad , \quad \left[\frac{d^4\Gamma^{(1)}}{d\varphi_2^4}\right]\Big|_{\varphi_1=0,\varphi_2=\langle\varphi_2\rangle} = \lambda_2 \quad , \quad \left[\frac{d^4\Gamma^{(1)}}{d\varphi_1^2\varphi_2^2}\right]\Big|_{\varphi_1=\langle\varphi_1\rangle,\varphi_2=\langle\varphi_2\rangle} = \lambda_{12}$$

$$\left[\frac{d^4\Gamma^{(1)}}{d\varphi_1^3\varphi_2}\right]\Big|_{\varphi_1=\langle\varphi_1\rangle,\varphi_2=\langle\varphi_2\rangle} = \delta_1 \quad , \quad \left[\frac{d^2\Gamma^{(1)}}{d\varphi_1\varphi_2^3}\right]\Big|_{\varphi_1=\langle\varphi_1\rangle,\varphi_2=\langle\varphi_2\rangle} = \delta_2 \tag{251}$$

From Eq. (251) we obtain the counterterms as follows [61],

$$\frac{1}{2}C_1\varphi_1^2 = -\frac{1}{2}\frac{\pi^2}{(2\pi)^4}\left[\Lambda^2(12\lambda_1+2\lambda_{12})+r_2\lambda_{12}\left(1+2\ln\left(\frac{r_2}{\Lambda^2}\right)\right)\right]\varphi_1^2 \tag{252}$$

$$\frac{1}{2}C_2\varphi_2^2 = -\frac{1}{2}\frac{\pi^2}{(2\pi)^4}\left[\Lambda^2(12\lambda_2+2\lambda_{12})+6r_2\lambda_2\left(1+2\ln\left(\frac{r_2}{\Lambda^2}\right)\right)\right]\varphi_2^2 \tag{253}$$

$$C_3\varphi_1\varphi_2 = -\frac{1}{2}\frac{\pi^2}{(2\pi)^4}\left[\Lambda^2(3\delta_1+3\delta_2)+\frac{3}{2}r_2\delta_2\left(1+2\ln\left(\frac{r_2}{\Lambda^2}\right)\right)\right]\varphi_1\varphi_2 \tag{254}$$

$$\begin{aligned}\frac{1}{4!}D_1\varphi_1^4 &= -\frac{1}{4!}\frac{\pi^2}{(2\pi)^4}\left[16\left(198+54\ln\left(\frac{12\lambda_1\langle\varphi_1\rangle^2}{\Lambda^2}\right)\right)\lambda_1^2+\right.\\ &+ \left. 8\lambda_{12}^2\left(11+3\ln\left(\frac{2\lambda_{12}\langle\varphi_1\rangle^2}{\Lambda^2}\right)\right)+54\delta_1^2\ln\left(\frac{1}{\Lambda^2}\right)\right]\varphi_1^4\end{aligned} \tag{255}$$

$$\begin{aligned}\frac{1}{4!}D_2\varphi_2^4 &= -\frac{1}{4!}\frac{\pi^2}{(2\pi)^4}\left[16\left(198+54\ln\left(\frac{12\lambda_2\langle\varphi_2\rangle^2}{\Lambda^2}\right)\right)\lambda_2^2+\right.\\ &+ \left. 8\lambda_{12}^2\left(11+3\ln\left(\frac{2\lambda_{12}\langle\varphi_2\rangle^2}{\Lambda^2}\right)\right)+54\delta_2^2\ln\left(\frac{1}{\Lambda^2}\right)\right]\varphi_2^4\end{aligned} \tag{256}$$

$$\begin{aligned}\frac{1}{4}D_3\varphi_1^2\varphi_2^2 &= -\frac{1}{4}\frac{\pi^2}{(2\pi)^4}\left[\left(90+36\ln\left(\frac{6\delta_1\langle\varphi_1\rangle\langle\varphi_2\rangle}{\Lambda^2}\right)\right)\delta_1^2+\right.\\ &+ 16\lambda_1\lambda_{12}\left(9+3\ln\left(\frac{12\lambda_1\langle\varphi_1\rangle^2}{\Lambda^2}\right)\right)+\\ &+ \left(90+36\ln\left(\frac{6\delta_2\langle\varphi_1\rangle\langle\varphi_2\rangle}{\Lambda^2}\right)\right)\delta_2^2+\\ &+ 16\lambda_2\lambda_{12}\left(9+3\ln\left(\frac{12\lambda_2\langle\varphi_2\rangle^2}{\Lambda^2}\right)\right)+\\ &+ \left. 18\delta_1\delta_2\ln\left(\frac{1}{\Lambda^2}\right)+16\lambda_{12}^2\ln\left(\frac{1}{\Lambda^2}\right)\right]\varphi_1^2\varphi_2^2\end{aligned} \tag{257}$$

$$\frac{1}{6}D_4\varphi_1^3\varphi_2 = -\frac{1}{6}\frac{\pi^2}{(2\pi)^4}\Bigg[8\left(99+27\ln\left(\frac{12\lambda_1\left\langle\varphi_1\right\rangle^2}{\Lambda^2}\right)\right)\lambda_1\delta_1 + \\ + 4\delta_2\lambda_{12}\left(27+9\ln\left(\frac{2\lambda_{12}\left\langle\varphi_2\right\rangle^2}{\Lambda^2}\right)\right)+36\delta_1\lambda_{12}\ln\left(\frac{1}{\Lambda^2}\right)\Bigg]\varphi_1^3\varphi_2 \quad (258)$$

$$\frac{1}{6}D_5\varphi_1\varphi_2^3 = -\frac{1}{6}\frac{\pi^2}{(2\pi)^4}\Bigg[8\left(99+27\ln\left(\frac{12\lambda_2\left\langle\varphi_2\right\rangle^2}{\Lambda^2}\right)\right)\lambda_2\delta_2 + \\ + 4\delta_1\lambda_{12}\left(27+9\ln\left(\frac{2\lambda_{12}\left\langle\varphi_1\right\rangle^2}{\Lambda^2}\right)\right)+36\delta_2\lambda_{12}\ln\left(\frac{1}{\Lambda^2}\right)\Bigg]\varphi_1\varphi_2^3 \quad (259)$$

Replacing the countertems into Eq. (250) one can find the renormalized *one-loop* effective potential at *zero-temperature* for coexistence case,

$$V^0_{eff}(\varphi_1,\varphi_2) = \underbrace{r_2\varphi_2^2+\lambda_1\varphi_1^4+\lambda_2\varphi_2^4+\lambda_{12}\varphi_1^2\varphi_2^2+\delta_1\varphi_1^3\varphi_2+\delta_2\varphi_1\varphi_2^3}_{classical\ term}+ \\ + \frac{\pi^2}{(2\pi)^4}\Bigg[\left(36\lambda_1^2\ln\left(\frac{b_1}{12\lambda_1\left\langle\phi_1\right\rangle^2}\right)+\lambda_{12}^2\ln\left(\frac{r_2+b_2}{2\lambda_{12}\left\langle\varphi_1\right\rangle^2}\right)\right)\varphi_1^4 + \\ + \left(36\lambda_2^2\ln\left(\frac{r_2+b_2}{12\lambda_2\left\langle\varphi_2\right\rangle^2}\right)+\lambda_{12}^2\ln\left(\frac{b_1}{2\lambda_{12}\left\langle\phi_2\right\rangle^2}\right)\right)\varphi_2^4 + \\ + \left(9\delta_1^2\ln\left(\frac{b_1}{6\delta_1\left\langle\varphi_1\right\rangle\left\langle\varphi_2\right\rangle}\right)+12\lambda_1\lambda_{12}\ln\left(\frac{b_1}{12\lambda_1\left\langle\varphi_1\right\rangle^2}\right)+\right. \\ \left. + 9\delta_2^2\ln\left(\frac{b_2}{6\delta_2\left\langle\varphi_1\right\rangle\left\langle\varphi_2\right\rangle}\right)+12\lambda_2\lambda_{12}\ln\left(\frac{b_2}{12\lambda_2\left\langle\varphi_2\right\rangle^2}\right)\right)\varphi_1^2\varphi_2^2 + \\ + \left(36\delta_1\lambda_1\ln\left(\frac{b_1}{12\lambda_1\left\langle\varphi_1\right\rangle^2}\right)+6\delta_2\lambda_{12}\ln\left(\frac{r_2+b_2}{2\lambda_{12}\left\langle\varphi_2\right\rangle^2}\right)\right)\varphi_1^3\varphi_2 + \\ + \left(36\delta_2\lambda_2\ln\left(\frac{r_2+b_2}{12\lambda_2\left\langle\varphi_2\right\rangle^2}\right)+6\delta_1\lambda_{12}\ln\left(\frac{b_1}{2\lambda_{12}\left\langle\varphi_1\right\rangle^2}\right)\right)\varphi_1\varphi_2^3 + \\ + \left(3r_2\delta_2\varphi_1\varphi_2+6r_2\lambda_2\varphi_2^2+r_2\lambda_{12}\varphi_1^2\right)\ln\left(\frac{r_2+b_2}{r_2}\right)+ \\ - \left(168\lambda_1^2\varphi_1^4+\frac{14}{3}\lambda_{12}^2\varphi_1^4+168\lambda_2^2\varphi_2^4+\frac{14}{3}\lambda_{12}^2\varphi_2^4+\frac{63}{2}\delta_1^2\varphi_1^2\varphi_2^2+\frac{63}{2}\delta_2^2\varphi_1^2\varphi_2^2+\right. \\ + 48\lambda_1\lambda_{12}\varphi_1^2\varphi_2^2+48\lambda_2\lambda_{12}\varphi_1^2\varphi_2^2+150\delta_1\lambda_1\varphi_1^3\varphi_2+150\delta_2\lambda_2\varphi_1\varphi_2^3+ \\ \left. + 21\delta_2\lambda_{12}\varphi_1^3\varphi_2+21\delta_1\lambda_{12}\varphi_1\varphi_2^3+\frac{3}{2}r_2\delta_2\varphi_1\varphi_2+3r_2\lambda_2\varphi_2^2+\frac{1}{2}r_2\lambda_{12}\varphi_1^2\right)+ \\ + \frac{\left(3\delta_1\varphi_1^2+3\delta_2\varphi_2^2+4\lambda_{12}\varphi_1\varphi_2\right)^2}{4}\left(\frac{B^2\ln(B^2)-b_1\ln(b_1)}{B^2-b_1}\right)\Bigg] \quad (260)$$

where,

$$b_1 = 12\lambda_1\varphi_1^2 + 2\lambda_{12}\varphi_2^2 + 6\delta_1\varphi_1\varphi_2 \ , \ b_2 = 12\lambda_2\varphi_2^2 + 2\lambda_{12}\varphi_1^2 + 6\delta_2\varphi_1\varphi_2 \ \texttt{and} \ B^2 = |r_2 + b_2| \ . \tag{261}$$

Note also that Eq. (260) can be rewritten as follows [61],

$$V_{eff}^0 = r_2\varphi_2^2 + \lambda_1'\varphi_1^4 + \lambda_2'\varphi_2^4 + \lambda_{12}'\varphi_1^2\varphi_2^2 + \delta_1'\varphi_1^3\varphi_2 + \delta_2'\varphi_1\varphi_2^3 + \tilde{\rho}(\varphi_{1,2}) + \frac{1}{(4\pi)^2}\eta\left[\ln\left(\frac{B^2}{r_2}\right) - \frac{1}{2}\right] \tag{262}$$

where $\tilde{\rho}(\varphi_{1,2})$ contains terms of higher orders in the fields and,

$$\eta = 3r_2\delta_2\varphi_1\varphi_2 + 6r_2\lambda_2\varphi_2^2 + r_2\lambda_{12}\varphi_1^2 \tag{263}$$

with,

$$\lambda_1' = \lambda_1 + \frac{\pi^2}{(2\pi)^4}\left[36\lambda_1^2\left(\ln\left(\frac{b_1}{12\lambda_1\left\langle\varphi_1\right\rangle^2}\right) - \frac{25}{6}\right) + \lambda_{12}^2\left(\ln\left(\frac{|r_2 + b_2|}{2\lambda_{12}\left\langle\varphi_1\right\rangle^2}\right) - \frac{25}{6}\right)\right] \tag{264}$$

$$\lambda_2' = \lambda_2 + \frac{\pi^2}{(2\pi)^4}\left[36\lambda_2^2\left(\ln\left(\frac{|r_2 + b_2|}{12\lambda_2\left\langle\varphi_2\right\rangle^2}\right) - \frac{25}{6}\right) + \lambda_{12}^2\left(\ln\left(\frac{b_1}{2\lambda_{12}\left\langle\varphi_2\right\rangle^2}\right) - \frac{25}{6}\right)\right] \tag{265}$$

$$\begin{aligned}\lambda_{12}' &= \lambda_{12} + \frac{\pi^2}{(2\pi)^4}\left[9\delta_1^2\left(\ln\left(\frac{b_1}{6\delta_1\left\langle\phi_1\right\rangle\left\langle\phi_1\right\rangle}\right) - 3\right) + 9\delta_2^2\left(\ln\left(\frac{|r_2 + b_2|}{6\delta_2\left\langle\phi_1\right\rangle\left\langle\phi_2\right\rangle}\right) - 3\right) + \right. \\ &+ \left. 12\lambda_1\lambda_{12}\left(\ln\left(\frac{b_1}{12\lambda_1\left\langle\phi_1\right\rangle^2}\right) - \frac{7}{2}\right) + 12\lambda_2\lambda_{12}\left(\ln\left(\frac{|r_2 + b_2|}{12\lambda_2\left\langle\phi_2\right\rangle^2}\right) - \frac{7}{2}\right)\right]\end{aligned} \tag{266}$$

$$\delta_1' = \delta_1 + \frac{\pi^2}{(2\pi)^4}\left[36\delta_1\lambda_1\left(\ln\left(\frac{b_1}{12\lambda_1\left\langle\varphi_1\right\rangle^2}\right) - \frac{25}{6}\right) + 6\delta_2\lambda_{12}\left(\ln\left(\frac{|r_2 + b_2|}{2\lambda_{12}\left\langle\varphi_2\right\rangle^2}\right) - \frac{7}{2}\right)\right] \tag{267}$$

$$\tilde{\delta}_2 = \delta_2 + \frac{\pi^2}{(2\pi)^4}\left[36\delta_2\lambda_2\left(\ln\left(\frac{|r_2 + b_2|}{12\lambda_2\left\langle\varphi_2\right\rangle^2}\right) - \frac{25}{6}\right) + 6\delta_1\lambda_{12}\left(\ln\left(\frac{b_1}{2\lambda_{12}\left\langle\varphi_1\right\rangle^2}\right) - \frac{7}{2}\right)\right] \tag{268}$$

$$\tilde{\rho}(\varphi_{1,2}) = \frac{\pi^2}{(2\pi)^4}\left[\frac{(3\delta_1\varphi_1^2 + 3\delta_2\varphi_2^2 + 4\lambda_{12}\varphi_1\varphi_2)^2}{4}\left(\frac{B^2\ln(B^2) - b_1\ln(b_1)}{B^2 - b_1}\right)\right] \tag{269}$$

where B^2 and $b_{1,2}$ are given in Eq. (261).

Again the prime quantities in Eq. (262) represent effective couplings renormalized by quantum corrections and are given together with the higher orders terms $\tilde{\rho}(\varphi_{1,2})$ [61].

It is worth to point out that the *one-loop* effective potential in Eq. (262), specifically in the η contribution, contains a φ_2^2 term with a small coefficient whose effect is just to renormalize the classical potential and does not produce qualitative changes in the classical phase diagram. However, the presence of a φ_1^2 term in η gives rise to interesting physical consequences that we now analyze in detail.

First, note that for $\delta_i = 0$ in Eq. (262) the term in brackets $[\cdots]$ multiplied by η and involving φ_1^2 is always negative. This term in turn couples to the product $r_2\lambda_{12}$ that is also negative since the system is in the ordered φ_2 phase, i.e., $r_2 < 0$. This implies that the coefficient of the φ_1^2 term due to the quantum correction, $\approx -1/(4\pi)^2 r_2\lambda_{12}$, is always positive. The physical significance of this positive φ_1^2 term is that the QCP of the φ_1 phase has been pushed away towards the QCP of the φ_2 phase due to the competition introduced by λ_{12} coupling between these phases [61]. The system that was at the QCP of the φ_1 phase is now in its disordered phase. The deeper the system is in the φ_2 phase, the larger is this effect since $|r_2|$ is larger. The effect also increases with the intensity of the interaction λ_{12} clearly manifesting the competitive nature of this coupling that acts in the sense of reducing the region of coexistence in the phase diagram [61].

If the same analysis is carried out at the new QCP, $r_1^{'}$ (see Fig. 15), the same effect occurs until $r_1^{'} = r_2$ and we arrive at the stable situation studied previously of a quantum bicritical point [61]. For completeness, we point out the rather trivial case of a negative λ_{12} in which case the opposite effect is observed and coexistence is enhanced by this coupling. As shown in Fig. 15, the new QCP of the φ_1 phase has moved to $r_1^{''}$ due to the negative interaction [61].

Next, we consider the case for quartic interaction $\lambda_{12} = 0$, but we turn on the couplings $\delta_{1,2}$. The terms multiplied by η that arise in the quantum corrections due to these couplings are proportional to $r_2\delta_2$ and in particular there are no terms in φ_1^2 coupled to $\delta_{1,2}$, as can be seen from Eq. (262). However, the coeffcient of the term $\varphi_1\varphi_2$ has an opposite behavior to that obtained for the coupling λ_{12}, since both r_2 and δ_2 are negative, with the negative sign coming from the terms in brackets of Eq. (262). We can then state that the quantum corrections arising from these couplings, unlike the case of the previous coupling λ_{12}, favor an increase of the region of coexistence [61].

Finally, we discuss the stability of the coexistence phase described by the complete effective potential in the presence of both kinds of couplings, i.e., the full Eq. (262). As shown before, at classical level, coexistence is always possible whenever $\delta_{1,2} < 0$, even when $r_2 = 0$, since this lowers the total condensation energy. This is also valid with quantum corrections. The complete effective potential assumes a Mexican hat shape, as shown in Fig. 16.

The minima of the *one-loop* effective potential in Eq. (262) occurs for finite values of both order parameters $\varphi_1 = \varphi_2$, and consequently there is a coexistence of phases. Nevertheless, as discussed previously, the λ_{12} parameter couples with φ_1^2 term and we

Figure 16 - *One-loop* effective potential with both couplings finite for r_2 small

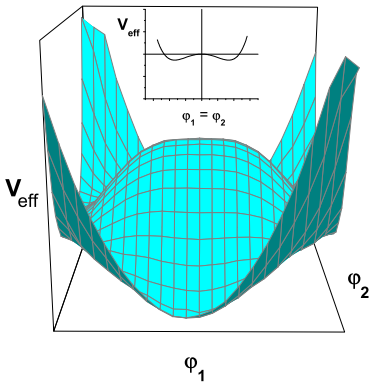

Legend: (Color online) Plot of the complete *one-loop* effective potential in Eq. (262) for r_2 small, with both couplings finite (schematic). The *minima* occurs for finite values of both order parameters, $\varphi_{1,2}$, such that, there is coexistence of phases (see text). For δ_i finite, the physical region of the phase diagram is that where φ_1 and φ_2 have the same sign. The inset shows a cut in a 3d graphic for $\varphi_1 = \varphi_2$ (2d graphic) in order to visualize the region of interest.

Source: Ref. [61].

have competition between the different orderings depending on the quantities r_2 and λ_{12}. In addition, the biquadratic and bilinear couplings also compete producing different trends for the coexistence of phases in the global phase diagram [61].

4.4 Quantum corrections for two-dimensional systems with linear dispersion relation

Let us now change the dimensionality of the system but preserve its Lorentz invariant character in order to investigate the effect of quantum fluctuations for 2d systems with linear dispersion relation [62], which comprise many interesting materials, like high T_c cuprates, heavy fermions compounds with tetragonal [12, 25, 26, 27, 28, 29, 84, 85] structures and Fe-based systems, where AFM and SC are in close proximity or coexist near a magnetic QCP [4, 62].

In general, we expect that lower dimensionalities enhance the effect of quantum fluctuations. With this motivation, we extend the results of the previous section to 2d systems [62]. Since we are still interested in systems with $z = 1$ the effective dimension for this case now is $d_{eff} = d + z = 3$, that is, $d_{eff} < d_c$. Then, we expect that quantum fluctuations will play an important role. It is clear that in this case the effective potential technique is not adequate to compute critical exponents. However, it captures the global

features of the phase diagram and in particular the stability of the critical point [62].

It is worth to emphasize that the procedure that will be applied in this section is entirely analogous to those one described in the previous section and it will persist all along this chapter. Therefore, taking again both phases associated with $z = 1$ we have the propagators as follows [62],

$$G^{(1)}(k) = G_0(w, \vec{q}) = \frac{1}{k^2 + r_1} \qquad \texttt{and} \qquad G^{(2)}(k) = G_0(w, \vec{q}) = \frac{1}{k^2 + r_2} \ . \tag{270}$$

Note that $\mathcal{F}$ in Eq. (204) is not affected by dimensionality, which means that the interacting term in Eq. (204) is not changed. Thus,

$$V_c^{int} = \lambda_1 \varphi_1^4 + \lambda_2 \varphi_2^4 + \lambda_{12} \varphi_1^2 \varphi_2^2 + \delta_1 \varphi_1^3 \varphi_2 + \delta_2 \varphi_1 \varphi_2^3 \tag{271}$$

Our starting point for calculating the first-order quantum corrections is Eq. (226), which for $d_{eff} = 3$ results [62],

$$\begin{aligned} \Gamma^{(1)} &= \frac{1}{2} \int \frac{d^3k}{(2\pi)^3} \ln \left[\left(1 + \frac{b_1}{k^2 + r_1} \right) \right] + \frac{1}{2} \int \frac{d^3k}{(2\pi)^3} \ln \left[\left(1 + \frac{b_2}{k^2 + r_2} \right) \right] + \\ &- \frac{\left(3\delta_1 \varphi_1^2 + 3\delta_2 \varphi_2^2 + 4\lambda_{12} \varphi_1 \varphi_2 \right)^2}{2(B^2 - A^2)} \int \frac{d^3k}{(2\pi)^3} \left(\frac{1}{k^2 + A^2} - \frac{1}{k^2 + B^2} \right) \end{aligned} \tag{272}$$

where,

$$\begin{aligned} b_1 &= 12\lambda_1 \varphi_1^2 + 2\lambda_{12} \varphi_2^2 + 6\delta_1 \varphi_1 \varphi_2 \ , \\ b_2 &= 12\lambda_2 \varphi_2^2 + 2\lambda_{12} \varphi_1^2 + 6\delta_2 \varphi_1 \varphi_2 \ , \\ A^2 &= r_1 + b_1 \ , \\ B^2 &= r_2 + b_2 \ . \end{aligned} \tag{273}$$

Using that $d^dk = S_d k^{d-1} dk$ where $S_d = (2\pi)^{d/2}/\Gamma(d/2)$ we obtain $S_3 = 4\sqrt{2}\pi$, since $\Gamma(3/2) = \sqrt{\pi}/2$. Therefore, we need to deal now with integrals of the type,

$$\frac{2\sqrt{2}}{(2\pi)^2} \int_0^\Lambda dk \ k^2 \ln \left(1 + \frac{b_i}{k^2 + r_i} \right) \tag{274}$$

and

$$\frac{2\sqrt{2}}{(2\pi)^2} \int_0^\Lambda dk \ k^2 \frac{1}{k^2 + (A, B)^2} \tag{275}$$

where Λ is the *cut-off* and A and B are constants with respect to k.

The solutions of the two first integrals in Eq. (272), or equivalently in Eq. (274),

close to the transition and in the limit $\Lambda \to \infty$ are given by

$$I_{1,2} = \frac{2\sqrt{2}}{(2\pi)^2}\left\{\frac{1}{3}\left[3\Lambda b_{1,2} - \pi r_{1,2}^{3/2}\left(1+\frac{b_{1,2}}{r_{1,2}}\right)^{3/2} + \pi r_{1,2}^{3/2}\right]\right\} \tag{276}$$

On the other hand, the solutions of the last two integrals in Eq. (272), or equivalently in Eq. (275), close to the transition and in the limit $\Lambda \to \infty$ are given by,

$$I_{3,4} = \frac{2\sqrt{2}}{(2\pi)^2}\left[\Lambda - \frac{\pi(A,B)}{2}\right] \tag{277}$$

Summing $I_{1,2}$+$I_{3,4}$ we get

$$\begin{aligned}\Gamma^{(1)}_{\varphi_{1,2}} &= \frac{2\sqrt{2}}{(2\pi)^2}\left[\Lambda(b_1+b_2) - \frac{\pi}{3}\left[r_1^{3/2}\left(1+\frac{b_1}{r_1}\right)^{3/2} + r_2^{3/2}\left(1+\frac{b_2}{r_2}\right)^{3/2}\right] + \right. \\ &+ \left. \frac{\pi}{3}\left(r_1^{3/2}+r_2^{3/2}\right) - \pi\frac{\left(3\delta_1\varphi_1^2+3\delta_2\varphi_2^2+4\lambda_{12}\varphi_1\varphi_2\right)^2}{4(B+A)}\right]\end{aligned} \tag{278}$$

where $b_{1,2}$, A and B are given in Eq. (273).

So, for this case we have counterterms as follows,

$$\frac{1}{2}C_1\varphi_1^2\ ,\ \frac{1}{2}C_2\varphi_2^2\ ,\ C_3\varphi_1\varphi_2\ . \tag{279}$$

4.4.1 Bicritical point

Analogously to section 4.3.1 we use in bicritical point that $r_{1,2} \approx 0$ in Eq. (278), as a first approximation, which yields [62],

$$\Gamma^{(1)}_{\varphi_{1,2}} = \frac{\sqrt{2}}{2\pi}\left[\frac{\Lambda}{\pi}(b_1+b_2) - \frac{1}{3}\left(b_1^{3/2}+b_2^{3/2}\right) - \frac{\left(3\delta_1\varphi_1^2+3\delta_2\varphi_2^2+4\lambda_{12}\varphi_1\varphi_2\right)^2}{4(B+A)}\right] \tag{280}$$

To calculate the counterterms we apply the following definitions [61],

$$\left[\frac{d^2\Gamma^{(1)}}{d\varphi_1^2}\right]\Big|_{\varphi_{1,2}=0} = r_1 = 0\ \ ,\ \ \left[\frac{d^2\Gamma^{(1)}}{d\varphi_2^2}\right]\Big|_{\varphi_{1,2}=0} = r_2 = 0\ \ ,\ \left[\frac{d^2\Gamma^{(1)}}{d\varphi_1\varphi_2}\right]\Big|_{\varphi_1=\langle\varphi_1\rangle,\varphi_2=\langle\varphi_2\rangle} = \gamma \tag{281}$$

where, again, $\langle\varphi_{1,2}\rangle$ are the *minimums* of the effective potential.

Thus, we obtain [62],

$$\frac{1}{2}C_1\varphi_1^2 = -\frac{1}{2}\frac{\sqrt{2}}{2\pi^2}\left[\Lambda(24\lambda_1+4\lambda_{12})\right]\varphi_1^2 \tag{282}$$

Figure 17 - The effective potential for bicritical point

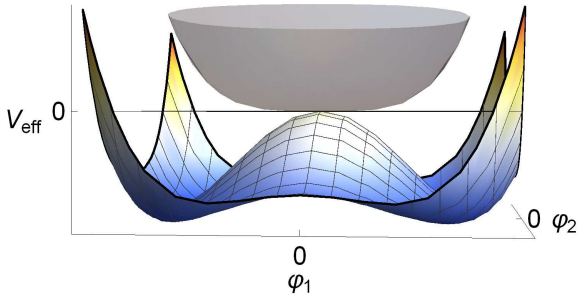

Legend: (Color online) The effective potential for bicritical point with (square lines) and without (gray smooth) quantum corrections. Quantum corrections induce coexistence, i.e., $\varphi_{1,2} = \varphi_c = 0$ is no longer a *minimum* of the effective potential (see text).
Source: Ref. [62].

$$\frac{1}{2}C_2\varphi_2^2 = -\frac{1}{2}\frac{\sqrt{2}}{2\pi^2}\left[\Lambda(24\lambda_2 + 4\lambda_{12})\right]\varphi_2^2 \tag{283}$$

$$C_3\varphi_1\varphi_2 = -\frac{\sqrt{2}}{2\pi^2}\left[\Lambda(6\delta_1 + 6\delta_2)\right]\varphi_1\varphi_2 \tag{284}$$

Replacing the counterterms into Eq. (280) one can obtain the renormalized *one-loop* effective potential at *zero-temperature* in (2+1) dimensions for bicritical point as follows [62],

$$\begin{aligned} V^0_{eff}(\varphi_1,\varphi_2) &= \underbrace{\lambda_1\varphi_1^4 + \lambda_2\varphi_2^4 + \lambda_{12}\varphi_1^2\varphi_2^2 + \delta_1\varphi_1^3\varphi_2 + \delta_2\varphi_1\varphi_2^3}_{classical\ term} + \\ &- \frac{\sqrt{2}}{2\pi}\left[\frac{1}{3}\left(b_1^{3/2} + b_2^{3/2}\right) + \frac{\left(3\delta_1\varphi_1^2 + 3\delta_2\varphi_2^2 + 4\lambda_{12}\varphi_1\varphi_2\right)^2}{4(\sqrt{b_2} + \sqrt{b_1})}\right] \end{aligned} \tag{285}$$

where,

$$b_1 = 12\lambda_1\varphi_1^2 + 2\lambda_{12}\varphi_2^2 + 6\delta_1\varphi_1\varphi_2 \quad \texttt{and} \quad b_2 = 12\lambda_2\varphi_2^2 + 2\lambda_{12}\varphi_1^2 + 6\delta_2\varphi_1\varphi_2\ . \tag{286}$$

The first important observation is that since $\Gamma^{(1)} < 0$ in Eq. (285), $\varphi_{1,2} = \varphi_c = 0$ is no longer a minimum of V^0_{eff} [62]. In fact, V^0_{eff} has a minimum for $\varphi_{1,2} = \varphi_c \neq 0$, signaling a SSB [62], as can be seen in Fig. 17.

Thus, the bicritical point is unstable and quantum fluctuations induce coexistence (see Fig. 18). Our *one-loop* effective potential results can be compared with a perturbative renormalization group analysis. In Ref. [86], a very detailed Wilson renormalization group scheme was implemented at *one-loop* order for an equivalent model (without linear couplings). Their results show that the Gaussian fix point is unstable with all coupling

Figure 18 - Schematic phase diagram showing temperature as a function of pressure for bicritical point with and without quantum corrections.

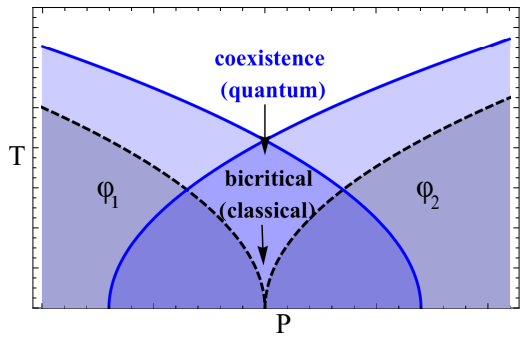

Legend: (Color online) Schematic phase diagram showing temperature as a function of pressure for bicritical point with (blue full line) and without (black dashed line) quantum corrections. Quantum corrections give rise to coexistence (see text).
Source: Ref. [62].

constants growing unbounded very quickly, signaling the absence of non-trivial critical points. These results are in complete agreement with ours.

Interestingly, this dramatic change in the MF phase diagram occurs for any finite (positive) value of the couplings λ_{12} as well as $\delta_{1,2}$. In other words, quantum fluctuations provide stability for the coexistence of phases, whatever the coupling [62]. This result is quite different from its 3d version, where the MF bicritical point is unstable under bilinear interactions, proportional to $\delta_{1,2}$. However, it is stable under the biquadratic interaction λ_{12}.

4.4.2 Coexistence region

Depending on the parameters of the theory, the MF phase diagram supports coexistence regions [61], see Fig. 11. In particular, coexistence is possible whether $\varphi_1 = \varphi_2$ and $\lambda_{12}^2 < 4\lambda_1\lambda_2 + \delta_2\lambda_1 + \delta_1\lambda_2 + \delta_1\delta_2/4$, with $\delta_{1,2} \leq 0$. Analogously to section 4.3.2, to compute quantum fluctuations in a coexistence phase we will focus in one of the QCPs, say $r_1 \approx 0$. At this point, $r_2 < 0$ and $\varphi_2 \neq 0$ since this is an ordered phase. The calculation in the opposite region, $r_2 \approx 0$ with $r_1 < 0$, is completely analogous since both phase have the same dynamic.

From Eq. (278) we get,

$$\begin{aligned}\Gamma^{(1)}_{\varphi_{1,2}} &= \frac{\sqrt{2}}{2\pi}\left\{\frac{\Lambda}{\pi}(b_1+b_2)-\frac{1}{3}\left[b_1^{3/2}+r_2^{3/2}\left(1+\frac{b_2}{r_2}\right)^{3/2}\right]+\right.\\ &+ \left.\frac{1}{3}r_2^{3/2}-\frac{\left(3\delta_1\varphi_1^2+3\delta_2\varphi_2^2+4\lambda_{12}\varphi_1\varphi_2\right)^2}{4(\sqrt{b_2+r_2}+\sqrt{b_1})}\right\} \qquad (287)\end{aligned}$$

To calculate the counterterms we use the definitions [61],

$$\left[\frac{d^2\Gamma^{(1)}}{d\varphi_1^2}\right]\Big|_{\varphi_{1,2}=0} = r_1 = 0 \quad , \quad \left[\frac{d^2\Gamma^{(1)}}{d\varphi_2^2}\right]\Big|_{\varphi_{1,2}=0} = r_2 \quad , \left[\frac{d^2\Gamma^{(1)}}{d\varphi_1\varphi_2}\right]\Big|_{\varphi_1=\langle\varphi_1\rangle,\varphi_2=\langle\varphi_2\rangle} = \gamma \qquad (288)$$

So, we obtain the counterterms as follows,

$$\frac{1}{2}C_1\varphi_1^2 = -\frac{1}{2}\frac{\sqrt{2}}{2\pi^2}\left[\Lambda(24\lambda_1+4\lambda_{12})\right]\varphi_1^2 \qquad (289)$$

$$\frac{1}{2}C_2\varphi_2^2 = -\frac{1}{2}\frac{\sqrt{2}}{2\pi^2}\left[\Lambda(24\lambda_2+4\lambda_{12})\right]\varphi_2^2 \qquad (290)$$

$$C_3\varphi_1\varphi_2 = -\frac{\sqrt{2}}{2\pi^2}\left[\Lambda(6\delta_1+6\delta_2)\right]\varphi_1\varphi_2 \qquad (291)$$

Replacing the counterterms into the *one-loop* effective potential at *zero temperature* in (2+1) dimensions for coexistence region results [62],

$$\begin{aligned}V^0_{eff}(\varphi_1,\varphi_2) &= \underbrace{r_2\varphi_2^2+\lambda_1\varphi_1^4+\lambda_2\varphi_2^4+\lambda_{12}\varphi_1^2\varphi_2^2+\delta_1\varphi_1^3\varphi_2+\delta_2\varphi_1\varphi_2^3}_{classical\ term}+\\ &+ \frac{\sqrt{2}}{(2\pi)}\left\{-\frac{1}{3}\left[b_1^{3/2}+r_2^{3/2}\left(1+\frac{b_2}{r_2}\right)^{3/2}\right]+\right.\\ &+ \left.\frac{1}{3}r_2^{3/2}-\frac{\left(3\delta_1\varphi_1^2+3\delta_2\varphi_2^2+4\lambda_{12}\varphi_1\varphi_2\right)^2}{4(\sqrt{r_2+b_2}+\sqrt{b_1})}\right\} \qquad (292)\end{aligned}$$

where,

$$\begin{aligned}b_1 &= 12\lambda_1\varphi_1^2+2\lambda_{12}\varphi_2^2+6\delta_1\varphi_1\varphi_2\ ,\\ b_2 &= 12\lambda_2\varphi_2^2+2\lambda_{12}\varphi_1^2+6\delta_2\varphi_1\varphi_2\ ,\\ B^2 &= r_2+b_2\ . \qquad (293)\end{aligned}$$

With this correction, the effective potential V^0_{eff} will continue to have minima for

Figure 19 - Schematic phase diagram showing temperature as a function of pressure for coexistence region with and without quantum corrections.

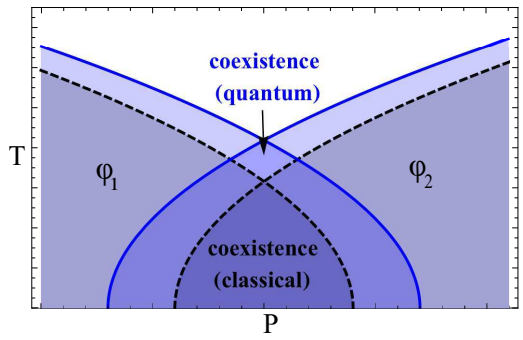

Legend: (Color online) Schematic phase diagram showing temperature as a function of pressure for coexistence region with (blue full line) and without (black dashed line) quantum corrections. Quantum corrections enhance coexistence region (see text).
Source: Ref. [62].

$\varphi_{1,2} \neq 0$. Note that this correction is quite different from the bicritical case, due to the appearance of the mass term contribution (r_2). On the other hand, it is clear that $|r_2| < b_2$. If this condition is not satisfied, the effective potential gets an imaginary part, signaling that the homogeneous coexistence is metastable [87]. In this case, the ground state is no longer homogeneous, giving rise to domain formation.

In the region of stability, i.e., for $|r_2| < b_2$, both λ_{12} and $\delta_{1,2}$ tends to enhance the coexistence region (see Fig. 19), which is consistent with the fact that in the bicritical phase, both interactions produce a symmetry breaking, tending to order both phases, thus ensuring the stability of the coexistence region [62]. However, this is in contrast to the 3d case, where λ_{12} does not increase any order. In fact, it tends to shrink the coexistence region due to simple competition already present at MF level.

4.5 Quantum corrections for two-dimensional systems with dissipative quadratic dispersion relation

In this section we discuss the quantum corrections within *one-loop* approximation for systems with $z = 2$ [4, 24, 51, 52], i.e., phases characterized by a different class of universality, which are usually associated with dissipative modes in SC or paramagnons in itinerant AFM/FM near their respective QCPs. Indeed, we are interested in dealing with SC and AFM competing orders, which are well described by this kind of dynamics [4, 24].

Consider, for instance, $\mathcal{F}$ for an AFM order parameter φ_1 coupled with a complex

SC order parameter Δ [62],

$$\mathcal{F} = V_c = r_1\varphi_1^2 + \lambda_1\varphi_1^4 + r_2\left|\Delta\right|^2 + \lambda_2\left|\Delta\right|^4 + \lambda_{12}\varphi_1^2\left|\Delta\right|^2 \ . \tag{294}$$

The SC order parameter can be parametrized as $\Delta = \varphi_2 + i\varphi_3$, or equivalently $\Delta = |\Delta|\, e^{i\theta}$. The free energy density in Eq. (294) is invariant under transformations of the group $U(1) \times Z_2$, where the $U(1)$ group is related with phase transformations, that is, $\theta \to \theta + \delta\theta$, and Z_2 denote sign changes of the real scalar order parameter φ_1. Since each order parameter transform with a different symmetry group, bilinear couplings are forbidden [62].

In the SC ordered phase, i.e., for $\Delta \neq 0$, there is one massless Goldstone mode associated with phase fluctuations $\delta\theta$. In two spatial dimensions at finite temperature, the $\theta(x)$ correlation function diverges logarithmically with the size of the sample, completely disordering the system. This is nothing but the Mermin-Wagner theorem [88] that states that a continuous symmetry cannot be spontaneously broken at finite temperature in 2d systems. However, at *zero-temperature*, time adds an extra dimension in the problem and the θ correlation function is infrared finite. At *one-loop* order, phase fluctuations decouple from the longitudinal ones and can be absorbed in a global normalization constant. Thus, in this case, the Goldstone mode cannot qualitatively change the character of the QPT [62]. This behavior is quite different in the presence of a magnetic field, since $\theta(x)$ couples with the vector potential, producing the Meissner effect.

Thus, we can safely choose in Eq. (294) a particular direction of the SC order parameter [62], for instance, $\varphi_3 = 0$, and compute the effect of the longitudinal fluctuations, φ_2. In these circumstances, the classical energy density is completely equivalent to Eq. (204) with $\delta_{1,2} = 0$ and the formal calculation of the effective potential V_{eff} follows the same lines of the previous cases [62].

Taking both dynamics with $z = 2$ we have now propagators as follows [62],

$$G^{(1)}(k) = G_0(w,\vec{q}) = \frac{1}{|w|\,\tau' + q^2 + r_1} \quad \texttt{and} \quad G^{(2)}(k) = G_0(w,\vec{q}) = \frac{1}{|w|\,\tau + q^2 + r_2} \ . \tag{295}$$

Note that the procedure to obtain the *one-loop* effective potential for this case will be completely analogous to those one described in the previous sections for Lorentz invariant systems and its *modus operandi* will persist for any calculation that is made within this approximation.

For simplicity, we take $\tau = \tau' = 1$ in Eq. (295). Moreover, due to the anisotropic character between time and space for this propagators, is convenient to solve the effective potential using a *cut-off* in the form $\Lambda^z = \Lambda^2$ for the frequency (ω) and restrict its integration to $0 < \omega + q^2 < \Lambda^2$ [4]. It is worth to emphasize that this different *cut-off* is not necessary and the effective potential is independent of this choice. However, for

Figure 20 - The effective potential for a bicritical point with and without quantum corrections

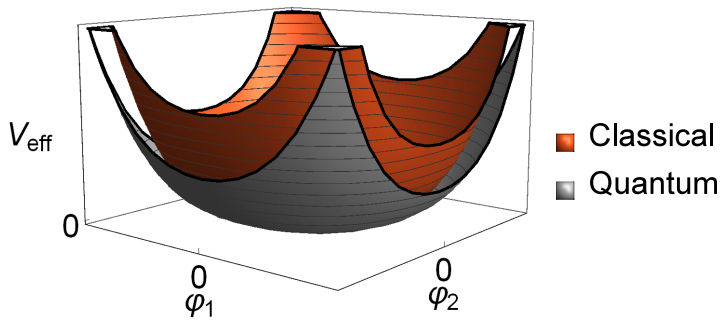

Legend: (Color online) The effective potential for a bicritical point with (gray (external plot)) and without (orange (internal plot)) quantum corrections. The only *minimum* of V^0_{eff} remains at origin (see text).

Source: Ref. [62].

convenience, we use this kind of *cut-off* for $z = 2$ case.

As we have seen in section 4.2, the first-order quantum corrections term is given by,

$$\Gamma^{(1)}(\phi_i) = \frac{1}{2}\int \frac{d^dk}{(2\pi)^d} \ln\left(\det\left[\mathbb{I} - M(k)\right]\right) + \texttt{counterterms} \tag{296}$$

where

$$[M]_{lm} = -G_0^{(l)}(k)\left[\frac{\partial^2 V_c^{int}(\phi_i)}{\partial\phi_l \partial\phi_m}\right]\Bigg|_{\phi_i=\phi_c} \tag{297}$$

Again, applying the *one-loop* effective potential formalism, with the help of Eq. (294), Eq. (295) into Eq. (296), we obtain the quantum corrections for 2d systems characterized by a dissipative behavior. So, after the renormalization process, the renormalized *one-loop* effective potential at *zero-temperature* for bicritical point in (2+2) dimensions results [62],

$$V^0_{eff}(\varphi_{1,2}) = \lambda_1''\varphi_1^4 + \lambda_2''\varphi_1^4 + \lambda_{12}''\varphi_1^2\varphi_2^2 + \frac{1}{(2\pi)^2}\left[8\lambda_{12}^2\varphi_1^2\varphi_2^2\left(\frac{b_1\ln(b_1) - b_2\ln(b_2)}{b_1 - b_2}\right)\right] \tag{298}$$

where,

$$b_1 = 12\lambda_1\varphi_1^2 + 2\lambda_{12}\varphi_2^2 \qquad \texttt{and} \qquad b_2 = 12\lambda_2\varphi_2^2 + 2\lambda_{12}\varphi_1^2\ . \tag{299}$$

Note that the double prime quantities are renormalized parameters. The important result is that the only *minimum* of V^0_{eff} in Eq. (298), computed from $\partial V^0_{eff}/\partial\varphi_i = 0$, is $\varphi_{1,2} = \varphi_c = 0$ [62], as can be seen in Fig. 20.

Then, the bicritical point is robust and survives at quantum level [62]. In other words, there are no qualitative changes in the MF phase diagram. For consistency reasons, it is very simple to check that the effective potential of Eq. (298) satisfies the Callan-Symanzik renormalization group equation [89], with β and γ functions signaling a stable fixed point. This result is in contrast with that obtained with $z = 1$ dynamics, discussed

in the previous section.

For coexistence region, the renormalized *one-loop* effective potential at *zero-temperature* is given by [62],

$$V^0_{eff}(\varphi_{1,2}) = r_1\varphi_1^2 + \lambda_1'''\varphi_1^4 + \lambda_2'''\varphi_2^4 + \lambda_{12}'''\varphi_1^2\varphi_2^2 + \left(\frac{2}{\pi}\right)^2 \left[|r_1|\left(\lambda_{12}\varphi_2^2 + 6\lambda_1\varphi_1^2\right)\ln\left(\frac{b_1+2r_1}{2r_1}\right)\right] \tag{300}$$

where b_1 is given in Eq. (299), and the prime quantities represent renormalized effective couplings.

The important observation here is that the contribution of quantum fluctuations is negative. This comes out because the argument of the ln function is always less than one. On the other hand, we are considering the coupling $\lambda_{12} > 0$. Therefore, the interaction between both order parameters enhance the region of coexistence, very similar to Fig. 19, despite that classically, λ_{12} tends to shrink this region, i.e., quantum fluctuations provide stability for the coexistence of different phases [62]. Once again, this is in contrast with the 3d non-dissipative case ($z = 1$), where λ_{12} tries to frustrate coexistence.

For completeness, we also investigate the *one-loop* approximation for the case where $d_{eff} > d_c = d + z = 4$, that is, for $d = 3$ and $z = 2$. For 3d systems with quadratic dispersion relations the bicritical point is robust and survives at quantum level, as in the case for $d = 2$ in the presence of dissipative dynamics [62]. This is the case of itinerant AFM/FM [51] or SC [4] with dissipative modes with quadratic dispersion near their QPTs. The result for $(3 + 2)$ dimensions is in agreement with the expectation that for effective dimensions $d_{eff} = d + z > 4$, we should not expect drastic changes of the MF results.

Finally, it is worth to point out that the effective potential in the case with $d = 2$, $z = 2$ and $d = 1$, $z = 3$ turns out be of the same form as that of $d = 3$, $z = 1$, as expected from the fact that both cases have the same effective dimension $d + z = 4$ [90]. Analogously, the case $d = 2$, $z = 3$ is the same as $d = 3$, $z = 2$.

5 FINITE TEMPERATURE EFFECTS IN QUANTUM SYSTEMS WITH COMPETING SCALAR ORDERS

In this chapter we apply the well-established Matsubara summation technique [57, 58, 59, 72, 73] from finite temperature QFT to introduce effects of thermal fluctuations on the *one-loop* effective potential of the systems previously investigated. This is an essential ingredient to make a direct contact with experiments. We present our results [63] for both 2d and 3d materials with dynamic critical exponent $z = 1$, such that time and space scale in the same way. Although our study here is carried out for QCPs with Lorentz invariance [4, 24, 41, 51, 61, 62], we expect that our general results will persist for arbitrary values of dynamic exponents [63].

5.1 Introduction

As we have discussed before, in CMP, and more specifically in SCES, one can find several systems [5, 6, 7, 8, 9, 10, 11, 12, 13, 14, 15, 16, 17, 18, 19] that at low temperatures exhibit very exotic experimental phase diagrams with competing/coexisting orders as a function of some fine tuned control parameter, such as pressure, doping or magnetic field [3, 4]. In this kind of systems, the interplay between finite temperature and quantum fluctuations may give rise to crucial effects and consequently provides clear predictions for the expected behavior of these systems [63]. In that sense, taking into account effects of thermal fluctuations brings our previous results to the new level of a testable theory.

Thus, in this chapter we extend the *one-loop* effective potential for finite temperatures in order to explore thermodynamic aspects that might be characteristic of these competing systems on the same scenarios discussed previously, i.e., the case of a bicritical point and that where two phases coexist. For consistency, we consider two real scalar order parameters interacting through quartic, as well as bilinear coupling terms, in both 2d and 3d systems. The dynamics of the systems here are characterized by Lorentz invariant critical theories [4, 24, 41, 51, 61, 62], i.e., with linear dispersion relations [62]. The effects of finite temperatures are introduced by means of the Matsubara summation formalism from finite temperature QFT [57, 58, 59, 72, 73].

5.2 Extension of the effective potential for finite temperatures

We apply the standard Matsubara summation [57, 58, 59, 72, 73] procedure to extend the *one-loop* effective potential to include finite temperature effects. Basically, its

consists of recognizing the following identifications and replacements in $\Gamma^{(1)}$,

$$\frac{1}{2}\int\frac{d^dk}{(2\pi)^d} \;\;\Rightarrow\;\; \frac{1}{2}\frac{1}{(2\pi)^d}\int d^{d-1}p\,\left(T\sum_{\omega_n}\right) \tag{301}$$

where $d^dk = S_dk^{d-1}dk$ with $S_d = (2\pi)^{d/2}/\Gamma(d/2)$ and $\omega_n = 2\pi nT$, with $n \in \mathcal{Z}$.

The Matsubara frequencies (ω_n) are discrete, due to the periodic boundary conditions for bosonic fields [57, 58, 59, 72, 73], i.e., $\varphi_i(0,x) = \varphi_i(\beta,x)$, and the fields should satisfy on the finite imaginary time axis $0 \leq \tau \leq \beta = 1/T$, where we consider the Boltzman constant $k_B = 1$ all along this dissertation.

It is worth to emphasize that finite temperature effects do not introduce any new divergence in the theory. For this reason, the only counterterms, necessary to renormalize the theory, are those introduced at *zero-temperature* [63]. Finally, note, from Eq. (301), that the dimensionality is encoded in the momentum integrations only.

Our starting point is Eq. (226), which is given by [63],

$$\begin{aligned}\Gamma^{(1)} &= \frac{1}{2}\int\frac{d^dk}{(2\pi)^d}\left\{\ln\left[\left(1+\frac{b_1}{k^2+r_1}\right)\right]+\ln\left[\left(1+\frac{b_2}{k^2+r_2}\right)\right]\right\}+ \\ &- \frac{\left(3\delta_1\varphi_1^2+3\delta_2\varphi_2^2+4\lambda_{12}\varphi_1\varphi_2\right)^2}{(B^2-A^2)}\frac{1}{2}\int\frac{d^dk}{(2\pi)^d}\left(\frac{1}{k^2+A^2}-\frac{1}{k^2+B^2}\right)+\texttt{counterterms}\end{aligned} \tag{302}$$

where

$$\begin{aligned} b_1 &= 12\lambda_1\varphi_1^2+2\lambda_{12}\varphi_2^2+6\delta_1\varphi_1\varphi_2\;, \\ b_2 &= 12\lambda_2\varphi_2^2+2\lambda_{12}\varphi_1^2+6\delta_2\varphi_1\varphi_2\;, \\ A^2 &= r_1+b_1\;, \\ B^2 &= r_2+b_2\;. \end{aligned} \tag{303}$$

Note that r_1 and r_2 are the distances to the *zero-temperature* critical points at which the order parameters φ_1 and φ_2 vanish, respectively. In addition, let us also introduce two energy scales $\Delta_{1,2} = \sqrt{b_{1,2}+r_{1,2}}$ that will play a role when we consider different regimes below [63].

Here we are interested in including finite temperature effects for both 2d and 3d systems with $z = 1$. So, for instance, in (3+1) dimensions Eq. (302) can be written as follows [63],

$$\begin{aligned}\Gamma^{(1)} &= \frac{1}{2}\int\frac{d^4k}{(2\pi)^4}\ln\left[\left(1+\frac{b_1}{k^2+r_1}\right)\left(1+\frac{b_2}{k^2+r_2}\right)\right]+ \\ &- \frac{\left(3\delta_1\varphi_1^2+3\delta_2\varphi_2^2+4\lambda_{12}\varphi_1\varphi_2\right)^2}{2(B^2-A^2)}\int\frac{d^4k}{(2\pi)^4}\left(\frac{1}{k^2+A^2}-\frac{1}{k^2+B^2}\right)+\texttt{counterterms}\end{aligned} \tag{304}$$

where $b_{1,2}$, A and B are given in Eq. (303).

From Eq. (304), we can identify two different types of integrals to be solved,

$$\frac{1}{2}\int \frac{d^4k}{(2\pi)^4}\ln\left(1+\frac{b_{1,2}}{k^2+r_{1,2}}\right) \quad \texttt{and} \quad \int \frac{d^4k}{(2\pi)^4}\frac{1}{k^2+(A,B)^2} \tag{305}$$

With the help of Eq. (301) one can introduce finite temperature effects on the effective potential through the following transformation in Eq. (304),

$$\frac{1}{2}\int \frac{d^4k}{(2\pi)^4} \;\Rightarrow\; \frac{1}{2}\frac{1}{(2\pi)^4}\int d^3p\int_0^\beta d\omega \Rightarrow \frac{1}{2}\frac{1}{(2\pi)^4}\int d^3p\;\left(T\sum_{\omega_n}\right) \tag{306}$$

where $d^3p = S_3\; p^2\; dp$ with $S_3 = 2\sqrt{2}(2\pi)$.

From Eq. (306) we get

$$\frac{1}{2}\int \frac{d^4k}{(2\pi)^4} \;\Rightarrow\; \frac{\sqrt{2}}{(2\pi)^3}\int dp\; p^2\left(T\sum_{\omega_n}\right) \tag{307}$$

The first kind of integrals in Eq. (305) can be rewritten, using Eq. (307), as follows,

$$\frac{1}{2}\int \frac{d^4k}{(2\pi)^4}\ln\left(1+\frac{b_{1,2}}{k^2+r_{1,2}}\right) \Rightarrow \frac{\sqrt{2}}{(2\pi)^3}\int dp\; p^2\; T\sum_{\omega_n}\ln\left(1+\frac{b_{1,2}}{k^2+r_{1,2}}\right) \tag{308}$$

where $k^2 = \omega_n^2 + p^2$.

Replacing $k^2 = \omega_n^2 + p^2$ into Eq. (308) we obtain,

$$\frac{\sqrt{2}}{(2\pi)^3}\int dp\; p^2\; T\sum_{\omega_n}\ln\left(1+\frac{b_{1,2}}{k^2+r_{1,2}}\right) = \frac{\sqrt{2}}{(2\pi)^3}\int dp\; p^2\; T\sum_{\omega_n}\ln\left(\frac{\omega_n^2+p^2+r_{1,2}+b_{1,2}}{\omega_n^2+p^2+r_{1,2}}\right) \tag{309}$$

Note that Eq. (309) can be rewritten in the form,

$$\begin{aligned} &\frac{\sqrt{2}}{(2\pi)^3}\int dp\; p^2\; T\sum_{\omega_n}\ln\left(\frac{\omega_n^2+p^2+r_{1,2}+b_{1,2}}{\omega_n^2+p^2+r_{1,2}}\right) = \\ = \;&\frac{\sqrt{2}}{(2\pi)^3}\int dp\; p^2\; T\sum_{\omega_n}\ln\left(\frac{(\omega_n^2+p^2+r_{1,2}+b_{1,2})T^2}{(\omega_n^2+p^2+r_{1,2})T^2}\right) \end{aligned} \tag{310}$$

From Eq. (310) we get

$$\frac{\sqrt{2}}{(2\pi)^3}\int dp\; p^2\;\left\{T\sum_{\omega_n}\ln\left(\frac{\omega_n^2+p^2+r_{1,2}+b_{1,2}}{T^2}\right) - T\sum_{\omega_n}\ln\left(\frac{\omega_n^2+p^2+r_{1,2}}{T^2}\right)\right\} \tag{311}$$

Therefore, from Eq. (311), one can recognize the structure,

$$\frac{\sqrt{2}}{(2\pi)^3}\int dp\; p^2\;\left\{T\sum_{\omega_n}\ln\left(\frac{\omega_n^2+\epsilon_{p_{1,3}}^2}{T^2}\right)-T\sum_{\omega_n}\ln\left(\frac{\omega_n^2+\epsilon_{p_{2,4}}^2}{T^2}\right)\right\} \tag{312}$$

where $\epsilon_{p_{1,3}}^2=p^2+r_{1,2}+b_{1,2}$ and $\epsilon_{p_{2,4}}^2=p^2+r_{1,2}$.

To perform the Matsubara summation we can use the following identity in Eq. (312),

$$\sum_{\omega_n}\ln\left(\frac{\omega_n^2+\epsilon_p^2}{T^2}\right)=\frac{\epsilon_p}{T}+2\ln\left(1-e^{-\frac{\epsilon_p}{T}}\right)+\texttt{constant} \tag{313}$$

where the constant term is temperature independent.

With the help of Eq. (313) one can write Eq. (312) in the form,

$$\frac{\sqrt{2}}{(2\pi)^3}\int dp\; p^2\left\{\left(\epsilon_{p_{1,3}}-\epsilon_{p_{2,4}}\right)+2T\;\ln\left[\frac{\left(1-e^{-\frac{\epsilon_{p_{1,3}}}{T}}\right)}{\left(1-e^{-\frac{\epsilon_{p_{2,4}}}{T}}\right)}\right]\right\} \tag{314}$$

Therefore, the first type of integrals in Eq. (305), after performing Matsubara summation, are given by,

$$\frac{1}{2}\int\frac{d^4k}{(2\pi)^4}\ln\left(1+\frac{b_{1,2}}{k^2+r_{1,2}}\right)=\frac{\sqrt{2}}{(2\pi)^3}\int dp\,p^2\left\{\left(\epsilon_{p_{1,3}}-\epsilon_{p_{2,4}}\right)+2T\;\ln\left[\frac{\left(1-e^{-\frac{\epsilon_{p_{1,3}}}{T}}\right)}{\left(1-e^{-\frac{\epsilon_{p_{2,4}}}{T}}\right)}\right]\right\} \tag{315}$$

where $\epsilon_{p_{1,3}}^2=p^2+r_{1,2}+b_{1,2}$ and $\epsilon_{p_{2,4}}^2=p^2+r_{1,2}$ with $b_{1,2}$ given by Eq. (303).

Note, at this point, that the two first terms in the *momentum* integral of Eq. (315) are related to the contribution of the effective potential at *zero-temperature*, and the temperature dependence is only in the last term of Eq. (315).

Let us focus now on the second type of integrals given in Eq. (305). So, from Eq. (306), we get

$$\frac{1}{2}\int\frac{d^4k}{(2\pi)^4}\frac{1}{k^2+(A,B)^2}\;\;\Rightarrow\;\;\frac{\sqrt{2}}{(2\pi)^3}\int dp\;p^2\;T\sum_{\omega_n}\frac{1}{k^2+(A,B)^2} \tag{316}$$

Once again, using that $k^2=\omega_n^2+p^2$ one can rewrite Eq. (316) in the form,

$$\frac{\sqrt{2}}{(2\pi)^3}\int dp\;p^2\;T\sum_{\omega_n}\frac{1}{\omega_n^2+p^2+(A,B)^2}=\frac{\sqrt{2}}{(2\pi)^3}\int dp\;p^2\;T\sum_{\omega_n}\frac{1}{\omega_n^2+\epsilon_{p_{5,6}}^2} \tag{317}$$

where $\epsilon_{p_{5,6}}^2=p^2+(A,B)^2$.

We can now use another identity to calculate the Matsubara summation in Eq. (317),

$$T\sum_{\omega_n}\frac{1}{\omega_n^2+\epsilon_p^2}=\frac{1}{2\epsilon_p}\left[1+2f_{BE}(\epsilon_p)\right] \tag{318}$$

where,

$$f_{BE}(\epsilon_p)=\frac{1}{e^{\epsilon_p/T}-1} \tag{319}$$

is the Bose-Einstein distribution function.

With the help of Eq. (318) we obtain

$$\frac{\sqrt{2}}{(2\pi)^3}\int dp\ p^2\ T\sum_{\omega_n}\frac{1}{\omega_n^2+\epsilon_{p_{5,6}}^2}=\frac{\sqrt{2}}{(2\pi)^3}\int dp\ p^2\left\{\frac{1}{2\epsilon_{p_{5,6}}}\left[1+2f_{BE}(\epsilon_{p_{5,6}})\right]\right\} \tag{320}$$

where $\epsilon_{p_{5,6}}^2=p^2+(A,B)^2$. Note that the first term in *momentum* integral of Eq. (320) is associated with the *zero-temperature* term on the effective potential.

Finally, using Eq. (315) and Eq. (320) one can rewrite the first-order quantum corrections term from Eq. (302) in order to take into account finite temperature effects as follows,

$$\begin{aligned}
\Gamma^{(1)} &= \frac{\sqrt{2}}{(2\pi)^3}\int dp\ p^2\Bigg\{\Bigg(\epsilon_{p_1}-\epsilon_{p_2}+\epsilon_{p_3}-\epsilon_{p_4}+\\
&- \frac{\left(3\delta_1\varphi_1^2+3\delta_2\varphi_2^2+4\lambda_{12}\varphi_1\varphi_2\right)^2}{(B^2-A^2)}\left[\frac{1}{2\epsilon_{p_5}}-\frac{1}{2\epsilon_{p_6}}\right]\Bigg)+\\
&+ 2T\ \ln\left[\frac{\left(1-e^{-\frac{\epsilon_{p_1}}{T}}\right)\left(1-e^{-\frac{\epsilon_{p_3}}{T}}\right)}{\left(1-e^{-\frac{\epsilon_{p_2}}{T}}\right)\left(1-e^{-\frac{\epsilon_{p_4}}{T}}\right)}\right]+\\
&- \frac{\left(3\delta_1\varphi_1^2+3\delta_2\varphi_2^2+4\lambda_{12}\varphi_1\varphi_2\right)^2}{(B^2-A^2)}\left[\frac{f_{BE}(\epsilon_{p_5})}{\epsilon_{p_5}}-\frac{f_{BE}(\epsilon_{p_6})}{\epsilon_{p_6}}\right]\Bigg\}
\end{aligned} \tag{321}$$

where

$$\begin{aligned}
\epsilon_{p_{1,3}}^2 &= p^2+r_{1,2}+b_{1,2}\ ,\\
\epsilon_{p_{2,4}}^2 &= p^2+r_{1,2}\ ,\\
\epsilon_{p_{5,6}}^2 &= p^2+(A,B)^2\ ,\\
f_{BE}(\epsilon_p) &= \frac{1}{e^{\epsilon_p/T}-1}\ ,
\end{aligned} \tag{322}$$

with $b_{1,2}$, A and B given in Eq. (303).

Note that finite temperature effects are encoded in the last two terms of Eq. (321). Furthermore, it is worth to emphasize that the contribution at *zero-temperature* in Eq. (321) was already calculated in section 4.3 and section 4.4.

Thus, for (3+1) dimensions we obtain [63]

$$
\begin{aligned}
V_{eff}^{(3+1)dim} &= V_{eff}^{0\ (3+1)dim} + \\
&+ \frac{\sqrt{2}}{(2\pi)^3}\int dp\ p^2\Bigg\{2T\ \ln\left[\frac{\left(1-e^{-\frac{\epsilon_{p_1}}{T}}\right)}{\left(1-e^{-\frac{\epsilon_{p_2}}{T}}\right)}\frac{\left(1-e^{-\frac{\epsilon_{p_3}}{T}}\right)}{\left(1-e^{-\frac{\epsilon_{p_4}}{T}}\right)}\right] + \\
&- \frac{\left(3\delta_1\varphi_1^2+3\delta_2\varphi_2^2+4\lambda_{12}\varphi_1\varphi_2\right)^2}{(B^2-A^2)}\left[\frac{f_{BE}(\epsilon_{p_5})}{\epsilon_{p_5}}-\frac{f_{BE}(\epsilon_{p_6})}{\epsilon_{p_6}}\right]\Bigg\}
\end{aligned}
\tag{323}
$$

where $\epsilon_{p_i}^2$ and $f_{BE}(\epsilon_p)$ are given in Eq. (322), and $b_{1,2}$, A and B given in Eq. (303).

It is worth to point out, at this point, that the only difference for the case in (2+1) dimension is that we have to consider $d^2p = S_2\ p\ dp$, where $S_2 = 2\pi$ in Eq. (301). So, we get the effective potential for (2+1) dimensions in the form [63],

$$
\begin{aligned}
V_{eff}^{(2+1)dim} &= V_{eff}^{0\ (2+1)dim} + \\
&+ \frac{1}{2}\frac{1}{(2\pi)^2}\int dp\ p\Bigg\{2T\ \ln\left[\frac{\left(1-e^{-\frac{\epsilon_{p_1}}{T}}\right)}{\left(1-e^{-\frac{\epsilon_{p_2}}{T}}\right)}\frac{\left(1-e^{-\frac{\epsilon_{p_3}}{T}}\right)}{\left(1-e^{-\frac{\epsilon_{p_4}}{T}}\right)}\right] + \\
&- \frac{\left(3\delta_1\varphi_1^2+3\delta_2\varphi_2^2+4\lambda_{12}\varphi_1\varphi_2\right)^2}{(B^2-A^2)}\left[\frac{f_{BE}(\epsilon_{p_5})}{\epsilon_{p_5}}-\frac{f_{BE}(\epsilon_{p_6})}{\epsilon_{p_6}}\right]\Bigg\}
\end{aligned}
\tag{324}
$$

where, again, $\epsilon_{p_i}^2$ and $f_{BE}(\epsilon_p)$ are given in Eq. (322), and $b_{1,2}$, A and B given in Eq. (303).

Below, we investigate in details the effects of finite temperature on the effective potential for both cases, i.e., for Eq. (323) and Eq. (324) separately. Initially, we study 2d systems and then we will discuss 3d materials [63].

5.3 Finite temperature effects for two-dimensional systems with linear dispersion relation

To investigate finite temperature effects and obtain some thermodynamic aspects on the phase diagrams of systems with multiple competing scalar orders in (2+1) dimensions we need to solve the *momentum* integrals given in Eq. (324). In that sense, we will do it for both situations of interest, i.e., bicritical point and coexistence region [63]. When it is not possible to get some analytical expression, we will solve these integrals numerically.

Figure 21 - Instability of the QCP in 2d systems for any finite couplings

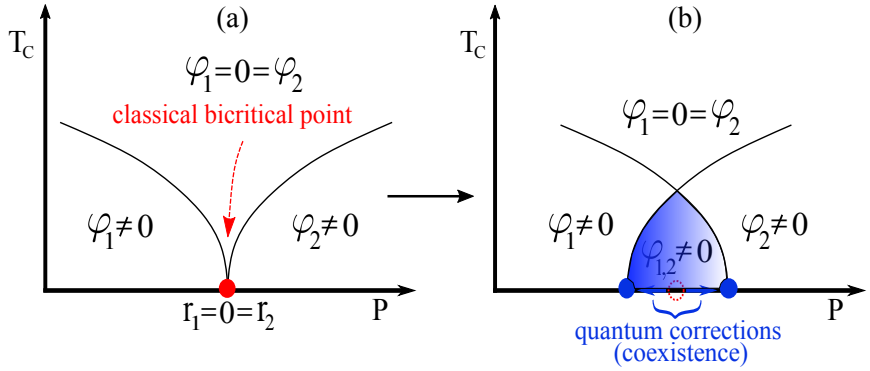

Legend: (Color online) (a) The ZTCBP (red) is unstable to quantum corrections in 2d for quartic and bilinear couplings [62]. In 3d it is stable for a quartic coupling between the fields but unstable to a bilinear interaction [61]. (b) The dynamics of the fields is described by Lorentz invariant critical theories and give rise, in the unstable cases, to a region of coexistence ($\varphi_{1,2} \neq 0$ (shaded (blue) region)), as shown schematically in the phase diagram.

Source: Ref. [63].

5.3.1 Bicritical point

Initially, let us briefly recall the expression of $V_{eff}^{0\ (2+1)dim}$ in Eq. (285) for a bicritical point, or equivalently, for a *zero-temperature* classical bicritical point (ZTCBP) [62],

$$\begin{aligned} V_{eff}^{0\ (2+1)dim} &= \lambda_1\varphi_1^4 + \lambda_2\varphi_2^4 + \lambda_{12}\varphi_1^2\varphi_2^2 + \delta_1\varphi_1^3\varphi_2 + \delta_2\varphi_1\varphi_2^3 + \\ &- \frac{\sqrt{2}}{2\pi}\left[\frac{1}{3}\left(b_1^{3/2} + b_2^{3/2}\right) + \frac{\left(3\delta_1\varphi_1^2 + 3\delta_2\varphi_2^2 + 4\lambda_{12}\varphi_1\varphi_2\right)^2}{4(\sqrt{b_2} + \sqrt{b_1})}\right] \end{aligned} \tag{325}$$

where $b_{1,2}$ are given by Eq. (286).

From Eq. (325) one can see that quantum corrections in 2d give rise to coexistence for any finite couplings, i.e., for quartic as well as bilinear interactions [62] (see Fig. 21). Conversely, in the 3d case, only the bilinear coupling gives rise to coexistence [61]. Below, we discuss the effects of finite temperature at a classical bicritical point.

We consider now the effects of finite temperature on the ZTCBP at $r_1 = r_2 = 0$ for 2d systems [63]. Note that these parameters appear in definitions of ϵ_{p_i} in Eq. (322). It turns out in this case that it is not possible to obtain an analytical expression for the full temperature dependent effective potential, Eq. (324), and we have to analyze particular limits.

First, we investigate the limit of low temperatures that correspond to $T << \Delta_{1,2}$. In this limit, one can neglect the last two terms depending on temperature in Eq. (324),

since the first one dominates at this temperature regime. Therefore, we get the following expression for the effective potential [63],

$$V_{eff}^{(2+1)dim} = V_{eff}^{0\ (2+1)dim} + \tfrac{1}{2}\tfrac{1}{(2\pi)^2}\int p\ dp \left\{ 2T\ \ln\left[\frac{\left(1-e^{-\frac{\epsilon_{p_1}}{T}}\right)}{\left(1-e^{-\frac{\epsilon_{p_2}}{T}}\right)} \frac{\left(1-e^{-\frac{\epsilon_{p_3}}{T}}\right)}{\left(1-e^{-\frac{\epsilon_{p_4}}{T}}\right)} \right] \right\} \tag{326}$$

where $\epsilon_{p_i}^2$ is given in Eq. (322), and $b_{1,2}$, A and B given in Eq. (303).

Since we are interested in bicritical case, i.e., for $r_{1,2} = 0$ in Eq. (326), it implies that the terms involving $\epsilon_{p_{2,4}}$ have to be treated differently from those depending on $\epsilon_{p_{1,3}}$. The former yields [63],

$$\int_0^\infty dp\ p\ \ln\left(1 - e^{-\frac{\epsilon_{p_{2,4}}}{T}}\right) = -T^2\zeta(3) \approx -1.2\,T^2 \tag{327}$$

The latter, in the low temperature regime, i.e., for $T << \Delta_{1,2}$, yields from Eq. (326),

$$\int_0^\infty dp\ p\ \ln\left(1 - e^{-\frac{\epsilon_{p_i}}{T}}\right) \approx -\int p\ dp\ e^{-\frac{\epsilon_{p_i}}{T}} \tag{328}$$

where we have used that $\ln(1-x) \approx -x$.

From Eq. (328) we finally get,

$$-\int_0^\infty dp\ p\ e^{-\frac{\epsilon_{p_{1,3}}}{T}} = -\int_0^\infty p\ dp\ e^{-\frac{\sqrt{p^2+b_{1,2}}}{T}} = -T^2\left[1 + \frac{\sqrt{b_{1,2}}}{T}\right] e^{-\frac{\sqrt{b_{1,2}}}{T}}. \tag{329}$$

With the help of Eq. (327), Eq. (329) and Eq. (325) we can rewrite Eq. (326) as follows [63],

$$\begin{aligned} V_{eff}^{(2+1)dim} \;=\; & \underbrace{\lambda_1\varphi_1^4 + \lambda_2\varphi_2^4 + \lambda_{12}\varphi_1^2\varphi_2^2 + \delta_1\varphi_1^3\varphi_2 + \delta_2\varphi_1\varphi_2^3}_{classical\ term} + \\ & \underbrace{-\frac{\sqrt{2}}{2\pi}\left[\frac{1}{3}\left(b_1^{3/2} + b_2^{3/2}\right) + \frac{\left(3\delta_1\varphi_1^2 + 3\delta_2\varphi_2^2 + 4\lambda_{12}\varphi_1\varphi_2\right)^2}{4(\sqrt{b_2} + \sqrt{b_1})}\right]}_{quantum\ corrections} + \\ & \underbrace{+\frac{T^3}{(2\pi)^2}\left\{-\sum_{i=1}^{2}\left[1 + \frac{\sqrt{b_i}}{T}\right] e^{-\frac{\sqrt{b_i}}{T}} + 2.4\right\}}_{finite\ temperature\ effects} \end{aligned} \tag{330}$$

where $b_{1,2}$ are given by Eq. (286).

Initially, we investigate the effects of finite temperature plotting the effective potential for bicritical point with $z = 1$, that is, Eq. (330), for different values of temperature. Without loss of generality, in numerical calculations we take $\lambda_1 = \lambda_2 = 0.05$ and $\lambda_{12} = 0.01$ in energy units to analyze the effects of the interaction term. For simplicity, one can also take $\delta_1 = \delta_2 = 0$ in Eq. (330) for 2d case since both couplings give rise to the

Figure 22 - The effective potential for a bicritical point in 2d systems with $z = 1$ for different values of temperatures

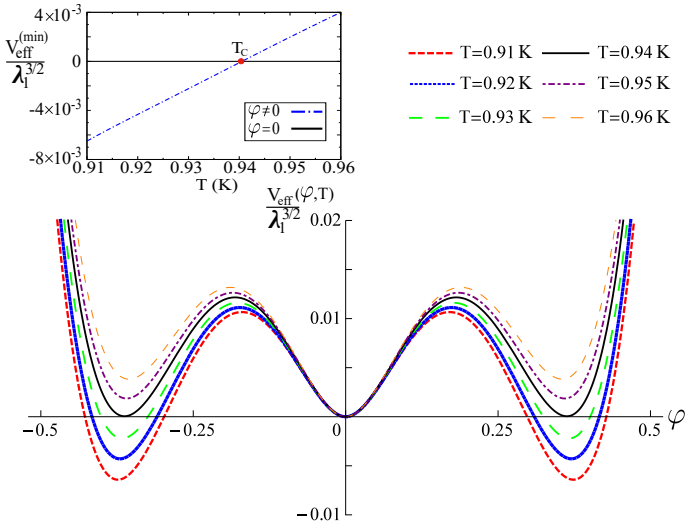

Legend: (Color online) The effective potential for a bicritical point in 2d systems with $z = 1$ for different values of temperatures (Eq. (330)). Without loss of generality, we take $\lambda_1 = \lambda_2 = 0.05\ (eV)^2$, $\lambda_{12} = 0.01\ (eV)^2$, $\delta_1 = \delta_2 = 0$, and $\varphi_{1,2} = \varphi$ (dimensionless). One can clearly see the signature of a first-order temperature phase transition (solid (black) line) at $T_c \approx 0.94\ K$, when the *minima* become degenerate. The tangent of the angle between the crossing energy lines (upper panel) is related to the latent heat L (see text).

Source: Ref. [63].

same behavior [62]. Furthermore, since we have coexistence from quantum corrections, in order to satisfy the particular analytical classical solution discussed in section 3.2.2 we take $\varphi_1 = \varphi_2 = \varphi$ and thus we can generate a two-dimensional plot since both order parameters are finite and equal in the coexistence region, as shown in Fig. 22.

The coexistence phase induced by quantum corrections [62] becomes unstable as we increase temperature, i.e., thermal fluctuations tend to disorder the system, as expected. This is shown in Fig. 22 (lower panel) where thermal fluctuations give rise to a *weak first-order temperature phase transition* [91, 92, 93] when the energy of the minima become degenerate (solid black line). This transition is associated with the interchange of stability of the two phases, ordered and disordered, as can be also seen in Fig. 22 (upper panel). The tangent of the angle between the crossing energy lines is related to the latent heat L [4]. Using the numerical values of Fig. 22 we obtain $L/(k_B T_c) \approx 0.21 < 1$, consistent with the *weak first-order* nature of this transition, i.e., this kind of transition presents a small latent heat compared to thermal fluctuations [4], making it difficult to be experimentally distinguished from a continuous transition.

Replacing the numerical values $\lambda_{1,2} = 0.05\ (eV)^2$, $\lambda_{12} = 0.01\ (eV)^2$, $\delta_{1,2} = 0$ and

Figure 23 - Scaling regimes of the specific heat for a bicritical point in 2d systems with $z = 1$

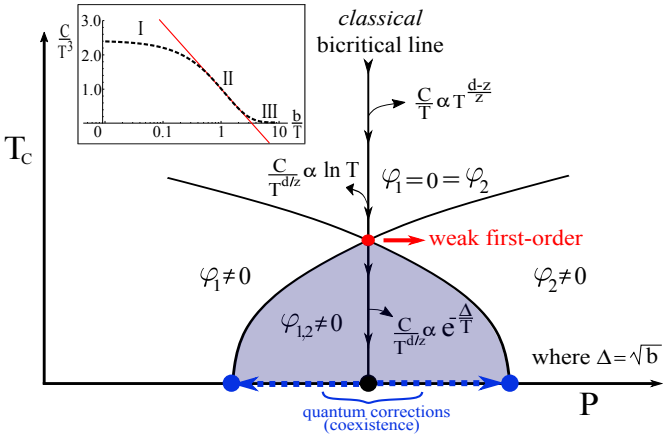

Legend: (Color online) Schematic phase diagram for a bicritical point in 2d systems with $z = 1$ showing the different scaling regimes of the specific heat. Quantum corrections (blue arrows) give rise to a coexistence region ($\varphi_{1,2} \neq 0$ (shaded gray)). At the classical bicritical line (see Fig. 21), we can identify three different scaling regimes for the specific heat. At the temperature T_c where both critical lines cross (red) there is a *weak first-order temperature phase transition*. Below T_c, in the coexistence region, there are gaps for thermal excitations, that is, $\Delta_{1,2} = \sqrt{b_{1,2}}$, where b_i is given by Eq. (286). The inset shows the numerical results for the specific heat calculated from the temperature dependent integral in Eq. (326) for $T \gtrsim T_c$. The intermediate regime, i.e., regime II, is distinguished by a logarithmic dependence (solid red line in the inset).

Source: Ref. [63].

$\varphi \approx 0.35$ (dimensionless) within the coexistence region, see Fig. 22, yields $\Delta_{1,2} \approx 0.28\ eV$. On the other hand, $k_B T \approx 8.0 \times 10^{-5}\ eV$, which corresponds to $T = 0.93\ K$ (within the coexistence region). Therefore, one can confirm our assumption that $T << \Delta_{1,2}$ at low temperatures.

If we tune the external parameter at the ZTCBP (see Fig. 21 (a)) whereupon quantum corrections give rise to a coexistence region [62] (see Fig. 21 (b)), we can study the effects of the temperature on the thermodynamic properties of the system.

For $T >> T_c$, we obtain, from Eq. (330), a cubic temperature dependence in the effective potential for the 2d case, in agreement with the expected scaling form of the free energy [4], i.e., $\mathcal{F} \propto T^{(d+z)/z}$, for a system approaching a Lorentz invariant QCP in d-dimensions. This implies that the specific heat scales as $C/T \propto T^{(d-z)/z}$ [4]. In fact, it presents three regimes for $T \gtrsim T_c$, as shown in Fig. 23. A high temperature one, for $T >> T_c$, where $C/T \propto T^{(d-z)/z}$ and the system appears to be unaware of both the existence of a weak first-order transition at lower temperatures and of a coexistence phase for $T < T_c$. In this regime it behaves as approaching a QCP in d-dimensions with dynamic

Figure 24 - Numerical results for 2d systems with $z = 1$

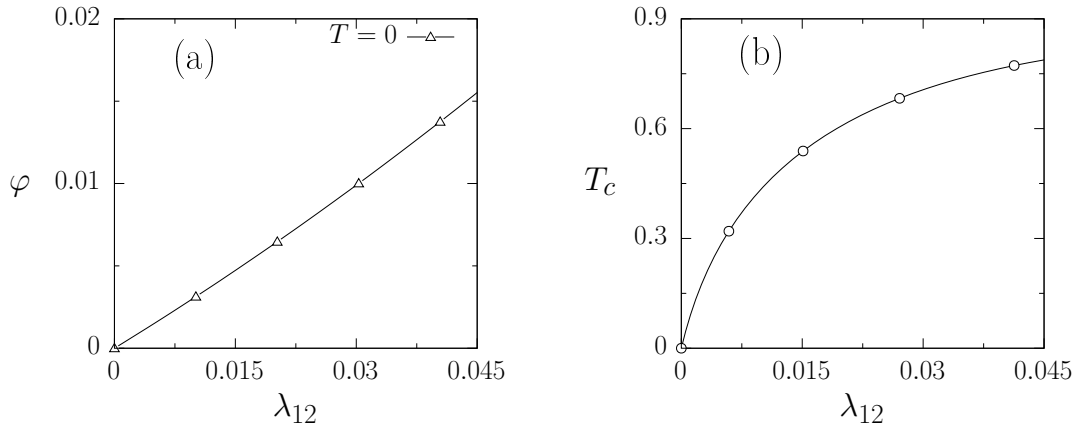

Legend: Numerical results obtained from the effective potential, Eq. (330), in the case of 2d systems with $z = 1$. (a) The order parameter ($\varphi_1 = \varphi_2 = \varphi$) as a function of the effective coupling at zero temperature. One can confirm that quantum fluctuations enhance the coexistence region since φ increases as a function of the quartic coupling λ_{12}. (b) The critical temperature T_c as a function of this coupling between the order parameters. These numerical results are consistent with the schematic phase diagrams exhibited in Fig. 21 and Fig. 23.

Source: Ref. [63].

exponent z. At lower temperatures, but still for $T \gtrsim T_c$, the specific heat crosses over to a less universal regime, where it behaves as $C/T^{d/z} \propto -\ln T$, see Fig. 23. Finally, at very low temperatures, $T << T_c$, the specific heat vanishes exponentially as a function of temperature, i.e., $C/T^{d/z} \propto \exp(-\Delta/T)$ [4] as can be seen from Eq. (330). In this regime, quantum corrections give rise to a coexistence region and there are gaps, $\Delta_{1,2} = \sqrt{b_{1,2}}$ for thermal excitations in finite size domains, see Eq. (329). Then, we can define two new length scales $\xi_{1,2} = 1/\sqrt{2b_{1,2}}$, that are essentially associated with the size of domains that begin to form once we reach the coexistence region cooling down the system [4], see arrows in Fig. 23.

For completeness, and again, without loss of generality, we can obtain some numerical results using the same numerical parameters as before. For consistency, we consider that the two *gaps* for thermal excitations are equal, see Eq. (286). This implies taking $\lambda_1 = \lambda_2$, such that $\varphi_1 = \varphi_2 = \varphi$. Observe from Fig. 24 (a) that at *zero-temperature* the order parameter (φ) increases as a function of the couplings (λ_{12}), as expected since quantum fluctuations stabilize coexistence [62]. Notice that T_c also depends on the coupling λ_{12} between the order parameters, as shown in Fig. 24 (b).

5.3.2 Coexistence region

Analogously to the previous section, let us firstly recall the effective potential at *zero-temperature* obtained for coexistence case in (2+1) dimensions, i.e., Eq. (292), which is given by [62],

$$\begin{aligned} V_{eff}^{0\ (2+1)dim}(\varphi_{1,2}) &= r_1\varphi_1^2 + \lambda_1\varphi_1^4 + \lambda_2\varphi_2^4 + \lambda_{12}\varphi_1^2\varphi_2^2 + \delta_1\varphi_1^3\varphi_2 + \delta_2\varphi_1\varphi_2^3 + \\ &- \frac{\sqrt{2}}{2\pi}\left[\frac{1}{3}\left((b_1+r_1)^{3/2} + b_2^{3/2}\right) - \frac{1}{3}\left|r_1\right|^{3/2} + \right. \\ &+ \left.\frac{\left(3\delta_1\varphi_1^2 + 3\delta_2\varphi_2^2 + 4\lambda_{12}\varphi_1\varphi_2\right)^2}{4(\sqrt{b_2}+\sqrt{b_1+r_1})}\right] \end{aligned} \tag{331}$$

where $b_{1,2}$ are given in Eq. (286).

For coexistence, the system is fine-tuned at the *zero-temperature* classical critical point (ZTCCP) of the phase characterized by φ_2, such that $r_2 = 0$. Notice that when $r_1 \to 0$ we recover Eq. (325) for bicritical case, as expected.

We point out that the main difference between this case and the bicritical one is that even at classical level there is a coexistence region that is enhanced by quantum corrections for both couplings, λ_{12} and $\delta_{1,2}$ [62]. In other words, both ZTCCPs move away due quantum fluctuations effects. Since the system is deep in the phase with $\varphi_1 \neq 0$ we can fix it at a constant (finite) value in order to analyze the temperature effects for this case, as we shall discuss later on. Moreover, we need to satisfy the condition $b_1 > r_1$ in Eq. (331), otherwise we have domains formation where coexisting phases become metastable [55, 62] giving rise to non-homogeneous ground states.

Similarly to the section above for the bicritical case, we are interested in investigating finite temperature effects on the effective potential of Eq. (324) now for the coexistence case. In order to obtain some analytical expressions, we apply the same approximation from previous section, i.e., we also consider the low temperature regime, that is, for $T << \Delta_{1,2}$. In other words, again, one can neglect the two last temperature dependent terms in Eq. (324). However, the only difference is that for coexistence case the quantum correction term is given now by Eq. (331).

Note that for coexistence case we take $r_1 \neq 0$ and $r_2 = 0$ in Eq. (322). So, we have the following integrals to solve [63],

$$\int_0^\infty dp\ p\ \ln\left(1 - e^{-\frac{\epsilon_{p_i}}{T}}\right) \approx T\left(\sqrt{b_i + r_i} + T\right) e^{-\frac{\sqrt{b_i+r_i}}{T}}. \tag{332}$$

The integral in ϵ_{p_2} has to be treated differently since $r_2 = 0$ [63]. Also,

$$\int_0^\infty dp\ p\ \ln\left(1 - e^{-\frac{\epsilon_{p_i}}{T}}\right) \approx T\left(\sqrt{|r_i|} + T\right) e^{-\frac{\sqrt{|r_i|}}{T}} \tag{333}$$

for $i \neq 2$, where we use again that $\ln(1-x) \approx -x$, for small x, since we are interested in the low temperature regime $T << \Delta_{1,2}$.

With the help of the Eq. (332), Eq. (333) and Eq. (331) we can rewrite the effective potential in Eq. (326), taking into account finite temperature effects, now for coexistence case [63],

$$
\begin{aligned}
V_{eff}^{(2+1)dim} &= \underbrace{r_1\varphi_1^2 + \lambda_1\varphi_1^4 + \lambda_2\varphi_2^4 + \lambda_{12}\varphi_1^2\varphi_2^2 + \delta_1\varphi_1^3\varphi_2 + \delta_2\varphi_1\varphi_2^3}_{classical\ term} + \qquad (334) \\
&\underbrace{- \frac{\sqrt{2}}{2\pi}\Big[\frac{1}{3}\left((b_1+r_1)^{3/2} + b_2^{3/2}\right) - \frac{1}{3}\left|r_1\right|^{3/2} + \frac{\left(3\delta_1\varphi_1^2 + 3\delta_2\varphi_2^2 + 4\lambda_{12}\varphi_1\varphi_2\right)^2}{4(\sqrt{b_2}+\sqrt{b_1+r_1})}\Big]}_{quantum\ corrections} \\
&\underbrace{+ \frac{T^3}{(2\pi)^2}\left\{ - \sum_{i=1}^{2}\left(\left[1 + \frac{\sqrt{b_i+r_i}}{T}\right] e^{\left(-\frac{\sqrt{b_i+r_i}}{T}\right)} - \left[1.2 + \frac{\sqrt{|r_i|}}{T}\right] e^{-\frac{\sqrt{|r_i|}}{T}} \right) \right\}}_{finite\ temperature\ effects}
\end{aligned}
$$

where $r_2 = 0$.

If $r_1 = 0$, we recover the result for bicritical case in the previous section, as expected (see Eq. (330)). Differently from the bicritical point discussed above, in coexistence case there is the emergence of a new characteristic length associated with the mass term (r_1) [4]. This can be seen directly from the solution of the integral in Eq. (333), i.e., the correlation length of the system is given by $\xi = 1/\sqrt{2r_1}$, which is related to the distance to the ZTCCP [4].

It is worth to point out that from the finite temperature terms in the effective potential, Eq. (334), we can recognize the same temperature scaling of the free energy as in the bicritical case, $\mathcal{F} \propto T^{(d+z)/z}$, for $T >> T_c$. Therefore, all the previous statements about the bicritical point, i.e., the *weak first-order temperature phase transitions* [91, 92, 93] and the specific heat regimes, hold even if we begin with a coexistence region in the classical phase diagram.

Analogously to the bicritical case, consider tuning the classical system to the ZTCCP of the phase characterized by φ_2, as in Fig. 25, at the point $r_2 = 0$ of the phase diagram. At this point, we have $< \varphi_2 >= 0$, and $\varphi_1 = \langle\varphi_1\rangle = \sqrt{|r_1|/(2\lambda_1)}$ (classical value). As the quantum corrections are turned on, $< \varphi_2 >$ becomes finite, due to the *repulsion* of the ZTCCPs that increases the region of coexistence [62]. This order parameter $< \varphi_2 >$, which was zero in the classical case now attains a finite value that for a fixed point in the phase diagram inside the coexistence region increases, as the coupling λ_{12} increases, see Fig. 25.

For numerical calculations we take the same previous parameters values. As temperature increases along the vertical line ($r_2 = 0, T \neq 0$) shown in Fig. 25, the phase with $< \varphi_2 >$ finite due to quantum corrections becomes unstable at a *weak first-order*

Figure 25 - Scaling regime of the specific heat for coexistence region in 2d systems with $z = 1$

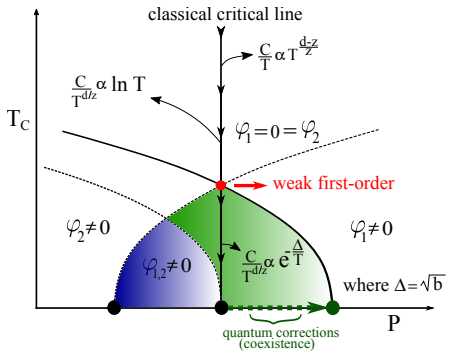

Legend: (Color online) Specific heat scaling regimes for coexistence region in 2d systems with $z = 1$. Quantum corrections enhance the coexistence region (arrow (green)). At the ZTCCP we can identify three different scaling regimes for the specific heat. Notice that in coexistence case there is the emergence of a new characteristic length of the system associated with the *mass* term, i.e. $\xi = 1/\sqrt{2r_1}$. The gaps for thermal excitations are now given by $\Delta_1 = \sqrt{b_1 + r_1}$ and $\Delta_2 = \sqrt{b_2}$, where $b_{1,2}$ appear in Eq. (303). Analogously to the bicritical case, the point where both lines cross (red) marks a *weak first-order temperature phase transition* point. The intermediate regime, i.e., regime II, is distinguished by a logarithmic dependence of the specific heat.

Source: Ref. [63].

transition. This is characterized by the minimum of the temperature dependent effective potential at $< \varphi_2 >= 0$ becoming degenerate with the minima at finite $< \varphi_2 >$.

Finally, once we introduce thermal fluctuations, we can also investigate how T_c behaves as a function of the distance to the ZTCCP in the coexistence region. This has important experimental consequences for the region of coexistence in systems with competing orders. Note from Fig. 26 that since we deviate from the ZTCCP the critical temperature decreases. This suggests that above the fine tuned value of the ZTCCP, we may find the highest T_c in the coexistence region [63]. In other words, at finite temperatures, above the ZTCCP the system presents the maximum T_c of the coexistence region as we consider both quantum and finite temperature effects on the effective potential.

5.4 Finite temperature effects for three-dimensional systems with linear dispersion relation

Let us now change the dimensionality of the system but preserve its dynamic critical exponent $z = 1$ in order to investigate finite temperature effects and consequently its thermodynamic signatures that we may expect for 3d systems whereupon time and space scales in the same way [63]. Again, when it is not possible to get some analytical

Figure 26 - T_c as a function of the distance to the ZTCCP (r_1) in the case of the 2d systems with $z = 1$

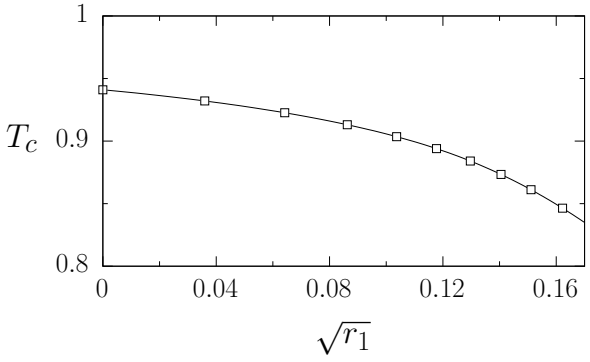

Legend: Numerical calculation of T_c as a function of the distance to the ZTCCP (r_1) in the case of the 2d systems with $z = 1$, i.e., using Eq. (334). T_c decreases as we deviate from the ZTCCP. This indicates that above where the ZTCCP is located, before including quantum corrections, the maximum T_c in the coexistence phase is attained. The numerical results are consistent with the schematic behavior presented in Fig. 25.
Source: Ref. [63].

expression, we will solve the integrals numerically.

5.4.1 Bicritical point and coexistence region

As we have mentioned before, the extension to include finite temperature effects in 3d systems with $z = 1$ is straightforward. Thus, using Eq. (323), for 3d systems with a linear dispersion relation and for $T << \Delta_{1,2}$ the effective potential becomes [63],

$$\begin{aligned} V_{eff}^{(3+1)dim} &= V_{eff}^{0\ (3+1)dim} + \\ &+ \frac{\sqrt{2}}{(2\pi)^3} 2T^4 \Bigg\{ - \frac{1}{T^3} \int_0^\infty dp\ p^2\ \left(e^{-\frac{\epsilon_1}{T}} + e^{-\frac{\epsilon_3}{T}} \right) + \\ &- \frac{1}{T^3} \int_0^\infty dp\ p^2\ \left(e^{-\frac{\epsilon_2}{T}} + e^{-\frac{\epsilon_4}{T}} \right) \Bigg\} \end{aligned} \tag{335}$$

where $V_{eff}^{0\ (3+1)dim}$ is the quantum corrections term at *zero-temperature* previously obtained [61] in Eq. (246) and Eq. (262) for bicritical point and coexistence region, respectively. Furthermore, again, $\epsilon_{p_i}^2$ and $f_{BE}(\epsilon_p)$ are given in Eq. (322), and $b_{1,2}$, A and B given in Eq. (303).

In the case of a bicritical point, i.e., for $r_1 = r_2 = 0$, to deal with the integration

over $\epsilon_{2,4}$, we now use the result,

$$\int_0^\infty dp\ p^2 \ln\left(1 - e^{-\frac{p}{T}}\right) = -\frac{1}{45}\pi^4 T^3 \tag{336}$$

Note the main differences when we compare Eq. (335) to the effective potential for 2d systems, i.e., Eq. (326). In $V_{eff}^{0\ (3+1)dim}$, the dependence of the integral on momentum in Eq. (335) is no longer linear but quadratic. The temperature dependent term in the effective potential now exhibits a T^4 dependence, instead of the T^3 in 2d. These results are consistent with the $T^{(d+z)/z}$ dependence of the free energy expected from scaling close to a QCP [4]. From the expression for $V_{eff}^{0\ (3+1)dim}$ we find that in 3d systems, with $z = 1$, the ZTCCPs are stable to quantum corrections in the presence of an exclusive quartic interaction [61]. However, in the case of the bilinear coupling these corrections give rise to coexistence [61], as in 2d systems [62].

The full results from Eq. (335) for both bicritical point and coexistence cases in 3d case have been obtained numerically. It turns out that the effects of thermal fluctuations in the case of bilinear coupling are very similar to those discussed above for the 2d case. Finite temperature effects, distinctively from quantum fluctuations, tend to disorder the system as we increase temperature. As in 2d case, there are three regimes with different thermal behaviors related to the existence of a *weak first-order transition* [91, 92, 93] at T_c. In the high temperature regime, $T >> T_c$ the free energy presents a temperature dependence of the form $T^{(d+z)/z}$ in agreement with the expected scaling behavior in the presence of a QCP [4]. The intermediate regime is distinguished by a logarithmic dependence of the specific heat. Finally, for the $T << T_c$ the specific heat is thermally activated with a gap related to the size of finite domains [4], see Fig. 23 and Fig. 25

SUMMARY AND CONCLUSIONS

SCES at low temperatures present complex phase diagrams [5, 6, 7, 8, 9, 10, 11, 12, 13, 14, 15, 16, 17, 18, 19] with competing or coexisting orders that can be tuned by varying external parameters, such as, pressure, doping, or magnetic field [3, 4]. Due to the electronic interaction may emerge ground states exhibiting exotic properties in these systems. The most notables among them are pnictides/iron-arsenide SC [25, 26, 27, 28, 29], U and Ce-based heavy fermions [8, 9, 11] and High-T_c cuprates materials [8, 9, 11]. For instance, one can observe FM, SDW, MI and CDW [1, 2] as a function of some external parameter. Moreover, it has been reported distinct ground states even for the same values of external parameters, which implies competing/coexistence of different orderings. All these experimental findings are very interesting ongoing research topics that need a fundamental theory to describe them.

In order to contribute to this issue, in this dissertation we have investigated the effects of quantum and thermal fluctuations on the phase diagrams of systems with competing scalar order parameters. We focused on two specific MF phase diagrams, i.e., the case of a bicritical point, where two phases vanish simultaneously and continuously, and also the region of this diagram where there is coexistence between the two phases. We studied these problems in the presence of two types of couplings between the order parameters. One is a conventional quartic coupling with a positive sign that describes competition between the different orderings [5, 38, 39, 40]. The other is a bilinear interaction that is allowed only in special cases where the order parameters have the same group symmetry [41, 42].

Initially, we have evaluated the *one-loop* effective potential at *zero-temperature* of two real scalar order parameters for both three [61] and two [62] spatial dimensions, considering dynamics characterized by linear and quadratic dispersion relations, i.e., by dynamic critical exponents $z = 1$ and $z = 2$ [24, 51, 52, 53], respectively. These possibilities cover most of the interesting cases of competing/coexisting phases observed in SCES.

We have obtained, for 3d systems with $z = 1$, that a classical bicritical point is stable to quartic interactions even when quantum fluctuations are taken into account. However, this is not the case in the presence of a bilinear coupling [61]. We have shown that any finite positive bilinear interaction breaks the symmetry of the bicritical point and gives rise to phase coexistence [61]. This is a purely quantum effect and resembles the physics of the Coleman–Weinberg mechanism [55] where coupling to a gauge field gives rise to symmetry breaking.

In the region of coexistence we obtained that the effect of quantum fluctuations in the presence of quartic interactions is to reduce the region of phase coexistence in the

phase diagram [61]. While in the classical case coexistence is allowed in the presence of a quartic coupling, if the condition $\lambda_{12} < 4\lambda_1\lambda_2$ is satisfied, when quantum corrections are included no coexistence is possible in the presence of these quartic interactions. This is not the case for a bilinear coupling that favors coexistence even when quantum fluctuations are included [61]. When both interactions are present, in fact for any finite bilinear coupling, the different phases can coexist at *zero-temperature* [61].

We also show that quantum fluctuations for 2d systems, characteristic of compounds with tetragonal structures, are stronger than 3d ones, producing more drastic effects on the MF phase diagram, as expected. We have found that for 2d systems with non-dissipative dynamics ($z = 1$), related to interacting magnetic excitons, where the effective dimensionality is simply increased by 1, the bicritical point is unstable and quantum fluctuations induce phase coexistence for both types of interactions between order parameters [62]. These effects are in contrast with the 3d case where, although the bilinear interaction spontaneously breaks global Z_2 symmetry, the biquadratic interaction does not modify the bicritical point. On the other hand, the bicritical point is robust and survives at quantum level, in $d = 2$ as well as in $d = 3$, in the presence of dissipative dynamics ($z = 2$) [62]. The latter is in agreement with the expectation that for effective dimensions $d_{eff} = d + z > 4$, we should not expect drastic changes of the MF results [4].

With respect to the region of coexistence, we found that quantum fluctuations for 2d systems with $z = 1$ enhance the coexistence region whatever is the dynamics [62]. Thus, quantum effects change the MF tendency of the biquadratic interaction to shrink this region, i.e., they provide stability for the coexistence of different phases [62]. Moreover, we obtain that there may be a sector of the phase diagram, under well-defined conditions, where the coexistence region is metastable, favoring domain formation and a non-homogeneous ground state [62], which may be observed experimentally.

Our results for the *one-loop* effective potential at *zero-temperature* [61, 62] provide requirements for the emergence of stable, unconventional coexisting phases, as observed experimentally in Fe-based [12, 25, 26, 27, 28, 29] SC, U and Ce-based [8, 9, 11, 84, 85] heavy fermions compounds, or even in high-T_c cuprates [8], through the effects of quantum fluctuations. In other words, while at MF level, the phase diagram only depends on symmetry, at a quantum level, dimensionality and dynamics are essential ingredients to ensure the stability of the coexistence of phases.

Next, we introduced finite temperature effects on the effective potential by means of the well-known Matsubara summation formalism from finite temperature QFT [4, 56, 57, 58, 59, 60, 72, 73]. We addressed the effects of finite temperature on our previous results concerning the stability of QCPs on the ground state of the phase diagrams of systems with competing scalar orderings for propagators described by $z = 1$ only [63].

We also investigated the interplay between the effects of quantum and thermal fluctuations on the phase diagram of the classical systems with $z = 1$ for 2d and 3d

cases [63]. It is worth to point out that the study of the effect of thermal fluctuations on the ground state with quantum corrections is very important and allow us to make the bridge between our results and experiments.

We show that for 2d systems, the ZTCBP is unstable for both quantum [62] and thermal fluctuations in the cases of quartic and bilinear couplings. Increasing temperature gives rise to a weak first-order temperature phase transition [91, 92, 93] at T_c, where the coexisting phases exchange stability with a disordered phase [63]. The weak first-order nature of this transition is confirmed by a calculation of the latent heat that turns to be small compared with the thermal fluctuations at T_c [63]. In addition, the observation of scaling behavior of the free energy and specific heat above T_c is consistent with the weak character of the transition [4, 63]. This has as consequence that it is difficult to distinguish it from a continuous second order transition.

Indeed, above T_c the system will present scaling behavior associated with the existence of a QCP in d-dimensions and with dynamic critical exponent $z = 1$ down to temperatures very close to T_c [63]. In this region of the phase diagram, i.e., for $T >> T_c$, the specific heat scales as $C/T \propto T^{(d-z)/z}$ that crosses over to a less universal behavior $(C/T)^{(d+z)/z} \propto -\ln(T)$ for $T \approx T_c$ in both 2d and 3d cases [63]. At low temperatures, that is, for $T << T_c$, in the coexistence region we can identify the appearance of a gap for thermal excitations [63]. This is related to excitations in finite domains that nucleate below T_c due to the first-order character of this transition. Experimentally this gap manifests in a thermally activated contribution to the specific heat at these low temperatures. The length of the domains introduces new length scales in the problem [4].

We have also studied the effects of thermal and quantum fluctuations in MF phase diagrams where there is a region of coexistence for $z = 1$ only [63]. In 2d systems, the ZTCCPs are unstable to quantum fluctuations that enhance the region of coexistence for both quartic and bilinear couplings [62]. However, at finite temperatures the coexisting phases exchange stability with a disordered phase at a weak first-order transition [63]. We also find the maximum T_c of a given phase occurs at temperatures above the ZTCCP of this phase [63]. As before, scaling behavior is found for $T > T_c$ and thermally activated excitations for $T << T_c$ [63].

In the case of a bilinear coupling the results for 3d systems are very similar to those in 2d [63]. We have to remark the stability of the ZTCBP to a quartic coupling in 3d [61]. In the case of coexistence, quantum fluctuations in the presence of a quartic coupling in 3d actually reduce the region of coexistence. In this sense, it competes with the bilinear interaction [61] that acts to increase this region.

From numerical calculations we note that in 3d, thermal fluctuations, in opposite to quantum fluctuations, present some common features with the 2d case. In both, 2d and 3d, thermal fluctuations lead to disorder in the system and give rise to weak-first order transitions as we increase temperature [63]. Above this transition we can identify

scaling behavior as approaching a QCP, consistent with its weak nature.

Note that the problem investigated in this dissertation is extremely relevant for many SCES in CMP. They range from high-T_c SCs, where different phases compete inside the SC dome, to heavy fermion materials [6, 7, 8, 9, 10, 11, 12]. In the latter AFM and SC have clearly been observed in coexistence close to an AFM-QCP.

Our results can be useful to identify the form of the interactions between the order parameters in this systems. In other words, we have shown the importance of considering the effect of quantum and thermal fluctuations on the MF phase diagrams of systems with competing scalar order parameters. The effect of quantum corrections is essential to understand the emergence of stable unconventional coexisting orders, experimentally observed in SCES. Our results show explicitly how symmetry, dynamic and dimensionality determine the nature of the phase diagrams. On the other hand, our study for finite temperature clearly points out the ubiquity of weak first-order transitions as well as scaling behavior for the free energy and specific heat in 2d and 3d systems with competing scalar order parameters. Although our analyze for finite temperature [63] has been carried out for QCPs with Lorentz invariance [24, 51, 52, 53, 61, 62], we expect that our general conclusions as the existence of these finite temperature transitions and the accompanying scaling behavior will persist for arbitrary values of the dynamic exponent.

REFERENCES

[1] T. Gruner, D. Jang, Z. Huesges, R. Cardoso-Gil, G. H. Fecher, M. M. Koza, O. Stockert, A. P. Mackenzie, M. Brando and C. Geibel, Nat. Phys. **13**, 967 (2017).

[2] F. Steglich and S. Wirth, Rep. Prog. Phys. **79** 084502 (2016).

[3] S. Sachdev, *Quantum Phase Transitions*, Cambridge University Press, UK (1999).

[4] M.A. Continentino, *Quantum scaling in many-body systems: an approach to quantum phase transitions*, Cambridge University Press, 2017.

[5] R.M. Fernandes and J. Schmalian, Phys. Rev. B **82**, 014521 (2010).

[6] R. Movshovich, T. Graf, D. Mandrus, J. D. Thompson, J. L. Smith, and Z. Fisk, Phys. Rev. **B 53**, 8241 (1996); N. D. Matur, F. M. Grosche, S. R. Julian, I. R. Walker, D. M. Freye, R. K. W. Haselwimmer and G. G. Lonzarich, Nature **394**, 39 (1998).

[7] T. Park, F. Ronning, H. Q. Yuan, M. B. Salamon, R. Movshovich, J. L. Sarrao and J. D. Thompson, Nature **440**, 65 (2006).

[8] P. G. Pagliuso, C. Petrovic, R. Movshovich, D. Hall, M. F. Hundley, J. L. Sarrao, J. D. Thompson, and Z. Fisk, Phys. Rev. **B 64**, 100503(R) (2001).

[9] K. Chen, F. Strigari, M. Sundermann, Z. Hu, Z. Fisk, E. D. Bauer, P. F. S. Rosa, J. L. Sarrao, J. D. Thompson, J. Herrero-Martin, E. Pellegrin, D. Betto, K. Kummer, A. Tanaka, S. Wirth, and A. Severing, Phys. Rev. **B 97**, 045134 (2018).

[10] V.A. Sidorov, M. Nicklas, P.G. Pagliuso, J.L. Sarrao, Y. Bang, A.V. Balatsky and J.D. Thompson, Phys. Rev. Lett., **89**, 157004 (2002).

[11] G.F. Chen, K.Matsubayashi, S. Bah, K. Deguchi and N.K. Sato, Phys. Rev. Lett., **97**, 017005 (2006).

[12] Z. Shermadini, A. Krzton-Maziopa, M. Bendele, R. Khasanov, H. Luetkens, K. Conder, E. Pomjakushina, S. Weyeneth, V. Pomjakushin, O. Bossen and A. Amato, Phys. Rev. Lett., **106**, 117602 (2011).

[13] D. Braithwaite, M. Vališka, G. Knebel, G. Lapertot, J.-P. Brison, A. Pourret, M.E. Zhitomirsky, J. Flouquet, F. Honda, and D. Aoki, Communications Physics **2**, 147 (2019).

[14] S. Sundar, S. Gheidi, K. Akintola, A. M. Côté, S. R. Dunsiger, S. Ran, N. P. Butch, S. R. Saha, J. Paglione, and J. E. Sonier, Physical Review B **100**, 140502(R) (2019).

[15] A. Narayan, A. Cano, A. V. Balatsky and N. A.Spaldin, Nature Materials **18**, 223-228 (2019).

[16] K. Dunnett, J.-X. Zhu, N. A. Spaldin, V. Juričić and A. V. Balatsky, Physical Review Letters **122**, 057208 (2019).

[17] Dai Aoki, A. Nakamura, F. Honda, D. Li, Y. Homma, Y. Shimizu, Y. J. Sato, G. Knebel, J.-P. Brison, A. Pourret, D. Braithwaite, G. Lapertot, Q. Niu, M. Vališka, H. Harima, and J Flouquet, Journal of the Physical Society of Japan **88**, 043702 (2019).

[18] J. R. Arce-Gamboa and G. G. Guzmán-Verri, Phys. Rev. Materials **2**, 104804 (2018).

[19] P. Gegenwart, Q. Si and F. Steglich, Nat. Phys. **4**, 186–197 (2008).

[20] M.A. Continentino, Brazilian Journal of Physics, vol. 35, no. 1, March (2005).

[21] M.A. Continentino, A.S. Ferreira, J. M. M. M. **310** 828 (2007).

[22] S. Doniach, Physica **B 91**, 231 (1977).

[23] J. D. Thompson and J. M. Lawrence in *Handbook on the Physics and Chemistry of Rare Earths, Lanthanides/Actinides:Physics-II*, edited by K.A. Gschneider Jr., L. Eyring, G.H. Lander, and G.R. Choppin , Elsevier Science B.V., Chapter 133 (19), 383 (1994).

[24] A.S. Ferreira, M.A. Continentino and E.C. Marino, Phys. Rev. B **70**, 174507 (2004).

[25] S. Raghu, X.L. Qi, C.X. Liu, D.J. Scalapino and S.C. Zhang, Phys. Rev. B , **77**, 220503(R) (2008).

[26] R.M. Fernandes and A.V. Chubukov, Rep. Prog. Phys., **80**, 014503 (2017).

[27] Y. Bang and G.R. Stewart, J. Phys.: Condens. Matter, **29**, 123003 (2017).

[28] M. Sunagawa, et al., Nature srep 04381 (2014).

[29] D. E. Almeida, R. M. Fernandes, and E. Miranda, Phys. Rev. **B 96**, 014514 (2017).

[30] H. Luetkens, H.-H. Klauss, M. Kraken, F. J. Litterst, T. Dellmann, R. Klingeler, C. Hess, R. Khasanov, A. Amato, C. Baines, M. Kosmala, O. J. Schumann, M. Braden, J. Hamann-Borrero, N. Leps, A. Kondrat, G. Behr, J. Werner, and B. Büchner, Nature Mater. **8**, 305 (2009).

[31] A. J. Drew, Ch. Niedermayer, P. J. Baker, F. L. Pratt, S. J. Blundell, T. Lancaster, R. H. Liu, G. Wu, X. H. Chen, I. Watanabe, V. K. Malik, A. Dubroka, M. Rössle, K. W. Kim, C. Baines, and C. Bernhard, Nature Mater. **8**, 310 (2009).

[32] C. R. Rotundu, D. T. Keane, B. Freelon, S. D. Wilson, A. Kim, P. N. Valdivia, E. Bourret-Courchesne, and R. J. Birgeneau, Phys. Rev. B **80**, 144517 (2009).

[33] T. Goko, A. A. Aczel, E. Baggio-Saitovitch, S. L. Bud'ko, P. C Canfield, J. P. Carlo, G. F. Chen, P. Dai, A. C. Hamann, W. Z. Hu, H. Kageyama, G. M. Luke, J. L. Luo, B. Nachumi, N. Ni, D. Reznik, D. R. Sanchez-Candela, A. T. Savici, K. J. Sikes, N. L. Wang, C. R. Wiebe, T. J. Williams, T. Yamamoto, W. Yu, and Y. J. Uemura, Phys. Rev. B **80**, 024508 (2009).

[34] D. Belitz, T. R. Kirkpatrick, and J. Rollbühler, PRL **94**, 247205 (2005).

[35] D. Belitz, T. R. Kirkpatrick, Thomas Vojta, Reviews of Modern Physics, vol. 77, April (2005).

[36] T. Vojta, D. Belitz, T. R. Kirkpatrick, and R. Narayanan, Ann. Phys. (Leipzig) 8 (1999) 7–9, 593 – 602.

[37] N. Goldenfeld, *Lectures on phase transitions and the renormalization group*, Addison-Wesley, 1992.

[38] P. Santini and G. Amoretti, Phys. Rev. Lett. **73**, 1027 (1994).

[39] V. Barzykin and L. P. Gor'kov, Phys. Rev. Lett. **70**, 2479 (1993).

[40] D.G. Barci, R.V. Clarim and N.L. Silva Júnior, Phys. Rev. B **94**, 184507 (2016).

[41] V. P. Mineev and M. E. Zhitomirsky, Phys. Rev. B **72**, 014432 (2005).

[42] D. F. Agterberg and M. B. Walker, Phys. Rev. B **50**, 563 (1994).

[43] A. P. Ramirez, P. Coleman, P. Chandra, E. Brück, A. A. Menovsky, Z. Fisk, and E. Bucher, Phys. Rev. Lett. **68**, 2680 (1992).

[44] H. Ikeda and Y. Ohashi, Phys. Rev. Lett. **81**, 3723 (1998).

[45] P. Chandra, P. Coleman, J. A. Mydosh, and V. Tripathi, Nature (London) **417**, 831 (2002);

[46] P. Chandra, P. Coleman, and J. A. Mydosh, Physica B **397**, 312–313 (2002).

[47] M. Zacharias, I. Paul and M. Garst, Phys. Rev. Lett. **115**, 025703 (2015).

[48] M. E. Zhitomirsky and V.-H. Dao, Phys. Rev. B **69**, 054508 (2004).

[49] A. L. Larkin and S. A. Pikin, Zh. Eksp. Teor. Fiz. **56**, 1664 (1969).

[50] T. R. Kirkpatrick, D. Belitz, Thomas Vojta, and R. Narayanan, Phys. Rev. Lett. **87**, 127003 (2001).

[51] J.A. Hertz, Phys. Rev. B **14**, 3 (1976).

[52] V.P. Mineev, Pis'ma Zh. Éksp. Teor Fiz. 66, 655 (1997)[JETP Lett. 66, 693 (1997)].

[53] V.P. Mineev, M. Sigrist, Phys. Rev. B **63**, 172504 (2001).

[54] G. Jona-Lasinio, Nuovo Cimento **34**, 1790 (1964).

[55] S. Coleman and E. Weinberg, Phys. Rev. D **7**, 1888 (1973).

[56] R.O. Ramos. D.G. Barci, C.A. Linhares and J. F. Medeiros Neto, Braz. J. Phys. [online]. 2007, vol.37, n.1b.

[57] T. Matsubara, Progress of Theoretical Physics, **14**, 4 (1955).

[58] J. I. Kapusta, *Finite-Temperature Field Theory* (Cambridge University Press, Cambridge, England, 1985).

[59] A. A. Abrikosov, L. P. Gorkov and I. E. Dzyaloshinski, *Methods of quantum field theory in statistical physics*, Dover publications, (1975).

[60] Z. Nussinov, I. Vekhter and A. V. Balatsky, Phys. Rev. B **79**, 165122 (2009).

[61] N.L. Silva Jr, M.A. Continentino and D.G. Barci, J. Phys.: Condens. Matter, **30** 255402 (2018).

[62] N. Lopes, M.A. Continentino and D.G. Barci, Physics Letters A **384**, 126095 (2020).

[63] N. Lopes, D.G. Barci and M.A. Continentino, J. Phys.: Condens. Matter **32** 415601 (2020).

[64] L.D. Landau and E.M. Lifshitz, *Statistical Mechanics*, Oxford: Pergamon Press (1980).

[65] P.S. Branicio, RBEF, vol. 23, no. 4 (2001).

[66] R. Zadorosny, A. Presotto, E.C.S. Duarte and E. Sardella, arXiv:1505.01150 (2015).

[67] A.A. Abrikosov, *Fundamentals of the theory of Metals*, Dover Publication Inc.; Reprint(2017).

[68] J. F. Annett, *Superconductivity, superfluids and condensates*, Oxford: Oxford Univ. Press (2004).

[69] A.S. Ferreira, *Transições Quânticas Induzidas por Flutuções em Sistemas Fortemente Correlacionados*, 112 p. Dissertation (Masters), Institute of Physics, Fluminense Federal University, Rio de Janeiro, 2005.

[70] B. Halperin, Physics Today **72**, 2, 42 (2019).

[71] L.P. Kadanoff, W. Gotze, D. Hamblen et al., Rev. Mod. Phys. **39**, 395 (1967).

[72] M.E. Peskin and D.V. Schroeder, *An introduction to quantum field theory*, CRC Press (2018).

[73] A. Altland and B. Simons, *Condensed Matter Field Theory*, Cambridge University Press (2010).

[74] M. A. Continentino and A. S. Ferreira, Physica A **339**, 461 (2004).

[75] B. Nienhuis and N. Nauenberg, Phys. Rev. Lett. **35**, 477 (1975).

[76] B. Nienhuis, A. N. Berker, E. K. Riedel and M. Schick, Phys. Rev. Lett. **43**, 737 (1979).

[77] J. Sólyom and P. Pfeuty, Phys. Rev. B **24**, 218 (1981).

[78] L. Turban and F. Igloi, Phys. Rev. B **66**, 014440 (2002)

[79] M. E. Fisher and A. N. Berker, Phys. Rev. B **26**, 2507 (1982).

[80] N. Boccara, *Symétries Brisées*, Hermann, Paris, p.120 (1979).

[81] J. Paglione,M. A. Tanatar, D. G. Hawthorn, E. Boaknin, R. W. Hill, F. Ronning, M. Sutherland, L. Taillefer, C. Petrovic and P. C. Canfield, Phys. Rev. Lett. **91**, 246405 (2003).

[82] R. Jackiw, Phys. Rev. D **9**, 1686 (1973).

[83] M. P. A. Fisher, P.B. Weichman, G. Grinstein and D. S. Fisher, Phys. Rev. B **40**, 546 (1989).

[84] D. P. Moore et al, Physica B, 312 & 313, **134** (2002).

[85] S. Fujimori et al, Journal of the Physical Society of Japan, **81**, 014703 (2012).

[86] J. Wang, G.-Z. Liu, Phys. Rev. D **90**, 125015 (2014).

[87] E.J. Weinberg and A. Wu, Phys. Rev. D, **36**, 2474 (1987).

[88] N.D. Mermin and H. Wagner, Phys. Rev. Lett., **17**, 1133 (1966).

[89] K.A. Meissner, H. Nicolai, Acta Phys. Pol. B **40** 2737 (2009).

[90] J.-H She, J. Zaanen, A. R. Bishop and A. V. Balatsky, Physical Review B **82**, 165128 (2010).

[91] S.A. Pikin, Physica A **194** 352-363 (1993).

[92] L.A. Fernández, J.J. Ruiz-Lorenzo, M.P. Lombardo and A. Taracón, Physics Letters B **277** 485-490 (1992).

[93] A. J. Millis, A. J. Schofield, G. G. Lonzarich, and S. A. Grigera, Phys. Rev. Lett. **88**, 217204 (2002).